Publications

ChemPubSoc Europe

DOI: 10.1002/slct.201601361

Chemistry SELECT Full Papers

Medicinal Chemistry & Drug Discovery

Anticancer Activity and DNA Binding Studies of Novel 3,7-Disubstituted Benzopyrones

Sunil Dutt Durgapal,[a] Rina Soni,[a] Shweta Umar,[b] Balakrishnan Suresh,[b] and Shubhangi S. Soman*[a]

We have designed and synthesized novel 7-substituted-3-acetyl-benzopyrones **9a**-**9g** and ethyl 7-substituted-3-carboxylate-benzopyrones **10a**-**10d** and screened for anticancer activity using MTT assay. Most of the tested compounds have shown very good activity against A549 cell line (lung cancer cell-line) and MCF7 cell line (breast cancer cell-line) compared to 5-Fluorouracil. Compound **9b** and **9e** exhibited excellent anticancer activity with IC_{50} 0.16 nM against A549 cell line and 84.8 nM against MCF7 cell line respectively. Compounds **9b** and **9e** showed excellent anticancer activity at very low concentration, well falling in nanomolar region. Compounds **9b** and **9e** exhibited very good binding constant for DNA binding through intercalation in UV based DNA titration which was further confirmed by fluorescence based EtBr displacement assay in DNA-EtBr complex.

Introduction

Cancer is one of the dreadful diseases after cardiovascular diseases and diabetes falling under category of non-communicable diseases all over the world. According to WHO, number of people affected by cancer will rise from 14 million in 2012 to 22 million within the next 20 years.[1] Most of the cancers are defined by uncontrolled growth of cells without differentiation due to the deregulation of essential enzymes and other proteins controlling cell division and proliferation.[2–3] Out of many therapeutic strategies, chemotherapy shows significant clinical responses. At the same time, these chemotherapeutic agents have a small therapeutic window with non-specificity and high-systemic toxicity. To get selective chemotherapeutics with very low side effects is a major challenge in treatment of cancer.[4] Second major problem after target selectivity in chemotherapy, is drug resistance to many anticancer agents. These have resulted in drug-induced toxicities and requirement of high doses of chemotherapeutic agents.[5–7] Therefore, discovering of new anticancer agent with high potency is urgent need in treatment of cancer.[8]

One of the important classes of natural products, coumarins are considered as useful source of potential drug candidates due to safety and efficacy exhibited by coumarin derivatives. The bioactivity of coumarin and more complex related derivatives is mostly coming from coumarin nucleus. Coumarin derivatives are known with variety of pharmacological activities including anti-inflammatory,[9,10] antioxidant,[11,12] antithrombotic,[13,14] antiviral,[15,16] antimicrobial,[17,18] antituberculosis,[19] and antihyperlipidemic[20] activities. Due to the potential applications of coumarins in medicinal chemistry, many efforts have been made on the design and synthesis of new coumarin derivatives with improved biological activities. Coumarins exhibited antitumor activities at different stages of cancer formation through various mechanisms, for example blocking cell cycle, inducing cell apoptosis, modulating estrogen receptor (ER), or inhibiting the DNA-associated enzymes, such as topoisomerase.[21]

Coumarin derivatives containing a substituted hydroxyl group at the position 7 showed antibiotic and antifungal activities, while 7-hydroxycoumarin derivatives showed very good cytotoxicity and cytostatic activity.[22] Recent studies on a variety of synthetic coumarin derivatives have demonstrated the influence of the coumarin skeleton and substitutions at positions 3 and 7 on antitumor activities.[23] Maciejewska *el al* reported series of *O*-aminoalkyl substituted 7-hydroxycoumarins with anticancer activity.[24] Compound **1** showed good activity against various cancer cell lines such as leukemia CCRFCEM, non-small cell lung cancer HOP92 and colon cancer HCC2998.

Antioxidant compounds play important role in biological system by removal of free radicals generated in body. Synthetic antioxidant compounds are showing toxicity and mutagenic effects. Several coumarin derivatives are reported with antioxidant activity. Recently, El-Hameed Hassan *et al* reported 7-hydroxycoumarin derivative **2** as very good antioxidant in DPPH assay with IC_{50} value 213 μg/mL.[25] Most of the anticancer drugs including 5-flourouracil, tamoxifen and paclitaxel exerts their cytotoxicity toward cancer cell by elevating cellular ROS production to a threshold level and this elevated ROS causes DNA damage and activate apoptotic pathway in cell.[26–29] To

[a] *S. D. Durgapal, Dr. R. Soni, Prof. S. S. Soman*
Department of Chemistry
The M. S University of Baroda
Department of chemistry, Faculty of Science, Vadodara. 390002, India
E-mail: shubhangiss@rediffmail.com
[b] *S. Umar, Prof. B. Suresh*
Department of Zoology
The M. S University of Baroda
Department of Zoology, Faculty of Science, Vadodara. 390002, India

Supporting information for this article is available on the WWW under http://dx.doi.org/10.1002/slct.201601361

counterbalance the effect of ROS, cell have an antioxidant defence system which combat the effect of increased ROS in cell. Thus, the presence of antioxidant eradicates the anticancer effect of an anticancer drug which mostly exerts its effect by mean of ROS. Therefore, a potent anticancer drug should have low antioxidant property. Thus, screening of antioxidant activity provides useful insight into the mechanism of action of anticancer activity.

Anticancer drugs have traditionally been targeted to damage aberrantly dividing cells by interrupting the cell division process. Some of them are DNA intercalating agents or DNA cross linking agents. Coumarins form interstrand as well as intrastrand cross linkages and act as intercalating agents.[30–31] However, there are limited reports on such interactions for 3,7-disubstituted coumarins with DNA. The novel 3,7-disubstituted coumarin derivatives **9a–g** and **10a–d** were synthesized and screened for their anticancer activity, DNA binding studies and antioxidant activity (Figure 1).

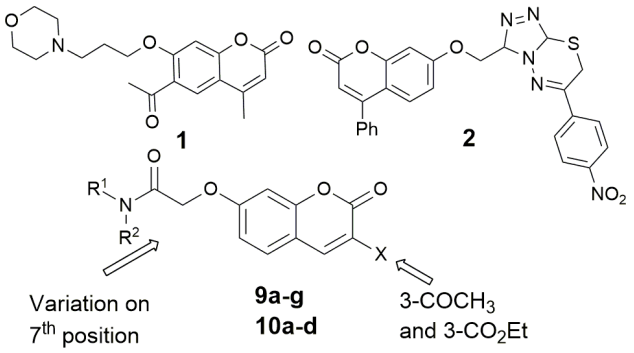

Figure 1. Coumarin derivatives with anticancer activity.

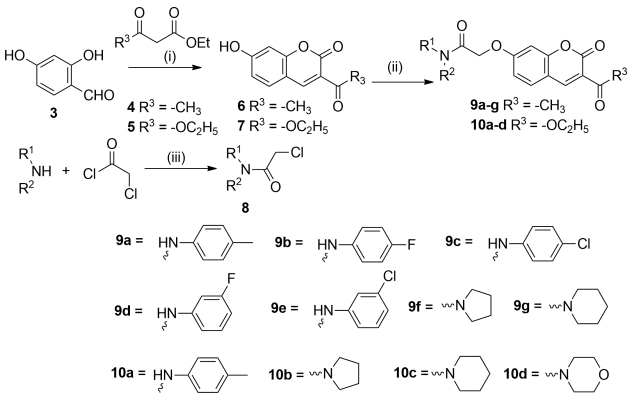

Scheme 1. Synthesis of 3,7-disubstituted coumarin derivatives **9a–g** and **10a–d.** Reagents and conditions: (i) Piperidine catalytic, pyridine, bulb oven (100 W), 70–80 °C, 14 h, 74–87%; (ii) 8, anhydrous K_2CO_3, KI pinch, DMF, 70–80 °C, 12–18 h, 43–91 %; (iii) TEA, DCM, 0–5 °C, 30 min, rt, 24 h, 85–95 %.

Results and Discussion

Chemistry

Novel 7-substituted-3-acetyl-benzopyrones **9a-9g** and ethyl 7-substituted-3-carboxylate-benzopyrones **10a-10d** (Scheme 1) were synthesized by reaction of 7-hydroxy-3-acetyl coumarin **6,** and ethyl 7-hydroxy-3-carboxylate coumarin **7** with different chloroacetamide derivatives. Knoevenagel Reaction of resorcaldehyde **3** with diethyl malonate **5** under similar conditions gave ethyl 7-hydroxy-3-carboxylate coumarin **7** as shown in **scheme 1.** The ^{1}H NMR spectrum of compound **6** exhibited singlet for -OH at 11.14 ppm, all aromatic protons were observed at δ 8.56-6.72. The methyl protons were observed as a singlet at δ 2.53. In the ^{13}C NMR spectrum, acetyl carbonyl carbon was observed at 195 ppm, the lactone carbonyl carbon of coumarin ring observed at δ 164, all aromatic carbons observed from δ 159–102 and methyl carbon at δ 30. The ^{1}H NMR spectrum of compound **7** exhibited singlet for -OH at 11.10 ppm, all aromatic protons observed at δ 8.67-6.72. The ethyl protons of ester group exhibited quartet at δ 4.25 and triplet at δ 1.29 with coupling constant 7.2 Hz for -CH_2 and -CH_3 respectively. In the ^{13}C NMR spectrum, the lactone carbonyl carbon of coumarin ring observed at δ 164 and ester carbonyl carbon was observed at δ 163 ppm, all aromatic carbons observed from δ 157–102 ppm and ethyl carbons at δ 61 and 14 ppm.

Various substituted amines on reaction with chloroacetyl chloride gave corresponding chloroacetamide derivatives **8** and these compounds were directly used for reaction with 7-hydroxy coumarins **6** and **7.** These chloroacetamide derivatives **8** were reacted with 7-hydroxy-3-substituted coumarins using anhydrous K_2CO_3 in DMF at 70–80 °C in presence of catalytic amount of KI to give compounds **9a–g** and **10a–d.** The structures of 3,7-disubstituted coumarin derivatives **9a–g** and **10a–d** were confirmed by different analytical techniques such as ^{1}H-NMR, ^{13}C-NMR, IR, ESI-MS and X-ray Single Crystal. In general, the IR spectra of compounds **9a–g** exhibited three strong bands in the range of 1734–1723 cm^{-1}, 1698–1681 cm^{-1} and 1670–1611 cm^{-1} for the lactone, ketone and amide carbonyl stretching frequency respectively. In the ^{1}H NMR spectra of **9a–g**, peaks for methyl protons of acetyl group observed in range of δ ~ 2.73-2.55, methylene protons observed in range of δ ~4.92-4.71, aromatic protons observed in range of δ 6.82-8.64 depending on effect of different amine substituted on it. For compounds **9a-e**, -NH protons are observed in range of 10.41-10.25. For compound **9e** D_2O exchange study was performed which showed disappearence of peak at δ 10.43 thus confirmed the peak for -NH proton at 10.43 ppm. In the ^{13}C NMR spectra of **9a–g**, peak for methyl carbon of acetyl group observed around 30 ppm, methylene carbon around 67 ppm, aromatic carbons in range of 101–161 ppm, amide carbonyl carbon in range of 163–161 ppm, coumarin lactone carbonyl carbon in range of 166–164 ppm and acetyl carbonyl carbon around 195 ppm.

For compounds **10a–d**, the IR spectra exhibited three strong bands in range of 1757–1747 cm^{-1}, 1708-1647 cm^{-1} and 1623–1602 cm^{-1} for the lactone, ester and amide carbonyls respectively. In the ^{1}H NMR spectra of **10a–d**, peak for methyl protons of ester group observed in range of δ ~1.42-1.30 as a

triplet and methylene protons observed in range of δ ~4.42-4.27 as a quartet. Protons for methylene linkage are observed in range of 5.02-4.71 and aromatic protons observed in range of 6.82-8.72 depending on effect of different amine substitution on it. For compound **10a** -NH proton is observed at δ 8.15 ppm, which was confirmed by D_2O exchange study. In the ^{13}CNMR spectra of **10a–d**, carbons for ethyl group observed around 14 ppm for methyl and 61 ppm for methylene. For compound **10a–d**, methylene linkage carbon observed around 67–66 ppm, aromatic carbon in range of 101–157 ppm, amide carbonyl group in range of 163–161 ppm, coumarin lactone carbonyl carbon in range of 163–164 ppm and ester carbonyl carbon at 165 ppm. All compounds **9a–g** and **10a–d** were analyzed by ESI-MS analysis to give $[M+H]^+$/$[M+Na]^+$ peak corresponding to their molecular weight. Structure of compound **10d** was confirmed by X-ray single crystal analysis (CCDC 1522100). All these new chemical entities were subjected to *in-vitro* studies for anticancer activity by MTT assay method, DNA binding studies and antioxidant activity by DPPH assay.

Anticancer Activity

Results from MTT assay were used to assess the growth inhibitory effect of the various compounds on A549 cancer cells (Lungs cancer cell line) and MCF7 (Breast cancer cell line). IC_{50} values were calculated to determine the concentration of test compound at which 50% of the cells are killed (Table 1). Compounds were studied for their DNA binding interaction (Table 2) and for their anti-oxidant activity against DPPH assay with respect to ascorbic acid as standard (Table 3).

Structure activity relationship (SAR) for anticancer activity

The MTT assay for 7-substituted-3-acetyl coumarin series showed better activity for compound **9a** with *p*-methyl substituent on aromatic amide against A549 and MCF7 with IC_{50} 2.40 μM and 0.65 μM respectively. On replacement of *p*-methyl with halogen such as compounds **9b** and **9c** resulted in compounds with excellent activity (Table 1). Compound **9b** with 4-fluoro substituent showed excellent activity with IC_{50} value 0.16 nM against A549 cell line, and showed good activity against MCF7 cell line with IC_{50} 23.53 μM. Moreover, compound **9c** with 4-chloro showed very good activity with IC_{50} value 0.82 μM and 13.02 μM against A549 and MCF7 cancer cell lines respectively. Interestingly, changing position of halogen from *-para* to *-meta* in compound **9d** and **9e** resulted in drop of anticancer activity against A549 cell line. Compound **9d** with 3-fluoro group showed moderate activity with IC_{50} value 9.16 μM and 14.04 μM, but compound **9e** showed very good anticancer activity against MCF7 cell line with IC_{50} 84.8 nM, while moderate anticancer activity observed against A549 cell line. Further, replacement of aromatic ring with saturated nitrogen heterocycles such as pyrrolidine **9f** and piperidine **9g** resulted in compounds with moderate to very good activity against A549 cell line with IC_{50} value 23.9 μM and 5.06 μM respectively. Against MCF7 cell line both compounds **9f** and **9g** showed good activity with IC_{50} value 3.08 μM and 1.11 μM respectively. Compounds **9a**-**9c**, **9g** and **10b** showed better anticancer activity in A549, while compounds **9a–g** and **10a–d** showed better activity in MCF7 compared to that of 5-Fluorouracil.

Table 1. Anticancer activity against A549 (Lungs cancer cell line), MCF7 (Breast cancer cell line) and anti-oxidant activity of compound **9a–g** and **10a–d.**

Compd no.	NR^1R^2	R^3	A549 IC_{50}[a]	MCF7 IC_{50}[a]
9a	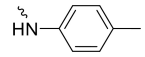	$-CH_3$	2.40 μM	0.65 μM
9b	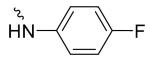	$-CH_3$	0.16 nM	23.53 μM
9c	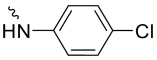	$-CH_3$	0.82 μM	13.02 μM
9d	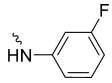	$-CH_3$	9.16 μM	14.04 μM
9e	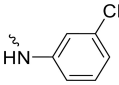	$-CH_3$	89.16 μM	84.8 nM
9f		$-CH_3$	23.9 μM	3.08 μM
9 g	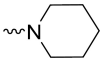	$-CH_3$	5.06 μM	1.11 μM
10a	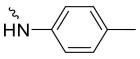	$-OC_2H_5$	NA	1.78 μM
10b		$-OC_2H_5$	3.11 μM	0.79 μM
10c		$-OC_2H_5$	NA	NA
10d		$-OC_2H_5$	23.2 μM	21.61 μM
5-Fluoro-uracil			11.13 μM	45.04 μM

[a]IC_{50} values were determined using Graph Pad Prism software by MTT assay using DMF. NA = Not active

Table 2. K_b and K_{SV} values for compound **9b** and **9e.**

Compd	λ_{max} nm	K_b (M^{-1}) UV based assay	Emission λ_{max} Nm	K_{SV} (M^{-1}) Fluorescence assay
9b	359	2.64×10^4	609	4.69×10^3
9e	356	8.29×10^5	610	4.23×10^3

Table 3. Anti-oxidant activity of compounds **9a–e** and **10b–c.**

Compoud no.	EC_{50} μg/mL[a]
9a	3436
9b	882
9d	48
9e	59
10b	46
10c	47
Ascorbic acid	11

[a]EC_{50} values were determined using Graph Pad. Prism software by DPPH assay using DMF.

Compound **10a**-**10d** containing carboxylate group at third position of coumarin ring showed good to poor anticancer activity, compared to corresponding 3-acetyl coumarin analogues. Compound **10a** showed good activity against MCF7 cell line with IC_{50} 1.78 μM, however remain inactive against A549 cell line.

Carboxylate analogue of compound **9f** *i.e* compound **10b** showed good activity against both tested cell lines A549 and MCF7 with IC_{50} 3.11 μM and 0.79 μM respectively. Compound **10c** remained inactive against both tested cell lines. However, morpholine analogue compound **10d** showed good activity against A549 and MCF7 cell lines. 5-Fluorouracil was used as standard and showed anticancer activity with IC_{50} 45.04 μM against MCF7 cell line

Anticancer activity data from NCI-60

Structures of all compounds were submitted to Division of Cancer Treatment and Diagnosis, National Cancer Institute Bethesda, USA to be evaluated in the full panel of 60 different cell lines. Out of all two compounds, *2-[(3-acetyl-2-oxo-2H-chromen-7-yl)oxy]-N-(3-fluorophenyl)acetamide* **9d** and *ethyl 7-[2-(morpholin-4-yl)-2-oxoethoxy]-2-oxo-2H-chromene-3-carboxylate* **10d** were selected for one dose analysis against 60 different cell lines. The growth inhibition (GI) was measured at the concentration of 10^{-5} M.[32] The relative growth was evaluated from no drug control from time zero number of cell, NCI allows detection of both growth inhibition (value between 0 to 100) to cell lethality (value below zero). Compound **9d** showed anticancer activity against melanoma cell-lines including LOX-IMVI, UACC-62 and UACC-257 causing 41.38%, 23.23% and 9.15% cell death at 10^{-5} M respectively. Whereas, showed no activity against ovarian cancer cell line and some cell lines of Breast cancer. Compound **10d** showed anticancer activity in prostate cancer cell line (DU145) with 34.74% cell death at 10^{-5} M, but remained inactive against leukemia cancer cell line.

DNA binding studies

Compounds **9b** and **9e** were selected for DNA-binding studies as they showed activity in nM concentration in MTT assay. For DNA binding UV based DNA titration and fluorescence emission study against DNA-EtBr complex were carried out as they provide more insight into mode of interaction of compounds with DNA.[21,33–34] UV absorption titrations for compounds **9b** and **9e** were performed with tris-HCl buffer (pH 7.2). The fixed concentration of compounds **9b** and **9e** were titrated against the known concentration of CT-DNA solution. Both the compounds showed good hypochromism shift (Figure 2**a**-**2b**). The strength of binding to CT-DNA was determined through the calculation of intrinsic binding constant K_b which is obtained by monitoring the changes in the absorbance of the compounds with increasing concentration of CT-DNA. Plot of [DNA]/ $(\varepsilon_A-\varepsilon_f)$ *versus* [DNA] (equation 1) is used to find out K_b.

$$[DNA]/(\varepsilon_A-\varepsilon_f) = [DNA]/(\varepsilon_b-\varepsilon_f) + 1/K_b(\varepsilon_b-\varepsilon_f) \quad (1)$$

Where [DNA] is the concentration of DNA, $\varepsilon_A = A_{observed}/[compound]$, ε_f is the extinction coefficient for unbound compound and ε_b is the extinction coefficient for the compound in the fully bound form. In plot of [DNA]/ $(\varepsilon_A-\varepsilon_f)$ *versus* [DNA], slope is equal to $1/(\varepsilon_b-\varepsilon_f)$ and Y-intercept is equal to $1/K_b$ $(\varepsilon_b-\varepsilon_f)$. K_b is obtained from the ratio of slope to the Y-intercept (Figure 2**c**-**2d**).

Compounds **9b** and **9e** showed the hypocromism shift with the intrinsic binding values 2.64 x 10^4 and 8.29 x 10^5 M^{-1} respectively in UV based DNA titrations which are indicative of DNA intercalative mode of binding (Table 2). To further confirm the mode of interaction of compounds **9b** and **9e** with DNA, fluorescence emmission based Ethidium bromide (EtBr) displacement assay was carried out. The emission spectra of DNA-EtBr (λ_{ex} = 546 nm) in the absence and presence of increasing amount of compounds were recorded (Figure 3**a**-**3b**). The data were plotted according to the Stern-Volmer equation (equation 2) were I_0 and I are the flurosence intensities in the absence and presence of compound.

$$I_0/I = 1 + K_{SV}[Q] \quad (2)$$

Ksv is the Stern-Volmer quenching constant which can be obtained from the slope of straight line in plot of I_0/I *versus* [Q]. Quenching of fluoroscence intensity was observed for compounds **9b** and **9e** with Ksv 4.69 x 10^3 and 4.23 x 10^3 M^{-1} respectively which supports the DNA intercalating property of these compounds (Table 2, Figure 3**c**-**3d**).

Antioxidant activity

The drug which showed good anticancer activity have poor antioxidant activity which give emphasis that the anticancer activity was may be due to reactive oxygen species.[35] Antioxidant activity of these entire synthesized compounds was screened by DPPH assay. Compounds which showed very good anticancer activity were found to be poor for antioxidant activity. Compounds **9a**-**9b** showed very poor antioxidant activity as compared to ascorbic acid (Table 3). Compounds **9d** and **9e** showed moderate anti-oxidant activity with EC_{50} 48 μg/mL and 59 μg/mL respectively. Interestingly, 3-carboxylate coumarin compounds **10b** and **10c** showed good antioxidant activity with EC_{50} 46 and 47 μg/mL respectively. Compounds **9d**-**9e** and **10b**-**10c** showed scavenging activity similar to ascorbic acid at 100 μM concentration. Compounds **9c**, **9f**, **9g**, **10a** and **10d** remained inactive as antioxidant agent in DPPH assay.

Conclusion

Our interest in synthesis of new 3,7-disubstituted coumarin derivatives is to develop more potent anticancer or antioxidant agents. All the newly synthesized compounds were obtained in good yields and characterized by spectral technique. Compounds **9a**-**9c**, **9g** and **10b** showed better anticancer activity

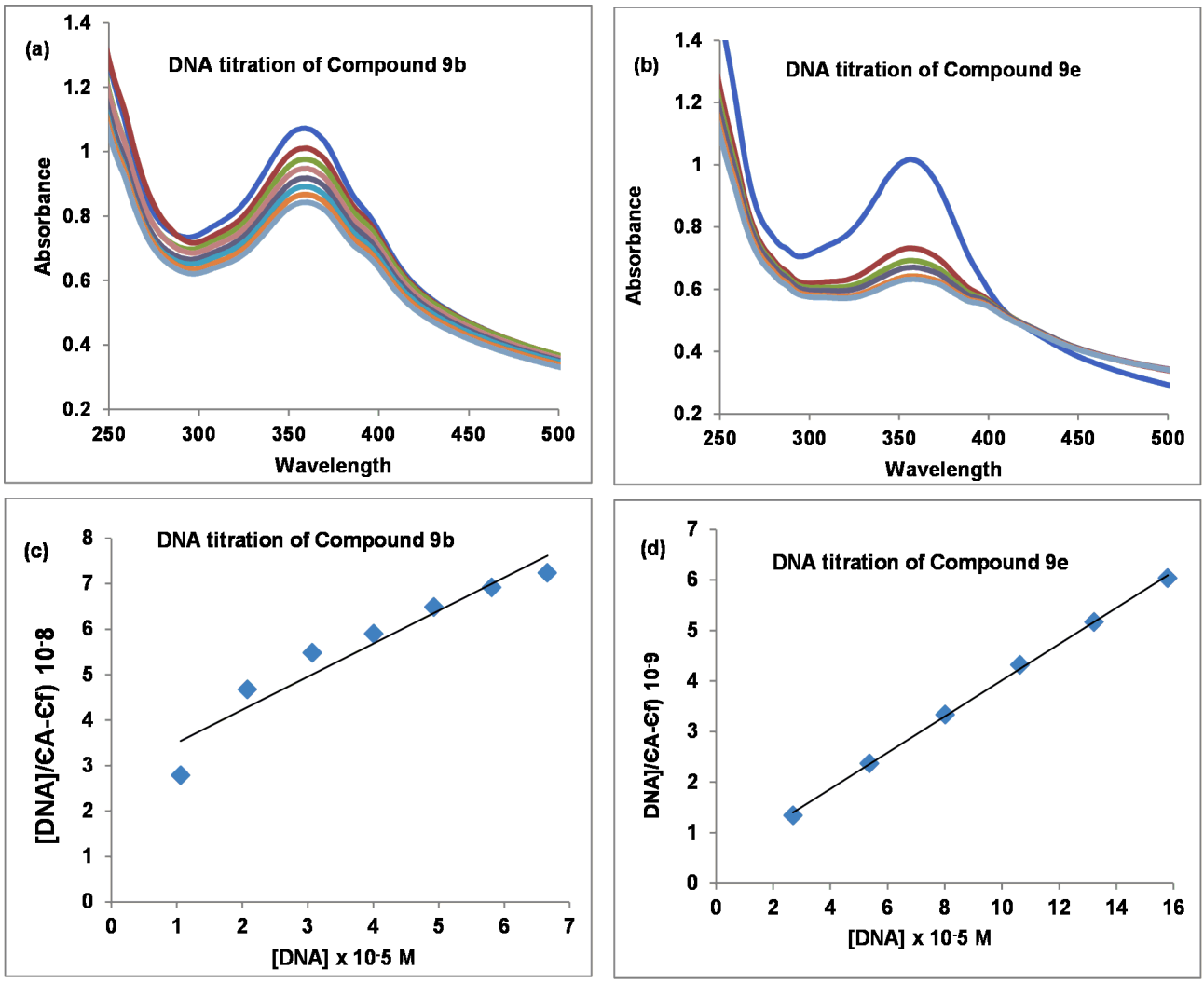

Figure 2. Titration plot of compounds **9b** and **9e** with DNA. Plot of Absorbance *versus* Wavelength (nm) for (a) compound **9b** and (b) compound **9e.** Plot of [DNA]/(ε_A-ε_f) versus [DNA] for (c) compound **9b** and (d) compound **9e.**

in A549 (Lungs cancer) cell line, while compounds **9a–g** and **10a–d** showed better activity in MCF7 (Breast cancer) cell line compared to that of 5-Fluorouracil.

Compounds **9b** and **9e** are showing excellent anticancer activity at very low concentration as compared to 5-Fluorouracil, well falling in nanomolar range. Both compounds **9b** and **9e** are exhibiting interaction with DNA through intercalation. The DNA interaction of compound **9e** is very good with intrinsic binding constant 8.29 x 10^5 M^{-1} compared to that of compound **9b** 2.64 x 10^4 M^{-1} in UV based DNA titration. Both compounds are showing good interaction with DNA by displacement of EtBr in DNA-EtBr complex by quenching its fluorescence. Further analysis is going on to confirm this finding that most of these derivatives also causing apoptosis in cancer cell line *via* p53 mediated induction of reactive oxygen species.

As per our target, structural modification of compound **3** was done to achieve more potent anticancer agent that has resulted in compound **9b** with excellent anticancer activity against A549 cell line with IC_{50} 0.16 nM. Thus strategy of modification of coumarin on 3rd position resulted in finding more active compound. Further work on identification of mechanism of anticancer activity is in progress.

Acknowledgement

One of the authors (RS) is thankful to Department of Science & Technology, Government of India for financial support vide reference no. SR/WOS–A/CS-1028/2014 under Women Scientist Scheme to carry out this work. One of the authors (SU) is thankful to UGC, Government of India for UGC-JRF vide reference no. 22/06/2014(i)EU–V. Authors are thankful to The Head, Department of Chemistry and Department of Zoology, Faculty of Science, The M. S. University of Baroda for providing laboratory facilities and also thankful to DST-PURSE programme for X-ray single crystal analysis, Zydus Research Centre, Ahmedabad, for the ESI-MS analyses.

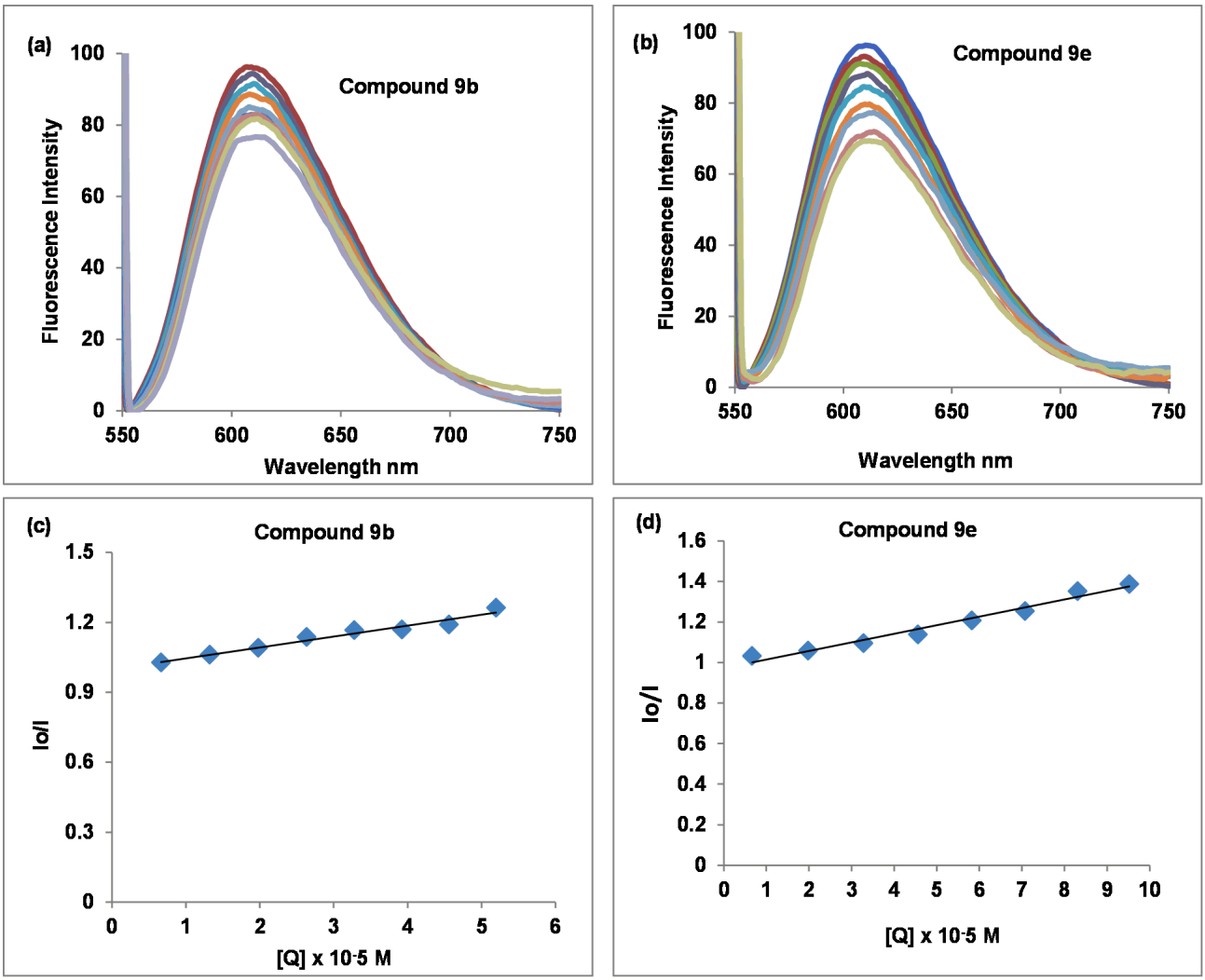

Figure 3. Plot of Fluorescence emission intensity I *versus* Wavelength (nm) for DNA-EtBr complex at different concentrations of (a) compound **9b** and (b) compound **9e.** Stem-Volmer quenching plot of DNA-EtBr for (c) compound **9b** and (d) compound **9e.**.

Conflict of Interest

The authors declare no conflict of interest.

Keywords: Anticancer · DNA Binding · Ethyl 7-substituted-3-carboxylate-benzopyrone · 7-Substituted-3-acetyl-benzopyrone

[1] Cancer fact sheet No-297, World Health Organisation (2015) Feb **2015.**
[2] M. Mareel, A. Leroy, *Physiol. Rev.* **2003**, *83*, 337–376.
[3] J. Wesche, K. Haglund, E. M. Haugsten, *Biochem. J.* **2011**, *437*, 199–213.
[4] S. K. Grant, *Cell. Mol. Life Sci.* **2009**, *66*, 1163–1177.
[5] G. I. Solyanik, *Exp. Oncol.* **2011**, *32*, 181–185.
[6] S. Vijayaraghavalu, C. Peetla, S. Lu, V. Labhasetwar, *Mol. Pharm.* **2012**, *9*, 2730–2742.
[7] H.-Y. Hung, E. Ohkoshi, M. Goto, K. F. Bastow, K. Nakagawa-Goto, K.-H. Lee, *J. Med. Chem.* **2012**, *55*, 5413–5424.
[8] S. Riedl, D. Zweytick, K. Lohner, *Chem. Phys. Lipids* **2011**, *164*, 766–781
[9] Y. Bansal, P. Sethi, G. Bansal, *Med. Chem. Res.* **2013**, *22*, 3049–3060.
[10] K. C. Fylaktakidou, D. J. Hadjipavlou-Litina, K. E. Litinas, D. N. Nicolaides, *Curr Pharm. Des.* **2004**, *10*, 3813–3833.
[11] M. J. Matos, C. Terán, Y. Pérez-Castillo, E. Uriarte, L. Santana, D. Viña, *J. Med. Chem.* **2011**, *54*, 7127–7137.
[12] A. Beillerot, J.-C. R. Domínguez, G. Kirsch, D. Bagrel, *Bioorg. Med. Chem. Lett.* **2008**, *18*, 1102–1105.
[13] K. M. Amin, N. M. Abdel Gawad, D. E. Abdel Rahman, M. K. El Ashry, *Bioorg. Chem.* **2014**, *52*, 31–36.
[14] M. Jain, W. R. Surin, A. Misra, P. Prakash, V. Singh, V. Khanna, S. Kumar, H. H. Siddiqui, K. Raj, M. K. Barthwal, *Chem. Biol. Drug Des.* **2013**, *81*, 499–505.
[15] M. Curini, F. Epifano, F. Maltese, M. C. Marcotullio, S. P. Gonzales, J. C. Rodriguez, *Aust. J. Chem.* **2003**, *56*, 59–60.
[16] J. R. Hwu, R. Singha, S. C. Hong, Y. H. Chang, A. R. Das, I. Vliegen, E. De Clercq, J. Neyts, *Antiviral Res.* **2008**, *77*, 157–162.
[17] D. A. Ostrov, J. A. Hernandez Prada, P. E. Corsino, K. A. Finton, N. Le, T.C. Rowe, *Antimicrob. Agents Chemother.* **2007**, *51*, 3688–3698
[18] S. Emami, A. Foroumadi, M. A. Faramarzi, N. Samadi, *Arch. Pharm. Chem. Life Sci.* **2008** *341* 42–48.
[19] A. Manvar, A. Bavishi, A. Radadiya, J. Patel, V. Vora, N. Dodia, K. Rawal, A. Shah, *Bioorg. Med. Chem. Lett.* **2011**, *21* 4728–4731.
[20] B. Yuce, O. Danis, A. Ogan, G. Sener, M. Bulut, A. Yarat, *Arzneim.-Forsch Drug Res.* **2009**, *59*, 129–134.
[21] P. Bhattacharya, S. M. Mandal, A. Basak, *Eur. J. Org. Chem.* **2016**, 1439–1448.
[22] D. Conley, E. M. Marshall, *Proc. Am. Assoc. Cancer Res.* **1987**, *28*, 63.

[23] S. Emami, S. Dadashpour, *Eur. J. Med. Chem.* **2015**, *102*, 611–630.
[24] J. T. Konc, E. Hejchman, H. Kruszewska, I. Wolska, D. Maciejewsk, *Eur. J. Med. Chem.* **2011**, *46*, 2252–2263.
[25] A. H. Halawa, A. A. E. Hassan, M. A. El-Nassag, M. M. A. El-All, G. E. El-Jaleel, E. M. Eliwa, A. H. Bedair, *Eur. J. Chem.* **2014**, *5*, 111–121.
[26] V. Sosa, T. Moliné, R. Somoza, R. Paciucci, H. Kondoh, M. E. Lleonart, *Ageing Res Rev.* **2013**, *12*, 376-390.
[27] S. Afzal, S. Jensen, J. Sørensen, T. Henriksen, A. Weimann, H. Poulsen, *Cancer Chemother. Pharmacol.* **2012**, *69*, 301-307.
[28] J. Alexandre, Y. Hu, W. Lu, H. Pelicano, P. Huang, *Cancer Res.* **2007**, *67*, 3512-3517.
[29] R. R. Nazarewicz, W. J. Zenebe, A. Parihar, S. K. Larson, E. Alidema, J. Choi, P. Ghafourifar, *Cancer Res.* **2007**, *67*, 1282-1290.
[30] A. Thakur, R. Singla, V. Jaitak, *Eur. J. Med. Chem.* **2015**, *101*, 476–495.
[31] Y. J. Li, C. Y, Wang, M. Y. Ye, G. Y. Yao, H. S. Wang, *Molecules* **2015**, *20*, 14791–14809.
[32] For details: http://dtp.nci.nih.gov and https://wiki.nci.nih.gov/display/NCIDTPdata/NCI-60+Growth+Inhibition+Data.html
[33] S. S. Mandal, U. Varshney, S. Bhattacharya, *Bioconjugate Chem.* **1997**, *8*, 798–812.
[34] C. V. Kumar, E. H. Asunsion, *J. Am. Chem. Soc.* **1993**, *115*, 8547–8553
[35] D. Dreher, A. F. Junod, *Eur. J. Cancer* **1996**, *32,* 30-38.

Submitted: September 20, 2016
Accepted: December 14, 2016

Received: 21 November 2017 | Revised: 15 February 2018 | Accepted: 21 February 2018

DOI: 10.1111/cbdd.13189

RESEARCH ARTICLE

WILEY

3-Aminomethyl pyridine chalcone derivatives: Design, synthesis, DNA binding and cytotoxic studies

Sunil Dutt Durgapal[1] | **Rina Soni**[1] | **Shweta Umar**[2] | **Balakrishnan Suresh**[2] | **Shubhangi S. Soman**[1]

[1]Department of Chemistry, Faculty of Science, The M. S. University of Baroda, Vadodara, India

[2]Department of Zoology, Faculty of Science, The M. S. University of Baroda, Vadodara, India

Correspondence
Shubhangi S. Soman, Department of Chemistry, Faculty of Science, The M. S. University of Baroda, Vadodara, India.
Email: shubhangiss@rediffmail.com

Herein we report design, synthesis, and anticancer activity of compounds **6a–h** and **11a–j**. Compounds **6a–f** were designed based on 3-aminomethyl pyridine attached to different acetamide derivatives and in compounds **6g–h** it was attached to coumarin moiety. Coumarin containing compounds **6g–h** showed very poor anticancer activity against both A549 (Lungs cancer cell line), and MCF-7 (Breast cancer cell line) cell lines in MTT assay. Compounds **11a–j** were designed as derivatives of 3-aminomethyl pyridine and 4-amino chalcones. A series of chalcone derivatives of 3-aminomethyl pyridine **11a–j** have been synthesized and screened for their in vitro anticancer activity and DNA binding affinity. Most of the compounds showed very good antimitotic activity against A549 cell line as compared to fluorouracil. Compounds **11g** and **11i** were selected for DNA-binding studies as they showed excellent activity against cancer cell lines in MTT assay. CT-DNA binding affinity of compounds **11g** and **11i** have been investigated by UV based DNA titration and fluorescence emission study against DNA-EtBr complex. Interestingly, compound **11i** has displayed excellent antiproliferative activity, with IC_{50} 0.0067 ± 0.0002 μM, against MCF-7 cell line. Compound **11i** has been studied for its cytotoxicity using MTT, LDH, as well as EtBr/AO assay and was found to induce apoptosis in the cancerous cell line.

KEYWORDS
aminomethyl pyridine, anticancer activity, chalcone derivatives, cytotoxic studies, DNA binding

1 | INTRODUCTION

Cancer is second leading cause of death worldwide. According to WHO report, the increase in number of new cases is expected to rise by 70% over next two decades.[1] Cancer progresses via multistep carcinogenesis, which involves various physiological processes of human body like uncontrolled growth of cells due to deregulation of essential enzymes, cell signaling, and apoptosis. Cancer is extremely complicated to combat.[2]The root cause was found out to be pattern of lifestyle adopted such as excessive use of tobacco, physical inactivity, and improper diet.[3] The increase in cancer incidence proves that even today it is not curable with the available therapy and medication. The major downsides of current therapy available to treat cancer include side-effects, lack of tumor specificity and multidrug resistance. Hence, there is a need of potent anticancer agents to overcome this hurdle. One of the important aspects in anticancer agent is designing of small molecules targeting DNA. The interaction of small molecule with DNA depends not only on ability of molecule to DNA recognition but also on type of interactions such as electrostatic, intercalation, and groove binding.[4,5]

α,β-Unsaturated ketones, commonly known as chalcones are important class of natural as well as synthetic products which show variety of biological activities. During last few

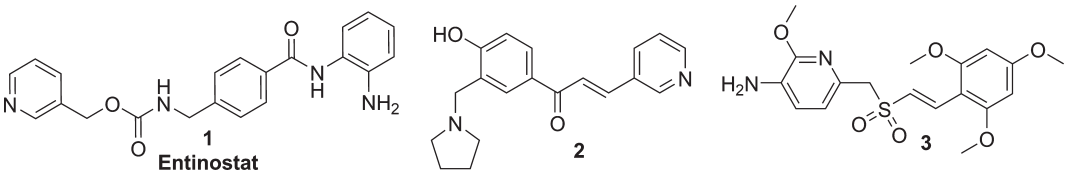

FIGURE 1 Compounds with anticancer activity

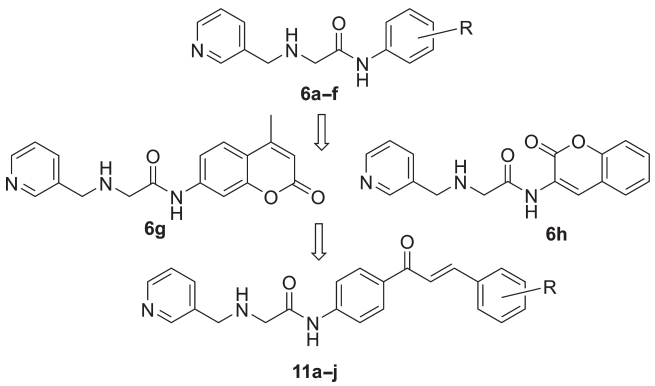

FIGURE 2 Designing of hybrid chalcone **11a–j** derived from 3-aminomethyl pyridine and 4-amino chalcones

decades, chalcone derivatives have been reported having potent anticancer activity with low side-effects and better solubility for therapeutic applications.[6,7] Simple structural modification in chalcone moiety with heterocycles, polyarene compounds, or organometal complexes may lead to new anticancer agents with promising activity.[8,9] Chalcone based small molecules provide advantage over other due to their low toxicity and mutagenicity profile. Yu et al. showed that 4-(dimethylamino)-4-amino chalcone can interact into base pair and created a new method to determine trace amount of DNA.[10]

Ifnterestingly, pyridine derivatives have shown very good effect on anticancer activity when substituted at 3rd position as in Entinostat **1** (MS-275), which is in phase II clinical trials for treatment of various types of cancers (Figure 1).[11] Inci Gul et al. have reported compound **2** as tumor selective cytotoxin containing both chalcone and pyridine moieties in a molecule.[12] Recently, Wang et al. have reported pyridine containing compound **3** with very good antitumor activity against xenograft A2780 ovarian cancer.[13]

As a part of our ongoing research on anticancer agents,[14,15] herein we report design, synthesis and anticancer activity of compounds **6a–h** and **11a–j**. compounds **6a–f** were designed based on 3-aminomethyl pyridine attached to different acetamide derivatives and in compounds **6g–h** it was attached to coumarin moiety (Figure 2). Compounds **11a–j** were designed as derivatives of 3-aminomethyl pyridine and 4-amino chalcones.

2 | EXPERIMENTAL

2.1 | Chemistry

Reagent grade chemicals and solvents were purchased from commercial supplier and used after purification. TLC was performed on silica gel F254 plates (Merck). Acme's silica gel (60–120 mesh) was used for column chromatographic purification. All reactions were carried out in nitrogen atmosphere. Melting points are uncorrected and were measured in open capillary tubes, using a Rolex melting point apparatus. IR spectra were recorded as KBr pellets on Perkin Elmer RX 1 spectrometer. ^{1}H NMR and ^{13}C NMR spectral data were recorded on Advance Bruker 400 spectrometer (400 MHz) with $CDCl_3$ or DMSO-d_6 as solvent and TMS as internal standard. *J* values are in Hz. Mass spectra were determined by ESI-MS, Mass spectra were determined by ESI–MS, using a Shimadzu LCMS 2020 apparatus (Shimadzu Scientific Instruments, Inc., USA). Elemental analyses were recorded on Thermo Finnigan Flash 11-12 series EA. All reactions were carried out under nitrogen atmosphere. 7-amino-4-methyl coumarin, 3-amino coumarin and chalcones were prepared as reported in literature.[16–18]

2.1.1 | Preparation of N-substituted bromoacetamide derivatives (5, 10)

To an ice-cold solution of substituted amines (10.0 mmol) in dichloromethane (DCM) (25 ml) was added triethylamine (TEA) (15.0 mmol) and stirred for 5–10 min. To this bromoacetyl bromide (12.0 mmol) was added dropwise over a period of 10 min under cooling. The resulting solution was stirred at 0–5°C for 30 min and at room temperature for 24 hr. The reaction mixture was diluted with water and extracted with DCM (2 × 30 ml). The organic layers were combined, washed with 0.5 N HCl solution (15 ml), dried over anhydrous Na_2SO_4, filtered and evaporated on a rotavapor to give compounds **5** and **10**. The substituted bromoacetamide **5** and **10** were directly used for next step without any purification

2.1.2 | General procedure for the preparation of compounds 6a–h and 11a–j

To a cold solution of substituted bromoacetamide **5/10** (1.0 eq) in DMF (20 ml) was added of 3-aminomethyl pyridine **4**

(0.5 g, 1.730 mmol) along with base triethylamine (1.5 eq) and stirred for 30 min. The resulting mixture was stirred at room temperature for 14-16 hr. The completion of reaction was checked by TLC using DCM:MeOH (9:1). The reaction mixture was poured into ice-cold water. The aqueous layer was extracted using ethyl acetate or dichoromethane (3 × 25 ml). The organic layers were combined, dried over anhy. Na_2SO_4, filtered and concentrated on a rotavapor to give crude product. The crude compound was purified by column chromatography using DCM:MeOH (95:5).

For compounds **6a–f**: To a cold solution of compounds **6a–f** in methanol (15 ml) was added 2 M HCl in methanol (1.2 eq). The resulting solution was stirred at 0–5°C for 30 min and concentrated on a rotavapor to give solid. The solid was triturated in diethyl ether, filtered and dried to give compounds **6a–f**.

For compounds **6g–h** and **11a–j**: Compounds **6g–h** and **11a–j** were obtained as a solid after column purification. All characterization data for synthesized compounds are provided in supporting information.

2.2 | Materials and methods for biological assays

2.2.1 | Reagent and cell culture

MTT, LDH assay kit (Pierce LDH Cytotoxicity Assay), *N*,*N*-dimethylformamide (DMF), EtBr and Acridine Orange, were purchased from Sigma-Aldrich, India. DMEM, Fetal Bovine Serum (FBS) and trypsin were sourced from (Gibco USA). Human lung carcinoma cell line A549 and human breast cancer cell line MCF-7 were purchased from NCCS, Pune, India. Cell line was maintained in Dulbecco's modified eagles medium (DMEM) supplemented with 2 mM l-glutamine and 10% fetal bovine serum (GIBCO, USA). Penicillin and streptomycin (100 IU/100 g) were adjusted to 1 ml/L. The cells were maintained at 37°C with 5% CO_2 in a humidified CO_2 incubator.

Stock solutions of derivatives were prepared in DMF and were diluted with PBS (Phosphate-buffered saline) to achieve working concentration. However, care was taken to maintain the final concentration of DMF not exceed more than 0.5% in any case.

2.2.2 | MTT assay

The half minimal inhibitory concentration was evaluated using MTT [3-(4,5-dimethylthiazol-2-yl)-2,5-diphenyltetrazolium bromide] assay as per standard protocol. Cells were plated in a 96-well plate (1×10^4 cells/well) and incubated overnight in 100 µl DMEM media supplemented with 10% FBS. Each compound was added in 0.5, 1, 10, 25, 50, 75, 100 µM conc. and incubated further for 48 hr. 20 µl of MTT solution (5 mg/ml in PBS) was added and further plate was incubated for 4 hr. Supernatant solution was removed and the blue formazan was dissolved in 100 µl of acidified isopropanol. The absorbance was measured using microplate reader at 570 nm (Metertech ∑960).

Cell viability (%) = (average absorbance of treated groups/average absorbance of control group) × 100%. IC_{50} values were calculated using GRAPHPAD PRISM. Each experiment was performed in triplicates.

2.2.3 | UV-Based Assay

PerkinElmer Lambda- 35 dual beam UV–Vis spectrophotometer was used for absorption spectral studies. Solution of calf thymus DNA (CT DNA) was prepared in water. The UV absorbance at 260 was found to 0.277 which is used to calculate the DNA concentrations ($\varepsilon = 6{,}600\ M^{-1}$) and was expressed in terms of base molarity. UV absorption titrations were carried out by keeping the concentration of compounds **11g** and **11i** (dissolved in DMSO) fixed and by adding a known concentration of CT DNA solution in both the cuvettes in increasing amount until hypochromism saturation was observed. Absorbance values were recorded after each successive addition of DNA solution and equilibration.

2.2.4 | Ethidium bromide displacement assay

DNA (100 µl, 8.4×10^{-4} M), EtBr (100 µl, 4.2×10^{-4} M), and Tris-HCl buffer pH 7.2 was used to make a total volume of 3 ml EtBr displacement fluorescence assay was employed to find DNA intercalation. Fluoroscence emission spectra ($\lambda_{max} = 600$ nm, excitation wavelength 546 nm, slit width 10 nm, 1 cm path length) were obtained at 30°C on a JASCO FP-6300 fluorescence spectrophotometer. The assays were performed by using different concentrations of compounds **11g** and **11i** in buffer solution (3 ml). I_0/I are plotted along with y axis against the concentration of compound, where in I and I_0 are the fluorescence intensities of the DNA-EtBr complex in the presence of and in the absence of compounds, respectively.

2.2.5 | Trypan blue

5×10^5 cells per well were seeded in 12 well plate and kept overnight for attachment. Next day cells were treated with IC_{50} conc. of compound **11i**, DMF and TritonX-100 and were incubated for 48 hr. DMF treated cells were taken as vehicle control and TritonX-100 as positive control. Following incubation, the supernatant pool was collected and adherent cells were trypsinized and collected. Cell viability was performed by the dye exclusion test with 0.5% trypan blue using a hemocytometer. Each experiment was performed in triplicates.

2.2.6 | LDH assay

Lactate dehydrogenase enzyme remains in cytoplasm, however during necrosis due to plasma membrane damage it leaches out. Cells were plated on 96 well plate (1×10^4 cells/well) for 24 hr in DMEM media without phenol red, then derivatives were added in the 0.5, 1, 10, 25, 50, 75, 100 μM concentration range. Subsequently, they were incubated for 48 h. Assay was performed according to the manufacture's instruction (Pierce LDH Cytotoxicity Assay, Thermo Scientific, USA). Absorbance was measured at 490 nm in a microplate reader and percentage cytotoxicity was calculated.

2.2.7 | Ethidium bromide/acridine orange staining assay

Morphological changes due to apoptosis and necrosis were visualized using EtBr/AO staining technique.[19] Cells were treated with IC_{50} concentration of compound **11i**. For positive control cell were treated with Triton-X 100 and incubated for 48 hr. Cells were washed with PBS and stained with 1 μl of 1:1 ratio of EtBr and AO (100 μg/ml). Cell to stain ratio was maintained as 1:25 μl. 10 μl of cell suspension was placed on microscopic slide and images were taken using Leica DM 2500 fluorescence microscope fitted with Leica EZ camera.

3 | RESULTS AND DISCUSSION

3.1 | Chemistry

Compounds **6a–h** were synthesized by reaction of bromoacetamide derivative **5** with 3-aminomethyl pyridine **4** (Scheme 1). Amino derivatives were reacted with bromoacetyl bromide to give bromoacetamide derivative **5**, which on reaction with 3-aminomethyl pyridine **4** using triethylamine in anhydrous *N*,*N*-dimethylformamide gave derivatives **6a–h** as shown in Scheme 1.

Compounds **6a**–**f** were isolated in the form of hydrochloride salts. The structures of compounds **6a–f** were confirmed by different analytical techniques such as ^{1}H-NMR, ^{13}C-NMR, IR, ESI-MS. In general, the IR spectra of compounds

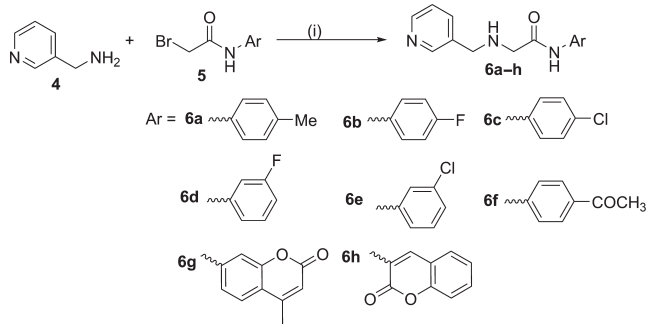

SCHEME 1 Synthesis of compound **6a–h**. Reagents and Conditions: (i) TEA, DMF, 0–5°C, 30 min, r.t 14–16 hr

6a–f exhibited three strong bands in the range of 3,421–3,383 cm^{-1}, 3,255–3,213 cm^{-1} and 3,200–3,176 cm^{-1} for secondary amine salt and N–H stretching respectively. Carbonyl stretching of amide was observed in the range of 1,691–1,670 cm^{-1}. In the ^{1}H NMR spectra of **6a–f**, peak for methylene next to amide group was observed in range of δ ~3.94 to 4.02 while methylene next to pyridine was observed in range of δ ~4.26 to 4.46, aromatic protons were observed in range of 6.92–9.67 depending on effect of different substituents on aromatic ring. For compounds **6a–f**, –NH protons of secondary amine salts were observed as broad singlet in range of 9.82–10.09 ppm, while amide -NH proton was observed in range of 10.75–11.30 ppm. In the ^{13}C NMR spectra of **6a–f**, peak for methylene carbons observed around 46.96–47.95 and 48.10–48.37 ppm, aromatic carbons in range of 106–161 ppm, amide carbonyl carbon in range of 164–165 ppm.

All compounds **6a–f** were analyzed by ESI-MS analyses to give $[M + H]^+/[M + Na]^+$ peak corresponding to their molecular weight. As modification in compounds **6a–f**, 3-aminomethyl pyridine was attached to comuarin moiety at 7th and 3rd position in compounds **6g** and **6h** respectively. Both compounds **6g** and **6h** were also fully characterized by ^{1}H-NMR, ^{13}C-NMR, IR and ESI-MS analysis and all data complies for formation of desired product.

As a structural modification of compounds **6g–h**, 3-aminomethyl pyridine was linked to 4-amino chalcone derivatives to study the effect of chalcone on activity profile. Compounds **11a–j** were synthesized by reaction of bromoacetamide derivative **10** with 3-aminomethyl pyridine **4** (Scheme 2). 4-Aminoacetophenone **7** on reaction with aldehyde **8** under basic conditions gave 4-amino chalcone derivatives **9** as shown in Scheme 2. 4-Amino chalcone **9** on reaction with bromoacetyl bromide gave **10**, which on reaction with 3-aminomethyl pyridine gave various derivatives **11a–j** (Scheme 2).

The structures of compounds **11a–j** were confirmed by different analytical techniques such as ^{1}H-NMR, ^{13}C-NMR, IR, ESI-MS. In general, the IR spectra of compounds **11a–j** exhibited two strong bands in the range of 3,333–3,236 cm^{-1} and 3,290–3,169 cm^{-1} for secondary amine and amide N–H stretching vibrations respectively. Carbonyl group of chalcone exhibited stretching frequency in range of 1693-1685 cm^{-1} and that of amide carbonyl in range of 1,658–1,649 cm^{-1}. In the ^{1}H NMR spectra of **11a–j**, peak for methylene next to amide group was observed in the range of δ ~3.34-4.13 while methylene next to pyridine was observed in range of δ ~3.78-4.50, aromatic protons and chalcone protons observed in range of 6.93–9.11 depending on effect of different substituents on aldehyde. For compounds **11a–j** –NH protons are observed between δ 9.42–11.49 ppm.

In the ^{13}C NMR spectra of **11a–j**, two peak for methylene carbons observed around 46.37–51.51 and 48.03–52.50 ppm, aromatic carbons between δ 113–161 ppm, amide carbonyl

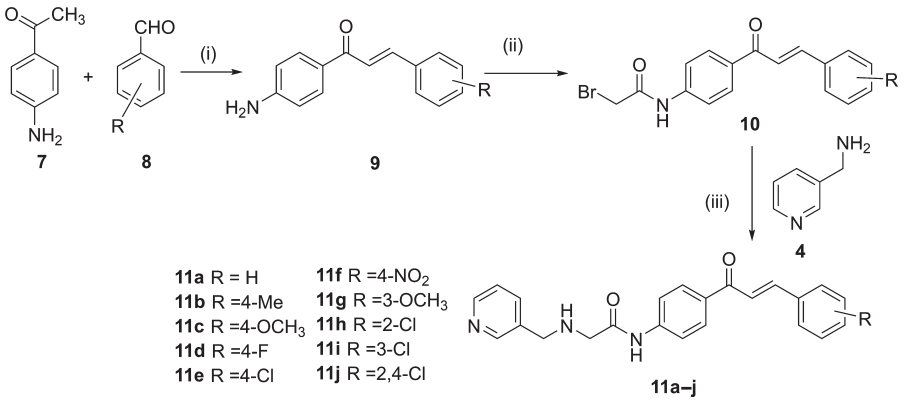

SCHEME 2 Synthesis of compound **11a–j**. Reagents and Conditions: (i) 40% aq NaOH, ethanol, r.t 5–10 hr; (ii) bromoacetyl bromide, TEA, DCM, r.t, 16–18 hr; (iii) TEA, DMF, 0–5°C, 30 min, r.t 14–16 hr

carbon around δ 164–171 ppm, chalcone carbonyl carbon between δ 187–189 ppm. All compounds **11a–j** were analyzed by ESI-MS analysis to give $[M + H]^+$/$[M + Na]^+$ peak corresponding to their molecular weight. All these new chemical entities were subjected to in-vitro studies for anticancer activity by MTT assay method.

3.2 | Biological activity

3.2.1 | MTT assay

Since the 70%–80% of total cancer diagnosed all over world are breast cancer and lung cancer, we have selected representative MCF7 and A549 cell lines for our study. 3-Aminomethyl pyridine derivatives **6a–h** were screened for their anticancer activity against A549 (Lungs cancer cell line), and MCF-7 (Breast cancer cell line) cell lines using MTT assay and compared the results with that of standard drug Fluorouracil (Table 1).[20]

TABLE 1 Anticancer activity against A549 (Lungs cancer cell line), MCF-7 (Breast cancer cell line) for compounds **6a–h**

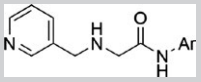

Compound no.	Ar	IC_{50} in μM[a]	
		A549	MCF-7
6a	4-MeC_6H_4	NA	NA
6b	4-FC_6H_4	1.186 ± 0.024	NA
6c	4-ClC_6H_4	0.213 ± 0.0031	950 ± 11.87
6d	3-FC_6H_4	NA	NA
6e	3-ClC_6H_4	NA	NA
6f	4-AcC_6H_4	32.63 ± 2.1	90.78 ± 6.24
6g	4-Me-coumarin-7-yl	177.10 ± 18.2	377.8 ± 29.32
6h	Coumarin-3-yl	69.1 ± 8.2	298.9 ± 21.2
Fluorouracil	11.13 ± 0.083	45.04 ± 1.02	

NA = Not active.

[a]IC_{50} values were determined based on MTT assay using GRAPHPAD PRISM software.

Compound **6a** with 4-methyl group found to be inactive against both the tested cell lines. Replacement of 4-methyl to 4-fluoro in compound **6b**, resulted in very good activity against A549 cell lines with IC_{50} 1.186 ± 0.024 μM, but remained inactive against MCF-7 cell line. Similar trend of activity was observed for compound **6c** with 4-chloro group with IC_{50} 0.213 ± 0.0031 μM against A549 cell lines. Interestingly, change in position of halogen from 4th to 3rd position in compounds **6d–e**, resulted in loss of anticancer activity. Compound **6f** with 4-$COCH_3$ group showed moderate activity against tested cell lines. However, coumarin containing compounds **6g–h** showed very poor anticancer activity against both cell lines.

3-Aminomethyl pyridine linked to 4-amino chalcones showed very good activity profile for anticancer activity in MTT assay against tested cell lines. Compounds **11a–b** and **11g–j** showed moderately good activity against MCF-7 cell line as compared to A549 cell line. Compound **11a** showed very good activity against A549 cell line with IC_{50} 6.18 ± 0.11 μM. On placing methyl group at 4th position on chalcone moiety in compound **11b** resulted in loss of activity against tested cell lines. Compound **11c** with methoxy group on 4th position showed very good activity against A549 cell line with IC_{50} 0.269 ± 0.0089 μM, however remained inactive against MCF-7 cell line. On replacement of methoxy group of compound **11c** by nitro group for compound **11f**, showed loss of activity against A549 cell line, while remained inactive against MCF-7 cell line. Compound **11e** having chloro at 4th position, showed very good activity with IC_{50} 5.14 ± 1.07 μM against A549 cell line. Further position change in methoxy group from 4th position in compound **11c** to 3rd position in compound **11g**, resulted in decrease in activity against A549 cell line, however this variation showed excellent activity against MCF-7 cell line with IC_{50} 0.174 ± 0.0076 μM.

On replacement of chloro from 4th to 2nd position in compound **11h** showed loss of activity against both tested cell lines. Interestingly, compound **11i** with chloro on 3rd position showed very good activity against A549 cell line and excellent activity against MCF-7 cell line. Furthermore, compound **11j** containing 2,4-dichloro showed moderate activity against tested cell lines.

Of all screened compounds **6a–h** (Table 1) and **11a–j** (Table 2), compounds **11g** and **11i** showed excellent activity with IC_{50} 0.174 ± 0.0076 μM and 0.0067 ± 0.0002 μM, respectively, as compared to standard drug Fluorouracil against MCF-7 cell line in MTT assay. Hence Compounds **11g** and **11i** were selected to study their DNA binding studies.

3.2.2 | DNA binding studies

Compounds **11g** and **11i** were selected for DNA-binding studies as they showed excellent activity against cancer cell lines in MTT assay. To explore mode of interaction of compounds **11g** and **11i** with DNA in cell, DNA binding UV based DNA titration and fluorescence emission study against DNA-EtBr complex were carried out.[21] UV based DNA binding studies gave information for possible interaction taking place between DNA and the lead compounds, while fluorescence based assay, i.e., EtBr displacement assay gave mode of interaction of our lead compounds is through intercalation.

The fixed concentration of compounds **11g** and **11i** was titrated against the known concentration of CT-DNA solution with Tris-HCl buffer (pH 7.2; Figure 3). The strength of binding to CT-DNA was determined through the calculation of intrinsic binding constant K_b which is obtained by monitoring the changes in the absorbance of the compounds with increasing concentration of CT-DNA. Plot of [DNA]/ ($\varepsilon_A - \varepsilon_f$) versus [DNA] (Equation 1) is used to find out K_b. Compound **11g** and **11i** showed the hypochromic shift with the intrinsic binding (k_b) values $2.12 \times 10^4\ M^{-1}$ and $1.06 \times 10^4\ M^{-1}$, respectively in UV based DNA titrations indicated intercalative mode of binding (λ_{max} = 325 nm; Figure 3, Table 3).

$$[DNA] / (\varepsilon_A - \varepsilon_f) = [DNA] / (\varepsilon_b - \varepsilon_f) + 1/K_b (\varepsilon_A - \varepsilon_f) \quad (1)$$

Fluorescence emmission based Ethidium bromide (EtBr) displacement assay was also performed with compound **11g** and **11i**. The emission spectra of DNA-EtBr (λ_{ex} = 546 nm) in the absence and presence of increasing amount of compound **11g** and **11i** were recorded at emission λ_{max} 608 nm (Figure 4). The data were plotted according to the Stern-Volmer equation (Equation 2). Quenching of fluoroscence intensity was observed for compound **11g** and **11i** with K_{sv} values $5.21 \times 10^3\ M^{-1}$ and $5.85 \times 10^3\ M^{-1}$ respectively (Table 3), which supports the DNA intercalating property of these compounds (Figure 4).

$$I_0/I = 1 + K_{SV}[Q] \quad (2)$$

3.2.3 | Cytotoxic studies

Compound **11i** induced cytotoxic studies in A549, MCF-7 cancer cell lines and NIH/3T3 noncancer cell line were performed. The cytotoxicity of compound **11i** was estimated using MTT assay and IC_{50} conc. of compound **11i** was measured in both the cancer cell line as well as in noncancer cell line. Mechanism of cytotoxicity was evaluated by Trypan blue and LDH assay in cancer cell lines. LDH assay is based on the release of cytosolic enzyme into culture medium due to the damage of cell membrane which is a hallmark of necrosis, while MTT assay is based on the activity of mitochondrial dehydrogenase enzyme activity and represent the metabolic rate or percentage viability of cell.[22–24]

In MTT assay, the percentage viability of cell line was decreased with increased concentration of compound **11i**. IC_{50} concentration of compound **11i** was estimated using GRAPHPAD

TABLE 2 Anticancer activity against A549 (Lungs cancer cell line), MCF-7 (Breast cancer cell line) compounds **11a–j**

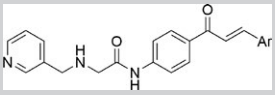

Compound no.	Ar	IC_{50} in μM[a] A549	MCF-7
11a	C_6H_5	6.18 ± 0.11	53.27 ± 3.56
11b	4-MeC_6H_4	132.00 ± 9.86	90.61 ± 5.96
11c	4-$OMeC_6H_4$	0.269 ± 0.0089	n/a
11d	4-FC_6H_4	16.04 ± 3.43	n/a
11e	4-ClC_6H_4	5.14 ± 1.07	n/a
11f	4-$NO_2C_6H_4$	28.19 ± 1.19	n/a
11g	3-$OMeC_6H_4$	32.42 ± 2.08	0.174 ± 0.0076
11h	2-ClC_6H_4	46.89 ± 6.08	71.72 ± 5.32
11i	3-ClC_6H_4	0.245 ± 0.011	0.0067 ± 0.0002
11j	2,4-$Cl_2C_6H_3$	62.26 ± 5.9	92.21 ± 7.21
Fluorouracil		11.13 ± 0.083	45.04 ± 1.02

NA = Not active.

[a]IC_{50} values were were determined based on MTT assay using GRAPHPAD PRISM software.

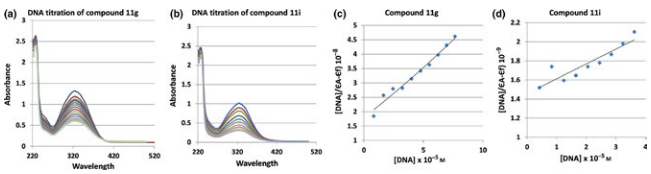

FIGURE 3 Titration plot of compounds **11g** and **11i** with DNA. Plot of Absorbance versus Wavelength (nm) (a) for compound **11g** and (b) compound **11i**. Plot of [DNA]/($\varepsilon_A - \varepsilon_f$) versus [DNA] (c) for compound **11g** and (d).for compound **11i** [Colour figure can be viewed at wileyonlinelibrary.com]

TABLE 3 K_b and K_{SV} values for compound **11g** and **11i**

Compound no.	λ_{max} nm	UV based assay K_b (M^{-1})	Emission λ_{max} nm	Fluorescence assay K_{SV} (M^{-1})
11g	325	2.12×10^4	610	5.21×10^3
11i	325	1.06×10^4	608	5.85×10^3

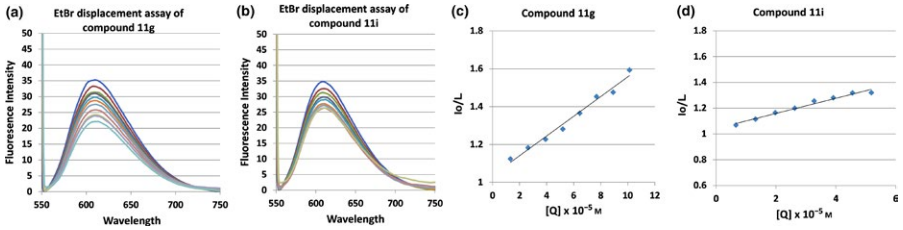

FIGURE 4 Plot of Fluorescence emission intensity I versus Wavelength (nm) for DNA-EtBr complex at different concentrations (a) for compound **11g** and (b) for compound **11i**. Stem-Volmer quenching plot of DNA-EtBr (c) for compound **11g** and (i) compound **11i** [Colour figure can be viewed at wileyonlinelibrary.com]

PRISM 5 software viz. 0.245 ± 0.011, and 0.0067 ± 0.0002 μM in A549 and MCF-7 cell line respectively (Figure 5a,b). Compound **11i** showed IC_{50} 79.31 ± 0.08 μM (Figure 5c) for non-cancer mouse fibroblast cell line (NIH/3T3), which was significantly high in compare to IC_{50} values against cancer cell lines A549 and MCF-7. These results prove beyond doubt that when cancer cell will be treated at such lower concentration of compound **11i**, will not be cytotoxic to nearby normal cells, hence, compound **11i** was very specific toward cancer cells. Therefore, it was taken further for the study of mechanism in cancer cell lines against A549 and MCF-7 cell line.

There are several mechanisms by which an anticancer compound exerts its effect on cancer cell in vitro. Apoptosis and necrosis are the most preferred mechanisms. To understand the mode of cytotoxicity of compound **11i** for cancer cell lines, LDH Assay was performed in both cancer cell lines. At lower concentration of compound **11i**, the LDH release was very low which revealed that at lower concentration the prevalent mechanism of cytotoxicity was apoptosis but with increased concentration of compound **11i** LDH release increases significantly therefore, at higher concentration

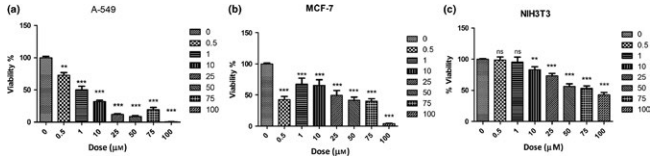

FIGURE 5 The cytotoxicity of compound **11i** against A549, MCF-7 and NIH/3T3 cell line. In MTT assay (a–c) cells were treated with 0.5, 1, 10, 25, 50, 75, 100 μM concentrations of compound **11i** graph was plotted against % viability v/s dose. Data were represented as mean ± *SD* from three independent experiments. ***$p < 0.001$

treated cells changed its fate toward the necrosis from apoptosis. As IC_{50} value of compound **11i** is very low for both cell lines therefore, it can be deduced that preferred mechanism of cytotoxicity for compound **11i** can be apoptosis (Figure 6a,b).

To confirm, that loss of percentage viability was either due to cell death or due to cell proliferation inhibition effect of compound **11i**, Trypan blue assay was performed in both A549 and MCF-7 cell lines. The percentage cell death at IC_{50} concentration of compound **11i** was approx. 36% ± 3% in A549 cell line and 45% ± 2.68% in MCF-7 cell line (Figure 7), from this it can be construed that compound **11i** is cytotoxic towards the MCF-7 whereas it might be cytotoxic or cytostatic toward A549 cell line, further experimental confirmation is required to explain the effect of compound **11i** on cancer cell lines.

In order to reaffirm the findings of LDH assay, the EtBr/AO staining assay was performed with compound **11i**. Acridine orange is a vital dye that stains both live and dead cells however, ethidium bromide stains only the cells that have lost their membrane integrity. EtBr/AO dye stains, necrotic cells red, live cells green, early apoptotic cell's nuclei green but with visible condensation whereas, late apoptotic cell's nuclei Orange with condensation and fragmentation.

Cells were treated with IC_{50} concentration of compound **11i** and it was found that most of the cells of A549 cell line (Figure 8a–c) were under late apoptosis, there were no cells under necrosis whereas, in MCF-7 cell line (Figure 8d–f) most of the cells were under early apoptosis with few under necrosis. Number of the cells under apoptosis and necrosis were negligible in control cell lines. Which confirmed the LDH assay finding that compound **11i** exhibits cytotoxic activity in both cell lines via apoptosis. To confirm the possible interaction of compound with DNA, compound **11i** was studied for DNA binding activity.

FIGURE 6 In LDH assay (a–b): Representation of cytosolic enzyme LDH (a) activity of LDH in A549 cell line (b) activity of LDH in MCF-7 cell line. Cells were treated with 0.5, 1, 10, 25, 50, 75, 100 μM concentrations of compound **11i**. Graph was plotted against LDH release versus dose. (***$p \leq .001$, **$p < .01$ significance one-way ANOVA (Tukey–Kramer). ANOVA, analysis of variance; LDH, lactic dehydrogenase

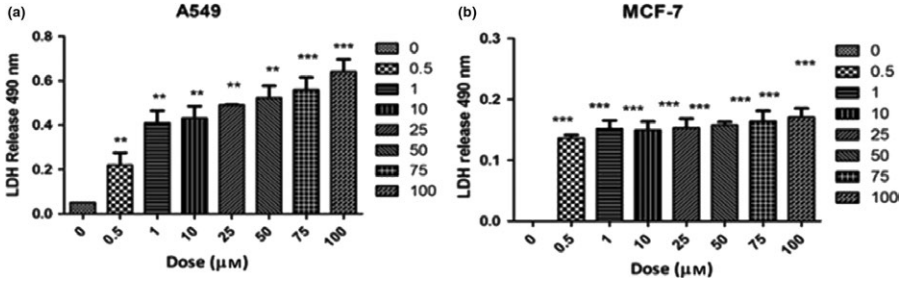

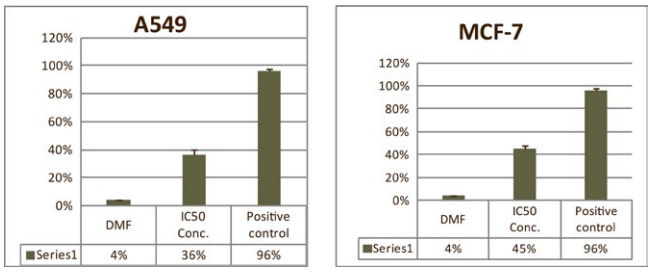

FIGURE 7 Trypan blue assay. The percentages cell death of A549 and MCF-7 cell line treated with DMF, with IC_{50} concentration of compound **11i** and with positive control was plotted. Data were represented as mean ± *SD* from three independent experiments

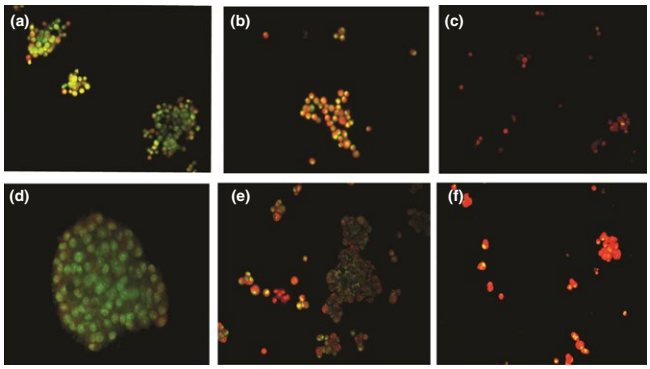

FIGURE 8 EtBr/AO assay**:** EtBr/AO assay was performed with A549 cell line (a–c) and MCF-7 (d–f). (a–c) images represent control, IC_{50} conc. compound **11i** treated and positive control in A549 cell line; (d–f) images represent control, IC_{50} conc. compound **11i** treated and positive control in MCF-7 cell line [Colour figure can be viewed at wileyonlinelibrary.com]

4 | CONCLUSIONS

In conclusion, a series of chalcone of 3-aminomethyl pyridine derivatives were synthesized and evaluated for their anticancer activity against A549 and MCF-7 cell lines. Based on MTT assay, one of the compounds **11i** has shown very good selectivity for MCF-7 cancer cell line as compared to NIH/3T3 normal cell line (noncancer mouse fibroblast cell line). DNA binding studies of compound **11i** indicated intercalation mode of binding with CT-DNA. The cytotoxic studies of compound **11i** have shown the apoptosis in MCF-7 cell line using LDH assay and the EtBr/AO assay. From the K_b binding values it can be concluded that compound **11g** has twofold higher affinity for CT-DNA binding than compound **11i.** Further study for sequence selectivity is undergoing for the lead compounds.

ACKNOWLEDGMENTS

One of the authors (RS) is thankful to Department of Science & Technology, Government of India for financial support vide reference no. SR/WOS-A/CS-1028/2014 under Women Scientist Scheme to carry out this work. One of the authors (SU) is thankful to UGC, Government of India for UGC-JRF vide reference no. 22/06/2014 (i) EU-V. Authors are thankful to The Head, Department of Chemistry and Department of Zoology, Faculty of Science, The M. S. University of Baroda for providing laboratory facilities, Zydus Research Centre, Ahmedabad, for the ESI-MS analyses.

CONFLICT OF INTEREST

The authors declare no conflict of interest.

ORCID

Shubhangi S. Soman http://orcid.org/0000-0002-1405-4064

REFERENCES

[1] World Health Organisation. Cancer fact sheet Feb 2017, World Health Organisation, **2017**.
[2] J. M. Reichert, J. B. Wenger, *Drug Discov. Today* **2008**, *13*, 30.
[3] American Cancer Society. Cancer Facts & Figures, **2017**.
[4] I. Haq, *Arch. Biochem. Biophys.* **2002**, *403*, 1.
[5] B. M. Zeglis, V. C. Pierre, J. K. Barton, *Chem. Commun.* **2007**, 4565.
[6] H. Kumar, A. Chattopadhyay, R. Prasath, V. Devaraji, R. Joshi, P. Bhavana, P. Saini, S. K. Ghosh, *J. Phys. Chem. B.* **2014**, *118*, 7257.
[7] L. D. Via, O. Gia, G. Chiarelotto, M. G. Ferlin, *Eur. J. Med. Chem.* **2009**, *44*, 2854.
[8] V. Markovic, N. Debeljak, T. Stanojkovic, B. Kolundzija, D. Stadic, M. Vujcic, B. Janovic, N. Tanic, M. Perovic, V. Tesic, J. Antic, M. D. Joksovic, *Eur. J. Med. Chem.* **2015**, *89*, 401.
[9] A. K. Singh, G. Saxena, S. Dixit, S. Hamidullah, S. K. Singh, M. Arshad, R. Konwar, *J. Mol. Struct.* **2016**, *111*, 90.
[10] X. Yang, G.-L. Shen, R.-Q. Yu, *Microchem. J.* **1999**, *62*, 394.
[11] T. Suzuki, T. Ando, K. Tsuchiya, N. Fukazawa, A. Saito, Y. Mariko, T. Yamashita, O. Nakanishi, *J. Med. Chem.* **1999**, *42*, 3001.
[12] S. Bilginer, H. I. Gul, E. Mete, U. Das, H. Sakagami, N. Umemura, J. R. Dimmock, *J. Enzyme Inhib. Med. Chem.* **2013**, *28*, 974.
[13] T. Lu, A. W. Goh, M. Yu, J. Adams, F. Lam, T. Teo, P. Li, B. Noll, L. Zhong, S. Diab, O. Chahrour, A. Hu, A. Y. Abbas, X. Liu, S. Huang, C. J. Sumby, R. Milne, C. Midgley, S. Wang, *J. Med. Chem.* **2014**, *57*, 2275.
[14] R. Soni, S. Umar, N. Shah, B. Suresh, S. S. Soman, *J. Heterocyclic Chem.* **2017**, *54*, 2501.
[15] S. Durgapal, R. Soni, S. Umar, B. Suresh, S. S. Soman, *Chemistryselect* **2017**, *2*, 147.
[16] R. L. Atkins, D. E. Bliss, *J. Org. Chem.* **1978**, *43*, 1975.
[17] Y. D. Kulkarni, D. Srivastava, D. A. Bishnoi, P. R. Dua, *J. Indian Chem. Soc.* **1996**, *73*, 173.
[18] L. J. Simons, B. W. Caprathe, M. Callahan, J. M. Graham, T. Kimura, Y. Lai, H. LeVine III, W. Lipinski, A. T. Sakkab, Y.

Tasaki, L. C. Walker, T. Yasunaga, Y. Ye, N. Zhuang, C. E. Augelli-Szafran, *Bioorg. Med. Chem. Lett.* **2009**, *19*, 654.
[19] S. Kasibhatla, G. P. Amarante-Mendes, D. Finucane, T. Brunner, E. Bossy-Wetzel, D. R. Green, *CSH Protocols* **2006**, *1*, pdb. prot4429.
[20] T. Mosmann, *J. Immunol. Methods* **1983**, *65*, 55.
[21] C. V. Kumar, E. H. Asunsion, *J. Am. Chem. Soc.* **1993**, *115*, 8547.
[22] M. Balduzzi, M. Diociaiuti, B. De Berardis, S. Paradisi, L. Paoletti, *Environ. Res.* **2004**, *96*, 62.
[23] C. M. Sayes, A. M. Gobin, K. D. Ausman, J. Mendez, J. L. West, V. L. Colvin, *Biomaterials* **2005**, *26*, 7587.
[24] G. Fotakis, J. A. Timbrell, *Toxicol. Lett.* **2006**, *160*, 171.

SUPPORTING INFORMATION

Additional supplemental material may be found online in the Supporting Information section at the end of the article.

How to cite this article: Durgapal SD, Soni R, Umar S, Suresh B, Soman SS. 3-Aminomethyl pyridine chalcone derivatives: Design, synthesis, DNA binding and cytotoxic studies. *Chem Biol Drug Des*. 2018;92:1279–1287. https://doi.org/10.1111/cbdd.13189

Arabian Journal of Chemistry (2019) **12**, 701–708

King Saud University

Arabian Journal of Chemistry

www.ksu.edu.sa
www.sciencedirect.com

ORIGINAL ARTICLE

Design, synthesis and anti-diabetic activity of chromen-2-one derivatives

Rina Soni [a,1], **Sunil Dutt Durgapal** [a,1], **Shubhangi S. Soman** [a,*], **John J Georrge** [b]

[a] *Department of Chemistry, Faculty of Science, The M. S. University of Baroda, Vadodara 390 002, India*
[b] *Biotechnology Department, Christ College, Rajkot, India*

Received 31 August 2016; accepted 21 November 2016
Available online 29 November 2016

KEYWORDS

Coumarin derivatives;
Molecular docking;
Antidiabetic activity;
DPP-IV inhibition

Abstract DPP-IV inhibitors have been immersed as promising pathway to treat Type 2 diabetes. Here we have reported designing of coumarin derivatives as DPP-IV inhibitors. Designed compounds have been studied for their binding with DPP-IV enzyme through molecular docking followed by synthesis. All synthesized compounds have been fully characterized and screened for DPP-IV inhibition activity. Two compounds showed very good inhibition at 10 μM concentration.

1. Introduction

Diabetes is chronic disease and the number of people with diabetes has risen from 108 million in 1982 to 422 million in 2014 (WHO, 2016). Out of two types of diabetes, type 1 diabetes is due to lack of insulin Type 2 diabetes which is due to body's ineffective use of insulin. Type 2 diabetes mellitus (T2DM) is a metabolic disease characterized by hyperglycemia or high blood sugar level. It is largely the result of excess body weight and physical inactivity (Abdullah et al., 2010). When it is not controlled or treated properly, it can lead to blindness, kidney failure, heart attacks, stroke and lower limb amputation into patients (Ripsin et al., 2009). Diabetes can be managed by healthy diet, regular physical activity and maintaining a normal body weight. It can be treated through various pathways by controlling blood glucose level (Bennett et al., 2011). Main disadvantage of these pathways is side effects such as weight gain, hypoglycemia and joint pains. Current treatment for type 2 diabetes is based upon increasing insulin availability, improving sensitivity to insulin, delaying the delivery of insulin and absorption of carbohydrates from gastrointestinal tract or increasing urinary glucose excretion (Sena et al., 2010). Recently, dipeptidyl peptidase IV (DPP-IV) inhibitors have been immerged as quite promising pathway to treat Type 2 diabetes. Inhibition of DPP-IV leads to increased half-life of endogenous incretins such as GLP-1, as active sites of enzyme which cleaves the *N*-terminal dipeptide with L-proline and L-alanine are blocked by inhibitors (Hansen et al., 1999). Different classes of DPP-IV have been reported and marketed to treat Type 2 Diabetes such as Vildagliptin and Sitagliptin (Villhauer et al., 2003; Kim et al., 2005) (Fig. 1). Recently, Omarigliptin has been reported as potent DPP-IV inhibitors with dose only once in a week for treatment of diabetes (Biftu et al., 2014) (Fig. 1).

Coumarin is one of the interesting heterocycle found in nature. Several coumarin derivatives have been reported with various activities such as anti-inflammatory, anticoagulant, anti-oxidant, anticancer, antifungal, and neuroprotective agents (Sandhu et al., 2014; Barot et al., 2015; Pisani et al., 2016). Synthetic coumarin derivatives have also been reported to treat diabetes by different pathways such as

* Corresponding author.
E-mail address: shubhangiss@rediffmail.com (S.S. Soman).
[1] These authors contributed equally.
Peer review under responsibility of King Saud University.

Production and hosting by Elsevier

http://dx.doi.org/10.1016/j.arabjc.2016.11.011
1878-5352

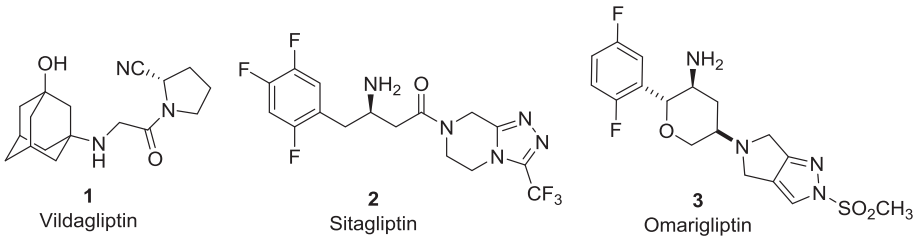

Fig. 1 Some potent DPP-4 inhibitors.

activation of phosphatidylinositol-3-kinase and α-glucosidase inhibitor (Dwivedi et al., 2008; Anand et al., 2011). The coumarin based drug dicumarol is in market since long time with minimum side effects. The pharmacological properties and application of coumarins depend on type and position of substitution on coumarin rings. There are only few reports on synthetic coumarin derivatives as DPP-IV inhibitors to treat Type 2 diabetes. In continuation to our work on coumarin containing DPP-IV inhibitors, we have designed compounds **10**, **14** and **15** based on our earlier coumarin derivatives as DPP-IV inhibitors **4** and **5** (Fig. 2). Compounds **4** and **5** have shown very good DPP-IV inhibition at micromolar concentration (Sharma and Soman, 2015, 2016). Molecular docking is a tool available to chemist to check whether the designed molecule is efficient in binding with receptor. So we have designed the molecules having glycine linkage between substituted amine and coumarin and studied its molecular docking with DPP-IV enzyme. Designed molecules were compared with Vildagliptin as they have same active pharmacophore. Compounds **10a–h**, **14a–h** and **15g–h** were synthesized and screened for DPP-IV inhibition activity.

2. Materials and methods

2.1. Chemistry

Reagent grade chemicals and solvents were purchased from commercial supplier and used after purification. TLC was performed on silica gel F254 plates (Merck). Acme's silica gel (60–120 mesh) was used for column chromatographic purification. All reactions were carried out in nitrogen atmosphere. Melting points are uncorrected and were measured in open capillary tubes, using a Rolex melting point apparatus. IR spectra were recorded as KBr pellets on Perkin Elmer RX 1 spectrometer. ^{1}H NMR and ^{13}C NMR spectral data were recorded on Advance Bruker 400 spectrometer (400 MHz) with $CDCl_3$ or DMSO-d_6 as solvent and TMS as internal standard. *J* values are in Hz. Mass spectra were determined by ESI-MS, using a Shimadzu LCMS 2020 apparatus. Elemental analyses were recorded on Thermo Finnigan Flash 11–12 series EA. All reactions were carried out under nitrogen atmosphere. Compounds *1-(bromomethyl)-3H-benzo[f]chromen-3-one* **9** (Dey and Sankaranarayan, 1934), *3-acetyl-7-hydroxy-2H-chromen-2-one* **11** (Shah and Shah, 1954) and *ethyl 7-hydroxy-2-oxo-2H-chromene-3-carboxylate* **12** (Bigi et al., 1999) were prepared using literature methods.

2.1.1. Preparation of substituted glycinamide derivatives (*6*)

A mixture of Boc-glycine (1.0 mmol), 1-ethyl-3-(3-dimethylaminopropyl) carbodiimide hydrochloride (1.5 mmol) (EDCI), 1-hydroxybenzotriazole (1.0 mmol) (HOBt), triethylamine (2.0 mmol) and amine (1° and 2°) (1.10 mmol) in dichloromethane (50 mL) (DCM) was stirred at room temperature for 16 h. The reaction was monitored using TLC. On completion of the reaction, it was washed with water (2 × 20 mL), brine (1 × 10 mL), dried over anhydrous sodium sulfate and the solvent evaporated under reduced pressure to give the crude product which was then purified by column chromatography using silica gel as stationary phase and DCM:MeOH (95:5) as eluent to yield desired *N*-Boc glycinamide **6**, as white solid.

2.1.2. Boc deprotection of glycinamide derivatives

Compound **6** was deprotected by stirring in 10% trifluoroacetic acid (TFA) in DCM. On completion of the reaction after monitored by TLC, the solvent was evaporated under reduced pressure. Compound was dissolved in DCM and concentrated under reduced pressure to remove to give compound **7** as trifluoroacetic acid salt and was directly used for next step without any purification.

2.1.3. General procedure for the preparation of compounds *10a–g*

4-Bromomethylnaphthopyrone **9** (0.5 g, 1.730 mmol) dissolved in DMF (20 mL) and substituted glycinamide **7** (1.1 eq), along with base triethylamine (1.5 eq) was added to it. The resulting mixture was stirred at room temperature for 16 h and then poured into cold water. The aqueous layer thus obtained was extracted using ethyl acetate and/or dichloromethane (checked by TLC) and solvent evaporated to give crude product. The product thus, obtained was purified by column chromatography using Pet ether: ethyl acetate.

Representative characterization data for compounds **10a**, **10b** and **10h**. Data for compounds **10c–g** are provided in supporting information.

*2.1.3.1. N-(4-methylphenyl)-2-{[(3-oxo-3H-benzo[f]chromen-1-yl)methyl]amino}acetamide (**10a**).* Yield: 45%; M.P.: 176–178 °C; IR (KBr): 3325, 3074, 2890, 1726, 1688, 1549, 1519, 1448, 1402, 1337, 1209, 1142, 999, 873, 814, 743 cm^{-1}; ^{1}H NMR (400 MHz, $CDCl_3$): 2.30 (s, 3H), 3.62 (s, 2H), 4.51 (s, 2H), 6.82 (s, 1H), 7.09 (d, *J* = 8.4 Hz, 2H), 7.29 (d, *J* = 8.4 Hz, 2H), 7.50 (d, *J* = 9.2 Hz, 1H), 7.59 (t, *J* = 7.2 Hz, 1H), 7.67–7.71 (m, 1H), 7.96 (dd, *J* = 0.8, 8.0 Hz, 1H), 8.01 (d, *J* = 9.2 Hz, 1H), 8.39 (d, *J* = 8.4 Hz, 1H), 8.75 (s, 1H); ^{13}C NMR (100 MHz, $CDCl_3$): 20.88, 52.52, 54.53, 113.18, 114.74, 117.99, 119.48, 125.02, 125.76, 128.44, 129.29, 129.49, 129.99, 131.42, 134.08, 134.14, 134.59, 154.51, 155.07, 160.41, 168.46; MASS: 372.90 $[M+H]^+$; Anal. Calc. for $C_{23}H_{20}N_2O_3$; C, 74.18; H, 5.41; N, 7.52; found: C, 74.38; H, 5.61; N, 7.32%.

*2.1.3.2. N-(4-chlorophenyl)-2-{[(3-oxo-3H-benzo[f]chromen-1-yl)methyl]amino}acetamide (**10b**).* Yield: 53%; M.P.: 182–184 °C; IR (KBr): 3322, 3277, 3075, 2845, 1712, 1675, 1590,

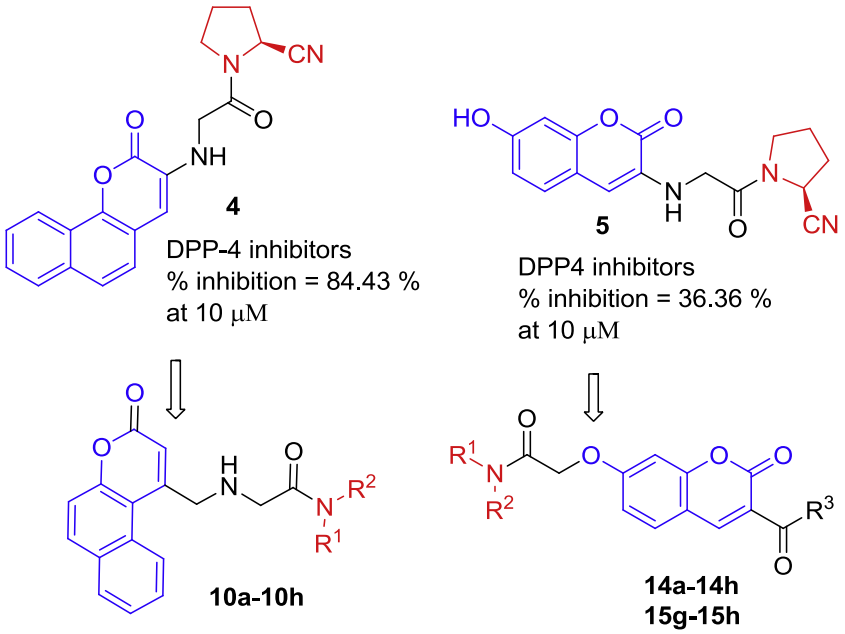

Fig. 2 Design of coumarin containing compounds **10**, **14** and **15** as DPP-4 inhibitors.

1553, 1512, 1398, 1304, 1207, 1092, 1020, 820, 747 cm^{-1}; ^1H NMR (400 MHz, $CDCl_3$): 3.63 (s, 2H), 4.52 (s, 2H), 6.79 (s, 1H), 7.22 (d, J = 8.8 Hz, 2H), 7.31 (d, J = 8.8 Hz, 2H), 7.49 (d, J = 8.8 Hz, 1H), 7.61 (t, J = 7.6 Hz, 1H), 7.68 (t, J = 8.0 Hz, 1H), 7.96–8.02 (m, 2H), 8.40 (d, J = 8.8 Hz, 1H), 8.86 (s, 1H); ^{13}C NMR (100 MHz, $CDCl_3$): 52.41, 54.65, 113.09, 115.06, 118.03, 120.59, 124.94, 125.79, 128.45, 128.97, 129.25, 129.34, 130.06, 131.45, 134.19, 135.70, 154.19, 155.14, 160.30, 168.66; MASS: 393.25 $[M+H]^+$; Anal. Calc. for $C_{22}H_{17}ClN_2O_3$; C, 67.26; H, 4.36; N, 7.13; found: C, 67.46; H, 4.55; N, 7.31%.

*2.1.3.3. 1-({[2-(morpholin-4-yl)-2-oxoethyl]amino}methyl)-3H-benzo[f]chromen-3-one (**10h**).* Yield: 56%; M.P.: 114–116 °C; IR (KBr): 3556, 3492, 3080, 2871, 2811, 1695, 1649, 1549, 1429, 1276, 1241, 1107, 859, 825, 744 cm^{-1}; ^1H NMR (400 MHz, $CDCl_3$): 3.38 (t, J = 4.8 Hz, 2H), 3.52 (s, 2H), 3.66–3.70 (m, 6H), 4.42 (s, 2H), 6.93 (s, 1H), 7.46 (d, J = 8.8 Hz, 1H), 7.55 (t, J = 7.6 Hz, 1H), 7.55 (dt, J = 1.2, 7.6 Hz, 1H), 7.91 (d, J = 7.6 Hz, 1H), 7.96 (d, J = 8.8 Hz, 1H), 8.45 (d, J = 8.8 Hz, 1H); ^{13}C NMR (100 MHz, $CDCl_3$): 42.20, 44.78, 49.57, 54.02, 66.38, 66.79, 113.90, 114.45, 117.80, 125.54, 125.72, 128.11, 129.53, 129.65, 131.29, 133.68, 154.84, 155.69, 160.86, 169.21; MASS: 352.90 $[M+H]^+$; Anal. Calc. for $C_{20}H_{20}N_2O_4$; C, 68.17; H, 5.72; N, 7.95; found: C, 68.30; H, 5.83; N, 7.87%.

2.1.4. Preparation of N-substituted chloroacetamide derivatives (13)

To an ice-cold solution of substituted amines (20 mmol) in dichloromethane (DCM) (25 mL) was added triethylamine (TEA) (20.2 mmol) and stirred for 5–10 min. To this chloroacetyl chloride (20 mmol) was added dropwise over a period of 10 min under cooling. The resulting solution was stirred at 0–5 °C for 30 min and at room temperature for 24 h. The reaction mixture was diluted with water and extracted with DCM (2 × 30 mL). The organic layers were combined, washed with HCl solution (0.5 N, 15 mL), dried over anhydrous Na_2SO_4, filtered and evaporated on a rotavapor to give compound **13**. The substituted chloroacetamide **13** thus obtained, was used directly for next step without any purification.

*2.1.5. General procedure for the synthesis of compounds **14a–g** and **15g–h***

To a solution of compound **11**/**12** (1.0 eq) in dry *N*,*N*-dimethylformamide (DMF) (15 mL) was added compound **13** (1.2 eq). To this anhydrous K_2CO_3 (1.5 eq) was added followed by pinch of KI. The resulting mixture was heated in water bath at 70–80 °C 12–18 h. The completion of reaction was checked by TLC using Pet. ether: ethyl acetate (1:1). The reaction mixture was poured in ice cold water. The solid separated out was filtered, washed with water and dried. When there was no solid separated out in water, the aqueous layer was extracted using DCM (3 × 20 mL). The organic layers were combined, washed with brine, dried over anhydrous Na_2SO_4, filtered and concentrated to give an oily residue. The residue was triturated in Pet. ether to give compound as solid. The crude compound was purified by column chromatography over silica gel using Pet. ether: ethyl acetate (40:60–20:80) to obtain pure compound as solid.

Representative characterization data for compounds **14a**, **14b** and **15g**. Data for compounds **14c–g** and **15h** are provided in supporting information.

*2.1.5.1. 2-[(3-Acetyl-2-oxo-2H-chromen-7-yl)oxy]-N-(4-methylphenyl)acetamide (**14a**).* Pale yellow solid, Yield: 91%; M.P.: 210–212 °C; IR (KBr): 3374, 3053, 2919, 1727, 1681, 1613, 1597, 1372, 1204, 1052, 820, 770 cm^{-1}; ^1H NMR (400 MHz, $CDCl_3$): δ 2.35 (s, 3H), 2.73 (s, 3H), 4.72 (s, 2H), 6.96 (d, J = 2.2 Hz, 1H), 7.04 (dd, J = 2.2, 8.8 Hz, 1H),

7.19 (d, J = 8.4 Hz, 2H), 7.48 (d, J = 8.4 Hz, 2H), 7.66 (d, J = 8.8 Hz, 1H), 8.10 (s, 1H), 8.52 (s, 1H); ^{13}C NMR (100 MHz, $CDCl_3$): δ ppm 20.95, 30.62, 67.71, 102.04, 113.29, 113.33, 120.35, 121.92, 129.71, 132.03, 133.84, 135.06, 147.31, 157.37, 159.27, 161.86, 164.37, 195.34; Anal. Calc. for $C_{20}H_{14}NO_5$; C, 68.37; H, 4.88; N, 3.99; found: C, 68.22; H, 4.90; N, 3.72%; ESI-MS: 352.0 $[M+H]^+$.

*2.1.5.2. 2-[(3-Acetyl-2-oxo-2H-chromen-7-yl)oxy]-N-(4-chlorophenyl)acetamide (**14b**)*. Pale yellow solid, Yield: 79%; M.P.: 216–218 °C; IR (KBr): 3364, 2925, 2355, 1728, 1682, 1615, 1593, 1531, 1454, 1372, 1260, 1203, 1127, 1056, 1010, 831, 770 cm^{-1}; ^{1}H NMR (400 MHz, DMSO-d_6): δ 2.56 (s, 3H), 4.91 (s, 2H), 7.10–7.12 (m, 2H), 7.38 (d, J = 6.8 Hz, 2H), 7.64 (d, J = 9.2 Hz, 2H), 7.91 (d, J = 9.2 Hz, 1H), 8.64 (s, 1H), 10.33 (s, 1H); ^{13}C NMR (100 MHz, DMSO-d_6): δ ppm 30.55, 67.75, 101.60, 112.75, 114.19, 121.23, 121.65, 127.83, 129.18, 132.70, 137.71, 147.95, 157.25, 159.27, 163.68, 166.21, 195.25; Anal. Calc. for $C_{19}H_{14}ClNO_5$; C, 61.38; H, 3.80; N, 3.77; found: C, 61.16; H, 4.02; N, 3.94%; ESI-MS: 394.00 $[M+Na]^+$.

*2.1.5.3. Ethyl 2-oxo-7-[2-oxo-2-(piperidin-1-yl)ethoxy]-2H-chromene-3-carboxylate (**15g**)*. Off white solid, Yield: 43%; M.P.: 128–130 °C; IR (KBr): 3052, 2993, 2937, 2848, 1756, 1659, 1603, 1556, 1502, 1445, 1431, 1380, 1292, 1204, 1181, 1112, 1051, 1035, 1010, 962, 862, 799 cm^{-1}; ^{1}H NMR (400 MHz, DMSO-d_6): 1.30 (t, J = 7.2 Hz, 3H), 1.44 (br s, 2H), 1.57 (br s, 4H), 3.34–3.42 (m, 4H), 4.27 (q, J = 7.2 Hz, 2H), 5.02 (s, 2H), 6.99–7.00 (m, 2H), 7.82–7.85 (m, 1H), 8.73 (s, 1H); ^{13}C NMR (100 MHz, DMSO-d_6): 14.59, 24.37, 25.70, 26.30, 42.61, 45.39, 61.40, 66.61, 101.50, 112.02, 113.80, 114.19, 131.96, 149.66, 156.72, 157.20, 163.28, 164.25, 164.90; Anal. Calc. for $C_{19}H_{21}NO_6$; C, 63.50; H, 5.89; N, 3.90; found: C, 63.23; H, 5.72; N, 3.63%; ESI-MS: 360.0 $[M+H]^+$.

2.2. Biological activity screening

In vitro enzyme (DPP-IV) inhibitory activity was determined using fluorescence based assay. Gly-Pro-Aminomethylcoumarin (AMC) was used as a substrate to measure DPP-IV activity. Cleavage of the peptide bond by DPP-IV releases the free AMC group, resulting in fluorescence that is analyzed using an excitation wavelength of 350–360 nm and emission wavelength of 450–465 nm. Human recombinant DPP-IV enzyme procured from Enzo Life Science (batch no. BML-SE434-9091), substrate, H-Gly-Pro-AMC procured from Enzo life science (batch no. BML-P189-9091) and assay buffer, having pH. 7.8 were used in the assay DPP-IV activity which was measured by mixing reagents in 96-well plate (order of addition of reagents: assay buffer, enzyme, solvent/inhibitor and finally substrate). Both the enzyme and 96-well plate were incubated for 30 min and the resulting fluorescence was measured using Spectra Max Fluorometer (Molecular Devices, Sunnyvale, CA) by exciting at 360 nm and emission at 460 nm with the excitation filter at 360 nm and emission filter at 460 nm at sensitivity of 45.

3. Results and discussion

3.1. Docking studies

The chain A of protein DPP-IV (PDB ID: 3W2T) was selected for docking study as the only crystallized structure of human DPP-IV complexed with an approved drug Vildagliptin available in PDB (Berman et al., 2002; Nabeno et al., 2013). Molecular docking studies were performed using glide XP (extra precision) scoring function of maestro version 9.0 (Repasky et al., 2007). All designed molecules and cocrystal Vildagliptin (Fig. 3) were docked flexibly with the target protein, and the QikProp and toxicity prediction applications were used to find the absorption, distribution metabolism and excretion (ADME) property (QikProp, 2009) and the toxicity level of the designed molecules respectively.

The softwares PyMol, a powerful and comprehensive molecular visualization product for rendering and animating 3D molecular structure (Schrodinger, 2015) and LigPlots were used to visualize the docking results. A schematic 2D representation of protein-ligand complex was generated by LigPlot, a graphical system of automatically generating multiple 2D diagrams of ligand protein interactions from 3D coordinates. The diagrams portray the hydrogen bond interaction patterns and hydrophobic contacts between the ligands and the main chain and side chain elements of proteins. To evaluate the reliability of docking algorithm, the RMSD between docked Vildagliptin and the X-ray solved Vildagliptin which is present in the protein complex was calculated and it has the value of 0.027 Å, which shows the algorithm is accurate (Nicolotti et al., 2009; Totrov and Abagyan, 2008) (Fig. 3a).

The docking results showed many of the designed molecules have considerable good binding affinity with the target protein than the cocrystal approved drug Vildagliptin, which has ΔG = −4.610 kcal/mol (Table 1, Fig. 4) and the designed molecules **10a–c** and **14a** bind in the large pocket of the target

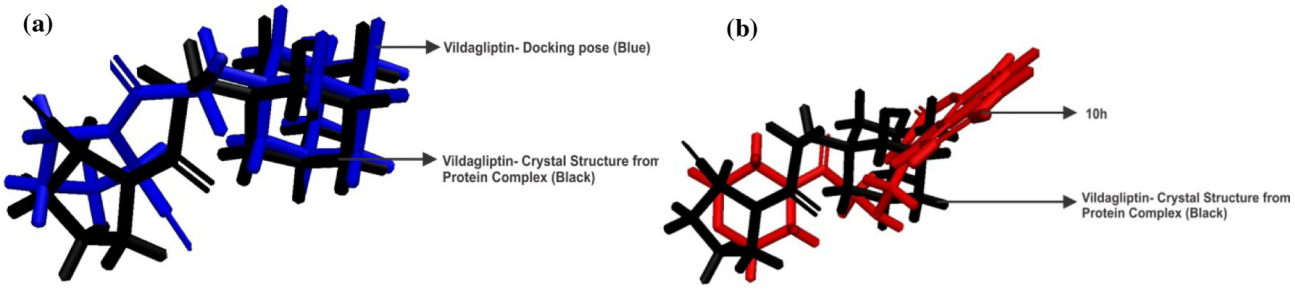

Fig. 3 (a) Superimposed structures of Vildagliptin in docking pose and crystal structure from protein complex and (b) superimposed structures of Vildagliptin (crystal structure from protein complex) and compounds **10h**.

Table 1 Glide XP docking score (kcal/mol) of compounds **10a–c**, **10g–h**, **14a** and Vildagliptin.

	10a[b]	**10b**[b]	**10c**[b]	**10g**[c]	**10h**[c]	**14a**[b]	**Vildagliptin**[c]
Glide XP Docking Score	−5.061	−5.307	−5.550	−4.369	−4.696	−4.719	−4.610
Interacting amino acid residues through Hydrogen bond[a]	Glu206, Tyr547, Tyr662	Glu205, Glu206, Ser209	Glu206, Tyr547, Gln553, Tyr585	Lys122, Gln123, Tyr238	Lys122, Gln123, Tyr238	Lys122, Asn710	Tyr238, Asp737

[a] Interacting amino acid residues through hydrogen bond from LigPlot.
[b] Compounds **10a–c** and **14b** bind in big pocket of DPP-IV enzyme (Fig. 4).
[c] Compounds **10g–h** and Vildagliptin bind in small pocket of DPP-IV enzyme (Fig. 4).

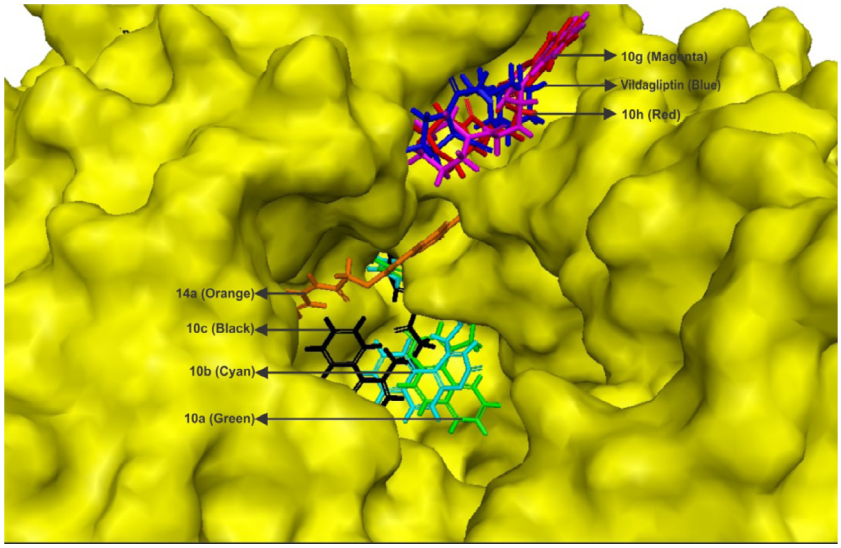

Fig. 4 Binding of Vildagliptin, compounds **10a–c**, **10g–h** and **14a** at the active site of DPP-IV. (Viewed in PyMol and LigPlot).

protein and among those molecules **10a–c**, **14a** had the best docking score than the co-crystal approved drug Vildagliptin. On other hand, the designed compounds **10g–h** fit well in smaller pocket of protein just like Vildagliptin. As compound **10h** binds in small pocket like Vildagliptin (Fig. 4), it was superimposed with Vildagliptin (Fig. 3b). RMSD between **10h** and the X-ray solved Vildagliptin which is present in the protein complex was calculated and it has the value of 0.246 Å.

The docking results with the interacting pattern including interacting amino acid residues showed that **10a–c** and **14a** bind in the large pocket of the target protein while Vildagliptin fit well in the smaller pocket of proteins DPP-IV (Fig. 4). On other hand, the designed compounds **10g–h** fit well in smaller pocket of protein just like Vildagliptin, thus confirmed our designing strategy is correct (Fig. 4). Interestingly, designed compounds **10a–c** and **10g–h** showed binding in different pockets of DPP-IV enzyme. These docking results prompted us to synthesize all designed compounds and to study their DPP-IV inhibition activity. Detailed docking results and LigPlots are given in supporting information.

3.2. Chemistry

The Boc-glycine on reaction with different amines in the presence of 1-(3-dimethylaminopropyl)-3-ethylcarbodiimide hydrochloride (EDC) and 1-hydroxybenzotriazole (HOBt) gave various amides **6**. Compound **6** was deprotected using trifluoroacetic acid in dichloromethane to give compound **7** which was used as such without purification for next step. On the other hand, ethyl acetoacetate was brominated using Br_2 to give 4-bromo-3-oxobutanoate **8** as red oil (Sousa et al., 2012).

Compound **8** on Pechmann reaction with β-naphthol in conc. H_2SO_4 gave 1-(bromomethyl)-3H-benzo[f]chromen-3-one **9** (Dey and Sankaranarayan, 1934). ^{1}H NMR for compound **9** showed presence of singlet at δ 4.90 for two protons indicated presence of —CH_2Br group and all other aromatic protons appeared in the range of δ 6.6–8.5 thereby confirming the formation of **9**. This compound **9** was used to carry out substitution reaction with compound **7** using triethylamine in DMF to form substituted aminomethylnaphthopyrone derivatives **10a–h** (Scheme 1).

The IR spectrum of compound **10a** exhibited strong band at 3325 cm^{-1} for the —NH stretching, another strong band at 1726 cm^{-1} for lactone carbonyl group of coumarin ring and 1688 cm^{-1} for amide carbonyl group. In the ^{1}H NMR spectrum of **10a**, all aromatic protons were observed at δ 8.39–6.82 and amide —NH at δ 8.75 as a singlet. The two methylene protons were observed as a singlet at δ 4.51 and 3.62 and methyl group at δ 2.30. In the ^{13}C NMR spectrum, the lactone carbonyl carbon of coumarin ring was observed at δ 160, amide carbonyl carbon at δ 168, all aromatic carbons at δ 155–113, two methylene carbons at δ 54 and 52, and

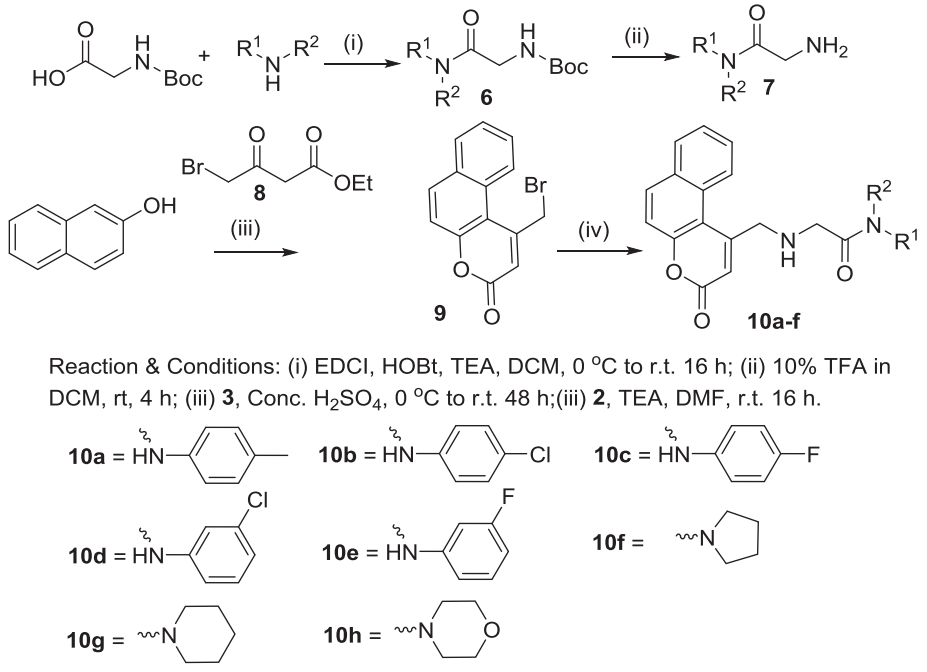

Scheme 1 Synthesis of substituted aminomethylnaphthopyrone derivatives.

methyl carbon at δ 20. In the ESI-MS spectrum of **10a** a peak at m/z 372.90 for $[M+H]^+$ confirmed its formation. The structures of all substituted aminomethylnaphthopyrones **10a–h** were confirmed by different analytical techniques such as ^{1}H NMR, ^{13}C NMR, IR, and ESI-MS. For compound **10h**, single crystal was developed and was studied its structure by X-ray single crystal analysis (CCDC No. 1500813) (Fig. 5) and used for docking (Fig. 3b).

In general, the IR spectra of compounds **10a–g** exhibited one strong band in the range of 1724–1711 cm^{-1} for the lactone carbonyl group of coumarin ring and amide carbonyl group at 1693–1622 cm^{-1}. In the ^{1}H NMR spectra of **10a–g**, peak for the methylene protons was observed in the range of δ ~ 5.01–3.91 depending on the effect of different amine substitution on it. All these new chemical entities were subjected to *in vitro* studies.

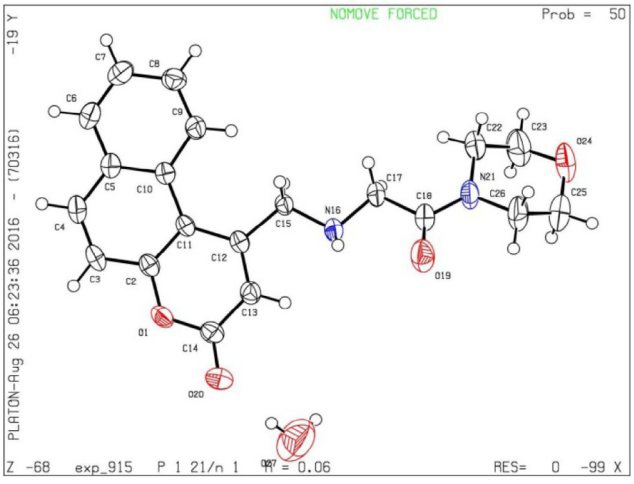

Fig. 5 X-ray crystal structure of compound **10h**.

3-Acetyl-7-hydroxy coumarin **11** and ethyl 3-carboxylate-7-hydroxy coumarin **12** were prepared by Knoevenagel condensation of resorcaldehyde with ethyl acetoacetate/diethyl malonate (Shah and Shah, 1954; Bigi et al., 1999). Various substituted amines on reaction with chloroacetyl chloride gave corresponding chloroacetamide derivatives **13** (Scheme 2) and these compounds were directly used for reaction with 7-hydroxy-3-substituted coumarins **11** and **12**. These chloroacetamide derivatives **13** were reacted with 7-hydroxy-3-substituted coumarins **11**–**12** using anhydrous K_2CO_3 in DMF at 70–80 °C in the presence of catalytic amount of KI to give compounds **14a–g** and **15g–h** (Scheme 2). All these compounds were characterized by different analytical techniques such as ^{1}H NMR, ^{13}C NMR, IR, and ESI-MS.

3.3. Biological evaluation

Preliminary *in vitro* DPP-IV inhibition assay was performed to screen compounds **10a–h** to study the effect of different amides at the P1 site on their inhibition potential at 100 μM concentration as shown in Table 2.

From the *in vitro* analysis as DPP-4 inhibitors, all tested compounds **10a–h** showed inhibition in the range of 26.7–66.9% at 100 μM concentration (Table 2). Compounds **10a–h** remained inactive at lower concentration such as 30 μM and 10 μM.

7-Substituted-3-acetyl coumarin derivatives showed interesting activities (Table 3). Compounds **14a** with p-methyl group, showed 62.2% inhibition in *in vitro* assay at 100 μM concentration. Aromatic amide derivatives **14b–e** remained poor at 100 μM concentration. Saturated amide derivatives, compound **14f** with pyrrolidine and compound **14g** with piperidine showed good activity with 84.5% and 65.7% inhibition respectively at 100 μM concentrations. Replacement of 3-acetyl group with ethyl 3-carboxylate group, resulted in enhancement of DPP-4 inhibition activity in compounds **15g**

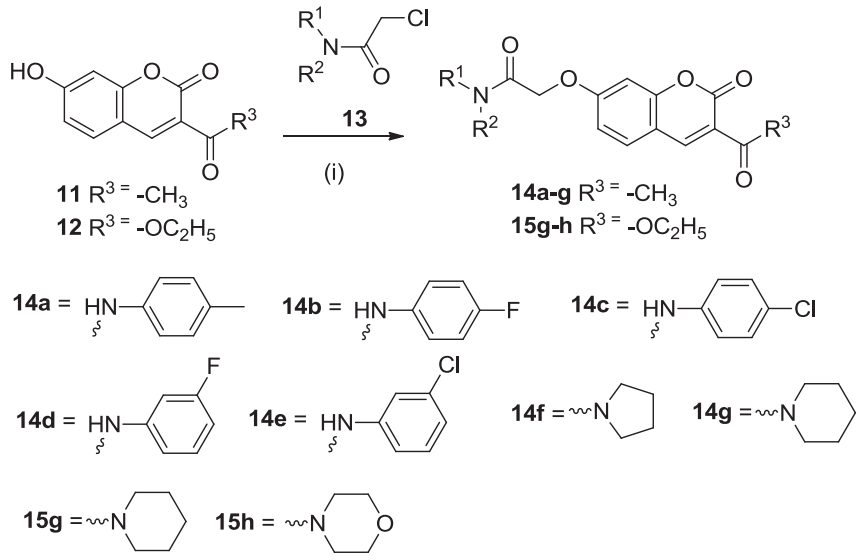

Reagents and conditions: (i) **13**, anhydrous K_2CO_3, KI pinch, DMF, 70-80 °C, 12-18 h.

Scheme 2 Synthesis of 3,7-disubstituted coumarin derivatives.

Table 2 DPP-IV inhibition activity of substituted aminomethylnaphthopyrones **10a–h**.

Compd	$-NR^1R^2$	Inhibition at 100 μM[a]	Compd	$-NR^1R^2$	Inhibition at 100 μM[a]
10a	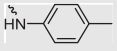	49.3%	**10e**		42.1%
10b		26.7%	**10f**		NA
10c	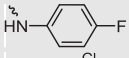	55.1%	**10g**		46.6%
10d		66.9%	**10h**		53.7%
Sitagliptin		62.7% at 0.1 μM	**Vildagliptin**		56.3% at 0.1 μM

[a] DPP-IV inhibitory activity determined by fluorescence-based assay was measured using Spectra Max fluorometer (Molecular Devices, CA). Values of % inhibition are mean of three independent determinations at 100 μM concentration of the test samples.

Table 3 DPP-IV inhibition activity of substituted aminomethylnaphthopyrones **14a–g** and **15g–h**.

Compd	$-NR^1R^2$	Inhibition at 100 μM[a]	Compd	$-NR^1R^2$	Inhibition at 100 μM[a]
14a	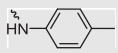	62.2%	**14f**		84.5%
14b	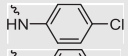	NA	**14g**		65.7%
14c	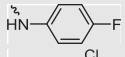	4.7%			At 10 μM
14d	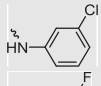	1.3%	**15g**		56.8%
14e		38.8%	**15h**		38.3%
Sitagliptin		62.7% at 0.1 μM	**Vildagliptin**		56.3% at 0.1 μM

[a] DPP-IV inhibitory activity determined by fluorescence-based assay was measured using Spectra Max fluorometer (Molecular Devices, CA). Values of % inhibition are mean of three independent determinations at 100 μM concentration of the test samples.

and **15h**. Compounds **15g** and **15h** showed DPP-4 inhibition at 10 μM concentration with 56.8% and 38.3% inhibition respectively (Table 3). Still it was less than Sitagliptin which showed 62.7% inhibition at 0.1 μM concentration.

4. Conclusion

We have designed small peptide linkage coumarin derivatives for DPP-IV inhibition and studied their docking with known pockets of enzyme. Docking studies showed interesting results as compounds **10a–e** with aromatic amines residue bind in big pocket of DPP-IV enzyme and **10f–h** with cyclic secondary amines residue bind like Vildagliptin in small pocket of DPP-IV enzyme. So we have synthesized various coumarin derivatives, and characterized their structures. Although synthesized compounds show less activity than standard drug Vildagliptin and Sitagliptin, two of our compounds showed promising DPP-IV inhibition activity at 10 μM concentration. Interestingly, compound **15g** showed very good activity with 56.8% inhibition at 10 μM.

Acknowledgments

One of the authors (RS) is thankful to Department of Science & Technology, Government of India for financial support vide reference no. SR/WOS-A/CS-1028/2014 under Women Scientist Scheme to carry out this work. The authors are thankful to The Head, Department of Chemistry Faculty of Science, The M. S. University of Baroda for providing laboratory facilities, Zydus Research Centre, Ahmedabad, for the activity and ESI-MS analyses and DST-PURSE for X-Ray crystallography facility.

Appendix A. Supplementary material

Supplementary data associated with this article can be found, in the online version, at http://dx.doi.org/10.1016/j.arabjc.2016.11.011.

References

Abdullah, A., Peeters, A., de Courten, M., Stoelwinder, J., 2010. Diabetes Res. Clin. Pract. 89, 309–319.
Anand, N., Jaiswal, N., Pandey, S.K., Srivastava, A.K., Tripathi, R. P., 2011. Carbohydr. Res. 346, 16–25.
Barot, K.P., Jain, S.V., Kremer, L., Singh, S., Ghate, M.D., 2015. Med. Chem. Res. 24, 2771–2798.
Bennett, W.L., Maruthur, N.M., Singh, S., Segal, J.B., Wilson, L.M., Chatterjee, R., Marinopoulos, S.S., Puhan, M.A., Ranasinghe, P., Block, L., Nicholson, W.K., Hutfless, S., Bass, E.B., Bolen, S., 2011. Ann. Intern. Med. 154 (9), 602–613.
Berman, H.M., Battistuz, T., Bhat, T., Bluhm, W.F., Bourne, P.E., Burkhardt, K., Feng, Z., Gilliland, G.L., Iype, L., Jain, S., Fagan, P., Marvin, J., Padilla, D., Ravichandran, V., Schneider, B., Thanki, N., Weissig, H., Westbrook, J.D., Zardecki, C., 2002. Acta Crystallogr. D 58, 899–907.
Biftu, T., Sinha-Roy, R., Chen, P., Qian, X., Feng, D., Kuethe, J.T., Scapin, G., Gao, Y.D., Yan, Y., Krueger, D., Bak, A., Eiermann, G., He, J., Cox, J., Hicks, J., Lyons, K., He, H., Salituro, G., Tong, S., Patel, S., Doss, G., Petrov, A., Wu, J., Xu, S.S., Sewall, C., Zhang, X., Zhang, B., Thornberry, N.A., Weber, A.E., 2014. J. Med. Chem. 57, 3205–3212.
Bigi, F., Chesini, L., Maggi, R., Sartori, G., 1999. J. Org. Chem. 64, 1033–1035.
Dey, B.B., Sankaranarayan, Y., 1934. J. Ind. Chem. Soc. 11, 687–689.
Dwivedi, A.P., Kumar, S., Varshney, V., Singh, A.B., Srivastava, A. K., Sahu, D.P., 2008. Bioorg. Med. Chem. Lett. 18, 2301–2305.
Hansen, L., Deacon, C.F., Orskov, C., Holst, J.J., 1999. Endocrinology 140, 5356–5363.
Kim, D., Wang, L., Beconi, M., Eiermann, G.J., Fisher, M.H., He, H., Hickey, G.J., Kowalchick, J.E., Leiting, B., Lyons, K., Marsilio, F., McCann, M.E., Patel, R.A., Petrov, A., Scapin, G., Patel, S.B., Roy, R.S., Wu, J.K., Wyvratt, M.J., Zhang, B.B., Zhu, L., Thornberry, N.A., Weber, A.E., 2005. J. Med. Chem. 48, 141–151.
Nabeno, M., Akahoshi, F., Kishida, H., Miyaguchi, I., Tanaka, Y., Ishii, S., Kadowaki, T., 2013. Biochem. Biophys. Res. Commun. 434, 191–196.
Nicolotti, O., Giangreco, I., Miscioscia, T.F., Carotti, A., 2009. J. Chem. Inf. Modell. 49, 2290–2302.
Pisani, L., Farina, R., Catto, M., Iacobazzi, R.M., Nicolotti, O., Cellamare, S., Mangiatordi, G.F., Denora, N., Soto-Otero, R., Siragusa, L., Altomare, C.D., Carotti, A., 2016. J. Med. Chem. 59, 6791–6806.
M.P. Repasky, M. Shelley, R.A. Friesner, 2007. Flexible Ligand Docking with Glide, Current Protocols in Bioinformatics, Unit 8.12 (Chapter 8).
Ripsin, C.M., Kang, H., Urban, R.J., 2009. Am. Fam. Phys. 79 (1), 29–36.
Sandhu, S., Bansal, Y., Silakari, O., Bansal, G., 2014. Bioorg. Med. Chem. 22, 3806–3814.
Schrodinger, LLC, 2015. The PyMOL Molecular Graphics System, Version 1.8.
Sena, C.M., Bento, C.F., Pereira, P., Seiça, R., 2010. EPMA J. 1, 138–163.
Shah, D.N., Shah, N.M., 1954. J. Org. Chem. 19, 1681–1685.
Sharma, R., Soman, S.S., 2015. Pharmanest 6, 2679–2684.
Sharma, R., Soman, S.S., 2016. Synth. Commun. 46, 1307–1317.
Sousa, C.M., Berthet, J., Delbaere, S., Coelho, P.J., 2012. J. Org. Chem. 77, 3959–3968.
Totrov, M., Abagyan, R., 2008. Curr. Opin. Struct. Biol. 18, 178–184.
v. QikProp, Schrödinger, LLC, 2009. New York, NY.
Villhauer, E.B., Brinkman, J.A., Naderi, G.B., Burkey, B.F., Dunning, B.E., Prasad, K., Mangold, B.L., Russell, M.E., Hughes, T.E., 2003. J. Med. Chem. 46, 2774–2789.
WHO, 2016. Diabetes Fact Sheet. World Health Organisation, March 2016.

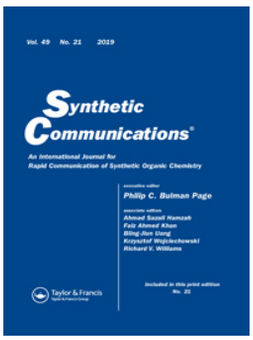

Taylor & Francis
Taylor & Francis Group

Synthetic Communications

An International Journal for Rapid Communication of Synthetic Organic Chemistry

ISSN: 0039-7911 (Print) 1532-2432 (Online) Journal homepage: https://www.tandfonline.com/loi/lsyc20

Evaluation of novel coumarin-proline sulfonamide hybrids as anticancer and antidiabetic agents

Sunil Dutt Durgapal & Shubhangi S. Soman

To cite this article: Sunil Dutt Durgapal & Shubhangi S. Soman (2019) Evaluation of novel coumarin-proline sulfonamide hybrids as anticancer and antidiabetic agents, Synthetic Communications, 49:21, 2869-2883, DOI: 10.1080/00397911.2019.1647439

To link to this article: https://doi.org/10.1080/00397911.2019.1647439

SYNTHETIC COMMUNICATIONS®
2019, VOL. 49, NO. 21, 2869–2883
https://doi.org/10.1080/00397911.2019.1647439

Taylor & Francis
Taylor & Francis Group

Evaluation of novel coumarin-proline sulfonamide hybrids as anticancer and antidiabetic agents

Sunil Dutt Durgapal and Shubhangi S. Soman

Department of Chemistry, Faculty of Science, M. S. University of Baroda, Vadodara, India

ABSTRACT

Cancer and diabetes are considered as two major diseases affecting human health worldwide. Various therapies are available for treatment of cancer and diabetes individually, peptide linkage containing proline sulfonamide can be a promising therapy for treatment of both cancer as well as diabetes. Here, we report design and synthesis of novel coumarin-proline sulfonamide derivatives as anticancer and antidiabetic agents. All the synthesized compounds were screened for their anticancer activity against lungs cancer cell line (A549) and breast cancer cell line (MCF7) using 3-(4,5-dimethylthiazol-2-yl)-2,5-diphenyltetrazolium bromide dye (MTT)assay and antidiabetic activity using DPP-IV inhibition assay. Compound **16b** showed excellent activity against breast cancer cell line (MCF7) with IC_{50} value of 1.07 μM. All compounds showed moderate DPP-IV inhibition.

GRAPHICAL ABSTRACT

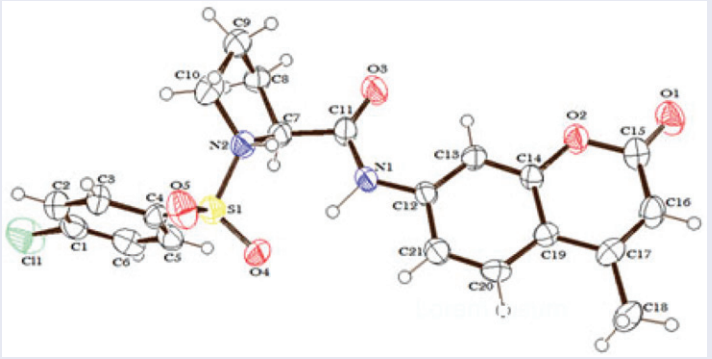

ARTICLE HISTORY
Received 25 April 2019

KEYWORDS
Aminocoumarin; anticancer; DPP-IV inhibitor; proline; sulfonamide

Introduction

Cancer and diabetes are two major diseases affecting human health worldwide. Cancer is considered as fatal disease, while type 2 diabetes is considered as one of the major threat to human health. According to WHO, around 18.1 million new cases of cancer

CONTACT Shubhangi S. Soman shubhangiss@rediffmail.com Department of Chemistry, Faculty of Science, M. S. University of Baroda, Vadodara 390 002, India

Supplemental data for this article can be accessed on the publisher's website.
Color versions of one or more of the figures in the article can be found online at www.tandfonline.com/lsyc.

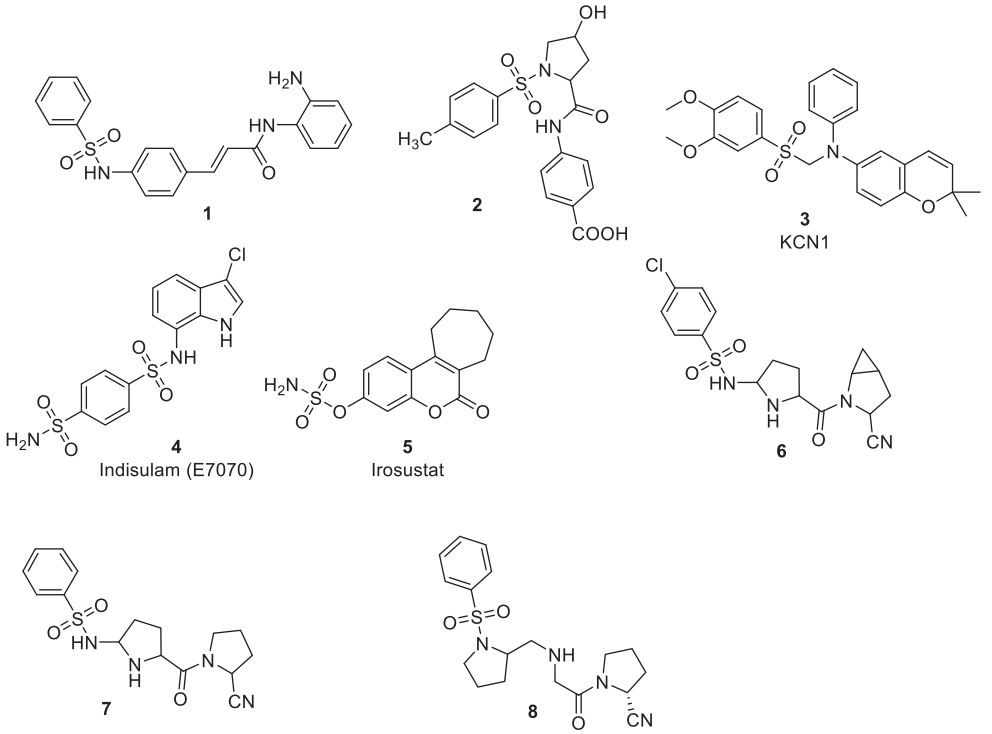

Figure 1. Sulfonamide derivatives **1–8** with anticancer and antidiabetic activity.

and 9.6 million cancer death was estimated to occur only in 2018.[1] In last few decades, there are several reports on development of sulfonamide derivatives with various biological activities. Sulfonamide derivatives are known for its antimicrobial, carbonic anhydrase, antitumor, and antidiabetic activities.[2–4] Various sulfonamide derivatives **1–8** having anticancer and antidiabetic activities are shown in Figure 1. Compound **1** (Figure 1) studied for histone deacetylase (HDAC) inhibitors that can induce hyperacetylation of histones in human cancer cells, which blocks the cell cycle and induce apoptosis in human cancer cells but not in normal cells.[5,6] Indisulam 4 (Figure 1) is a novel sulfonamide anticancer agent in clinical development for treatment of solid tumor, which includes renal, breast and colorectal cancer.[7,8] Dipeptidyl peptidase IV (DPP-IV E.C.3.3.145, CD 26) is a serine protease enzyme formed in various tissues and body fluids of mammals. It plays important roles in variety of disease like autoimmune disease, AIDS, and melanoma. DPP-IV is associated with glucose metabolism, immune regulation, signal transduction and apoptosis and regulating cancer. Compounds **6–8** (Figure 1) have been reported as potent DPP-IV inhibitors.[9–11]

The findings from meta-analysis indicated positive association between diabetes primarily Type II diabetes and breast cancer risk. Results showed that women with diabetes may have 20% increased risk of breast cancer. The association between diabetes and breast cancer was consistent for case–control and cohort studies and for studies carried out in North America, Europe, and Asia.[12,13] In diabetic patients, cancer may be favored by two types of mechanisms: (i) general mechanisms that promote cancer

initiation or progression in any organ due to hyperglycemia, hyperinsulinemia or drugs that affect all tissues, (ii) site-specific mechanisms affecting cancerogenesis of a particular organ.[14]

Metformin is one of the most widely prescribed drugs for the treatment for type 2 diabetes and also used in cardiovascular disease prevention.[15] Epidemiological observations have suggested that the use of metformin in diabetes mellitus patients is correlated with a reduction in cancer incidence.[16]

Coumarin is a class of natural and synthetic compound which shows versatile pharmacological activities like anticarcinogenic,[17] antiviral,[18] antimicrobial,[19] antidepressant,[20] antinflamatory,[21] antioxidant,[22] antidiabetic,[23] etc. Several compounds containing coumarin scaffold are clinically well-known agents.[24–26]

In our previous study, we did several modifications on third and seventh position of coumarin, which led to excellent anticancer activity and antidiabetic activity.[23,27,28] Keeping in mind the activity of various coumarin derivatives and sulfonamides and in continuation of our work on designing new compounds with anticancer and antidiabetic activity, we have designed pharmacophore which can have binary application. Hereby we report synthesis of coumarin proline sulfonamide hybrids to get a potent compound having both anticancer and antidiabetic activity. All the compounds were screened for their in vitro anticancer activity using MTT assay and antidiabetic activity as DPP-IV inhibition assay.

Results and discussion

In search of some novel compounds with potent anticancer activity and antidiabetic activity, compounds **16a–c** have been synthesized from 7-amino-4-methylcoumarin **12** (Scheme 1). Compound **12** was synthesized in three steps starting with carbamate protected 3-aminophenol **10**, which on Pechmann reaction with ethyl acetoacetate in 70% ethanolic sulfuric acid gave 7-carboethoxy amino coumarin **11** followed by deprotection in sulfuric acid/acetic acid (1:1) to give 7-amino-4-methyl coumarin **12**. (L)-N-Boc-proline **13** was first stirred with ethyl chloroformate in tetrahydrofuran (THF) at 0–5 °C followed by dropwise addition of solution of compound **12** and triethylamine (TEA) in THF, which further refluxed for 8 hours to give compound **14**. Deprotection of Boc group in compound **14** was carried out using trifluoroacetic acid (TFA) to give compound **15**. Compound **15** was reacted with different benzene sulfonyl chloride derivatives at room temperature using $NaHCO_3$ in DCM:water (1:1) gave compounds **16a–c** (Scheme 1).

^{1}H-NMR spectra of compound **14** showed peak at δ 1.53 ppm for nine protons of three methyl groups of Boc. Proline protons were observed in region from δ 1.92 to 4.55 and methyl protons of coumarin at δ 2.27. Aromatic protons were observed in region from δ 6.03 to 7.70 and amide proton was observed at 10.04 ppm. ^{13}C-NMR spectra of compound **14** showed peaks in region from 18.41 to 80.95 for aliphatic carbons of boc group and proline moiety, while aromatic carbons were observed from δ 106.84 to 155.78 ppm and carbonyl carbon of amide and lactone ring of coumarin at 161.17 and 171.36 ppm, respectively. The proton NMR of Boc-deprotected compound **15** exhibited different peaks at δ 1.77–2.81 ppm for aliphatic protons of proline, –NH

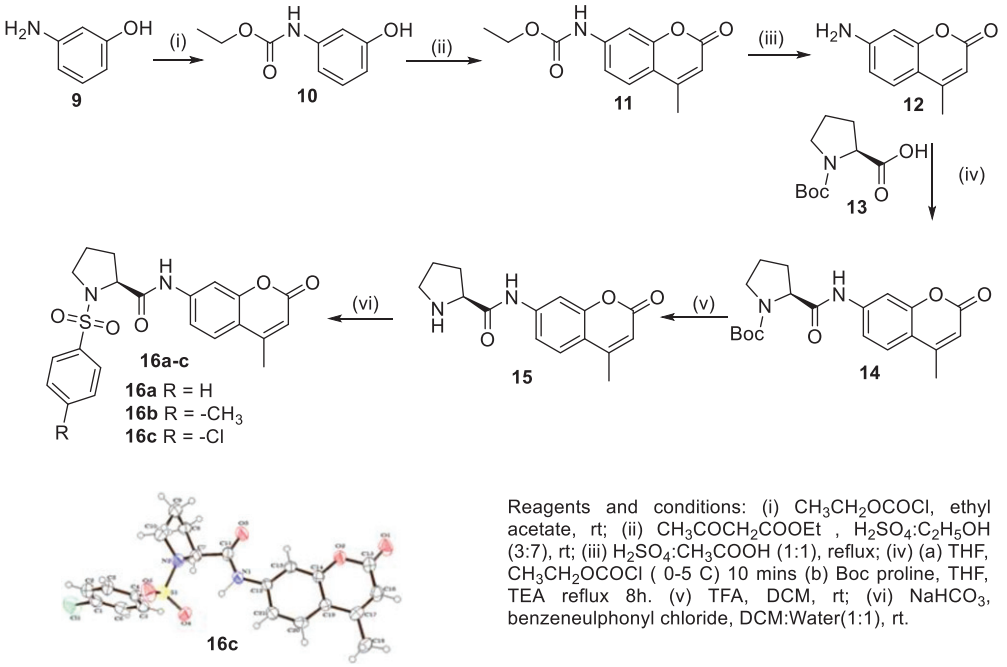

Scheme 1. Synthesis of 7-Amino-4-methylcoumarin derivatives **16a–c**.

proton as broad singlet around δ 2.12 ppm, methyl group of coumarin at δ 2.41 ppm. Protons of proline next to nitrogen were observed at δ 2.98–3.08, 3.01–3.14 and 3.91 ppm. Aromatic protons of coumarin ring were observed in the region of δ 7.51–7.64 ppm and amide proton at δ 10.05 ppm. In ^{13}C-NMR spectrum of compound **15** showed peaks at δ 18.67–61.02 ppm for carbons of methyl group and proline ring, peaks at δ 106.66–154.32 ppm for aromatic carbons and peak at δ 161.24 ppm for amide carbonyl and 174.08 ppm for carbonyl carbon of lactone ring. In IR spectrum of compound **15** showed bands at 3304–3082 cm^{-1} is for N–H and C–H stretching, bands at 1724 cm^{-1} and 1679 cm^{-1} corresponds to lactone carbonyl and amide functional groups respectively.

The structures of compounds **16a–c** were confirmed by its IR, ^{1}H-NMR, ^{13}C-NMR and ESI-MS analyses. ^{1}H-NMR of compound **16c** exhibited peaks at δ 1.61–4.21 for aliphatic protons, peaks at δ 6.23–7.85 for aromatic protons and peak at δ 9.02 ppm for amide proton. ^{13}C spectrum of compound **16c** showed peaks at δ 18.65–63.03 for aliphatic carbons and the peaks for aromatic carbons were observed in the range of 107.55–154.28 ppm. Amide carbonyl carbon was observed at 161.04 ppm and lactone carbonyl carbon was observed at 169.09 ppm. IR spectrum of compound **16c** showed one band at 3338 cm^{-1} for –NH stretching vibrations and band at 1716 and 1695 cm^{-1} is for carbonyl stretching of lactone and amide, respectively. Sulfonamide group showed peak at 1226–1201 cm^{-1}. Mass spectrum of compound **16c** showed $[M+H]^{+}$ peak at 477. The structure of **16c** was also confirmed by its single crystal analysis with CCDC number 1876142.

Similar set of proline sulfonamide hybrid compounds **28a–c** and **29a–c** were synthesized from 3–aminocoumarin **21–22** (Scheme 2). 3-Aminocoumarins **21–22** were

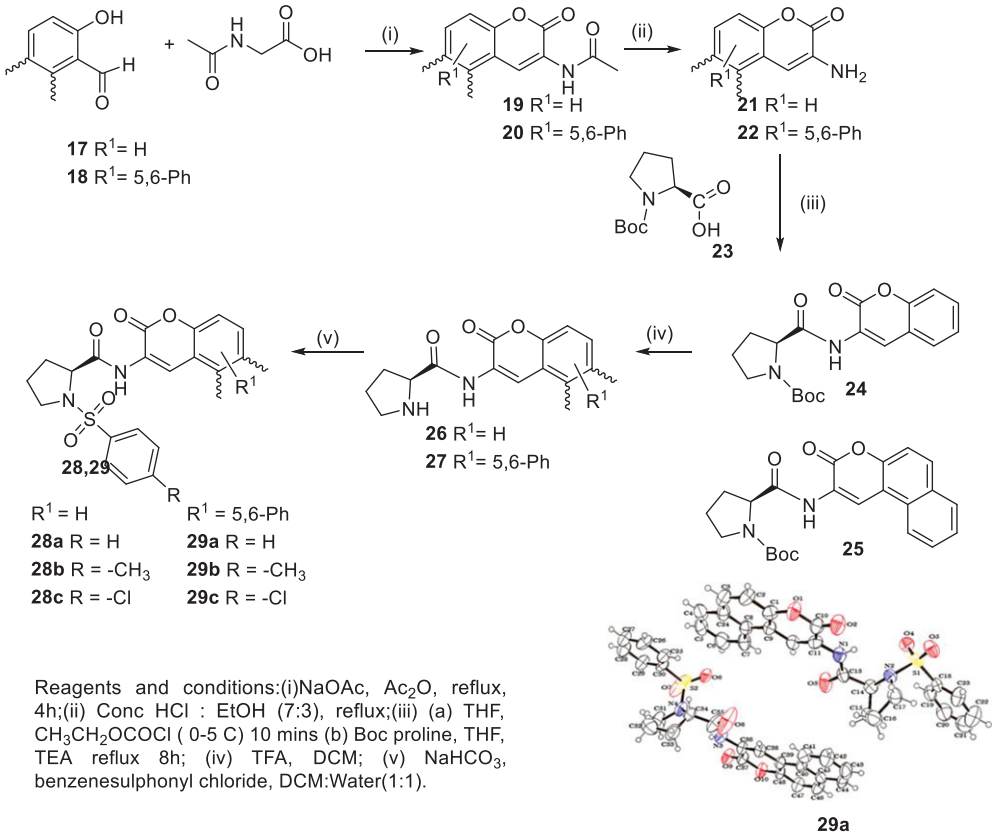

Scheme 2. Synthesis of 3-Aminocoumarin derivatives **28a–c** and **29a–c**.

synthesized using Perkin reaction of o-hydroxy benzaldehyde **17** or *β*-hydroxy naphthaldehyde **18** with N-acetyl glycine in presence of sodium acetate and acetic anhydride to give 3-acetamido coumarin derivatives **19–20**, followed by hydrolysis of acetyl group using ethanol: conc. HCl (7:3) to yield compounds 3-amino-2H-chromen-2-one (**21**) and 2-amino-3H-benzo[f]chromen-3-one (**22**). Compounds **28a–c** and **29a–c** were synthesized from compounds **21–22** using similar set of reaction conditions as discussed for synthesis of 7-amino coumarin derivatives **16a–c** from compound **15**. All compounds **28a–c** and **29a–c** were well characterized using spectral techniques such as ^{1}H-NMR, ^{13}C-NMR, IR and ESI-MS.

The ^{1}H-NMR spectrum of representative compound **28c** showed multiplet at δ 1.84 and singlet at δ 2.27 for protons at third and fourth position of proline ring, multiplet at δ 3.30 and singlet at δ 3.61 were observed for the protons at fifth position of proline ring and doublet at δ 4.31 was observed for second position proton of proline ring. Aromatic protons were observed in the region from δ 7.29 to 8.67 ppm and sharp singlet for amide proton at δ 9.29 distinctively. ^{13}C-NMR of compound **28c** showed proline ring carbons at δ 24.69, 30.54, 49.89, 62.75, aromatic region carbons from δ 116.45 to 150. Carbonyl carbon of amide and lactone were observed at δ 158.41 and δ 170.60 ppm, respectively.

Table 1. Anticancer activity against A549 (Lungs cancer cell line), MCF-7 (Breast cancer cell line) for coumarin-proline sulfonamide hybrid derivatives.

		IC_{50} in μM[a]	
Compound	R	A549	MCF-7
15		2.34	5.42
16a	H	18.09	2.58
16b	$-CH_3$	27.54	1.07
16c	–Cl	27.32	7.05
26		12.40	17.14
28a	H	9.34	4.39
28b	$-CH_3$	NA	7.759
28c	–Cl	7.39	3.81
27		3.75	11.74
29a	H	19.95	22.94
29b	$-CH_3$	11.95	7.37
29c	–Cl	23.09	50.99
Fluorouracil		11.13	45.04

NA: not active.
[a]IC_{50} values were determined based on MTT assay using GraphPad Prism software.

In IR spectrum of compound **28c** bands for N-H and C-H stretching were observed at 3311 and 3093 cm^{-1}, carbonyl stretching for lactone at 1724 and amide at 1693 cm^{-1}, respectively. The ESI-MS at 433.00 $[M+H]^+$ confirms the formation of desired compound **28c**. Formation of compound **29a** was also confirmed by its single crystal X-ray analysis (CCDC NO: 1876145)

Anticancer activity

Coumarin-proline sulfonamide hybrids **16a–c**, **28a–c** and **29a–c** were synthesized from 7-amino-4-methyl coumarin and 3-amino coumarin having one electron withdrawing group, electron releasing group and without any group on benzene sulfonamide. All compounds **16a–c**, **28a–c** and **29a–c** were screened initially for their anticancer activity using MTT assay against A549 (Lungs cancer cell line), MCF-7 (Breast cancer cell line) and compared with fluorouracil. Anticancer activity of coumarin-proline sulfonamide hybrids were also compared with their precursor coumarin-proline derivatives **15** and **26–27**.

Compound **15** with proline linked to 7-amino-4-methyl coumarin, showed good activity against both A549 and MCF7 cancer cell line with IC_{50} values 2.34 μM and 5.42 μM (Table 1). Compound **16a** with benzene sulfonamide group, showed drop in activity against A549 cell line, while showed good activity in MCF7 cell line with IC_{50} value of 2.58 μM. Methyl substitution on benzene ring at para to sulfonamide group in compound **16b** resulted in loss of activity against A549 cell line, but showed excellent activity with IC_{50} 1.07 μM against MCF7 cell line (Table 1). Compound **16c** with 4-chlorobenzene sulfonamide, showed moderate activity against both tested cell lines.

3-Aminocoumarin-proline hybrid compound **26** showed moderate activity against both the tested cell lines. While benzene sulfonamide derivative **28a** showed relatively good activity compared to compound **26** against both tested cell lines. Compound **28b**

Table 2. DPP-IV inhibition activity of amino coumarin-proline sulfonamide derivative **16a–c**, **28a–c** and **29a–c**.

	% DPP-4 enzyme inhibition activity[a]		
Compounds	25 μM	50 μM	100 μM
16a	11.11	16.29	19.36
16b	5.05	7.54	13.96
16c	10.90	17.08	20.76
28a	9.87	13.60	20.17
28b	13.76	19.36	20.73
28c	13.04	18.67	22.00
29a	7.06	10.44	14.32
29b	9.12	12.90	16.02
29c	11.68	15.31	19.79
Vildagliptin		56.3 % at 0.1μM	

[a]DPP-IV inhibitory activity determined by fluorescence-based assay was measured using Spectra Max fluorometer (Molecular Devices, CA). Values of % inhibition are mean of three independent determinations at 25, 50 and 100 μM concentrations of the test samples.

showed moderate activity against MCF7 cell line and lost the activity against A549 cell line (Table 1).

However, 4-chlorobenzene sulfonamide compound **28c** exhibited good activity with IC_{50} value of 7.39 μM and 3.81 μM against A549 and MCF7 cell lines, respectively. Compound **27** with extension of aromatic ring on amino coumarin part as compared to compound **26**, showed good activity against A549 cell line with IC_{50} value of 3.75 μM and moderate activity against MCF7 cancer cell line (Table 1). Interestingly, conversion of compound **27** to substituted benzene sulfonamide derivatives **29a–c** resulted in loss of activity against both tested cancer cell lines.

DPP-IV inhibition activity

Recently, coumarin containing compounds have been reported with very good DPP-IV inhibition activity. Interestingly, position of attachment with coumarin moiety and type of attachment showed drastic effect on DPP-IV inhibition activity of coumarin containing compounds. Proline containing derivatives as substrate like inhibitors are known and reported with excellent DPP-IV inhibition activity. As these compounds **16a–c**, **28a–c** and **29a–c** are hybrid of coumarin-proline and sulfonamide, they were also selected to screen for their initial DPP-IV inhibition activity at three different concentrations of 25, 50 and 100 μM and compared with Vildagliptin.

Compound with 7-amino-4-methyl coumarin with proline sulfonamide **16a** showed poor activity with 19.36% DPP-IV inhibition at 100 μM concentration, substituting methyl group on para position of benzene ring of sulfonamide resulted in compound **16b** with decrease in activity with 13.96% DPP-IV inhibition at 100 μM (Table 2). Change of methyl group by chloro resulted in compound **16c** slightly increase in DPP4 inhibition of 20.76% in 100 μM concentration. Change of attachment of proline-sulfonamide moiety with coumarin from seventh positions to third position did not show much change in DPP-IV inhibition activity for compounds **28a–c**. 3-Aminocoumarin analogs of proline-sulfonamide derivatives compound **28a** showed poor activity with 20.17% inhibition at 100 μM concentration. Compound **28b** with para-methyl and **28c**

with para-chloro on benzene sulfonamide showed moderate DPP4 inhibition at 100 µM (Table 2).

Further, extension of aromatic ring on 3-aminocoumarin resulted in compound **29a–c** with 3-aminobenzocoumarin proline-sulfonamide derivatives. Compounds **29a–c** were also showed similar trend of inhibitions with moderate activity at all three tested concentrations. All synthesized compounds were compared with standard drug vildagliptin with 56.3% inhibition at 0.1 µM concentration.

Conclusion

In this work, novel amino coumarin-proline sulfonamide hybrids were synthesized and their *in vitro* anticancer activity and DPP-IV inhibition activity were evaluated. Among the tested compounds almost all compounds showed moderate activity in A549 cell line and excellent activity in MCF7 cancer cell line. Compounds were also screened for their DPP-IV inhibition activity, Compounds **16a–c, 28a–c** and **29a–c** were found to be inactive. The active compounds could be considered as useful templates for further development to obtain more potent anticancer agents.

Experimental

General procedure for preparation of coumarin tert-butyl pyrrolidine-1-carboxylate derivatives (14, 24, 25)

To an ice cold solution of ethyl chloroformate (2.55 mmol) in THF, the mixture of N-Boc proline **13** (1.5 mmol) and TEA (1.5 mmol) in THF (10 mL) was added dropwise followed by stirring for 10–15 min. To this mixture, the solution of aminocoumarin **12/21/22** (1.5 mmol) and TEA (1.5 mmol) in THF (20 mL) was added dropwise over a period of 30 min at 0–5 °C. The resulting mixture was stirred for another 30 min at 0–5 °C, brought to room temperature and then refluxed for 8 h at 60 °C. The completion of reaction was monitored by TLC. After completion of reaction, solvents were removed under reduced pressure to give residue. The residue was dissolved in dichloromethane (DCM). The organic layer was washed with water, dil. HCl and sodium bicarbonate. The organic layer was dried over sodium sulfate, and concentrated to give compound. The product was used in next step without any further purification.

Characterization data for Boc-protected compounds 14, 24, and 25

Tert-Butyl 2-((4-methyl-2-oxo-2H-chromen-7-yl)carbamoyl)pyrrolidine-1-carboxylate (14). Pale yellow solid, Yield: 78%; *M.P*: 165–168 °C; IR (KBr) 3312, 3055, 2976, 2891, 1718, 1689, 1622, 1577, 1531, 1448, 1406, 1390, 1369, 1269, 1215, 1174, 1126, 1068, 1016, 904, 881, 829, 773, 754, 711, 638, 576, 524 cm^{-1}; ^{1}H-NMR(400 MHz, $CDCl_3$): δ 1.53 (s, 9 H), 1.92–1.98 (m, 1 H), 2.08 (br s, 2 H), 2.27 (br s, 1 H) 2.34 (s, 3 H), 3.43–3.45 (m, 1 H), 3.56–3.61 (m, 1 H), 4.56 (br s, 1 H), 6.03 (s, 1 H), 6.99 (d, $J = 7.6$ Hz, 1 H), 7.33 (d, $J = 8.4$ Hz, 1 H), 7.70 (s, 1 H), 10.04 (s, 1 H); ^{13}C-NMR(100 MHz, $CDCl_3$): δ ppm 18.41, 24.56, 28.48, 29.12, 47.35, 60.57, 80.95, 106.84, 112.83, 115.14, 115.31, 124.57, 141.74,

152.52, 153.76, 155.78, 161.17, 171.36; Anal. Calc. for $C_{20}H_{24}N_2O_5$; C,64.50; H, 6.50; N, 7.52; found: C, 64.58; H, 6.61; N, 7.45%; ESI-MS: 373.10 $[M+H]^+$.

Tert-Butyl 2-((2-oxo-2H-chromen-3-yl)carbamoyl)pyrrolidine-1-carboxylate (24). Pale yellow solid, Yield: 81%; *M.P*: 138–140 °C; IR (KBr) 3365, 3250, 3211, 3045, 2972, 2931, 2877, 2866, 1730, 1697, 1674, 1626, 1608, 1537, 1477, 1458, 1452, 1404, 1352, 1294, 1263, 1197, 1188, 1172, 1126, 1101, 1030, 981, 956, 923, 910, 881, 856, 763, 721 cm^{-1}; ^{1}H-NMR(400 MHz, $CDCl_3$): δ 1.50 (s, 9 H), 1.95–2.06 (m, 2 H), 2.23–2.36 (m, 2 H), 3.40–3.54 (m, 2 H), 4.33–4.49 (m, 1 H), 7.42 (br s, 2 H), 7.47 (m, 2 H), 8.65 (s, 1 H), 9.39 (s, 1 H); ^{13}C-NMR (100 MHz, $CDCl_3$): δ ppm 24.60, 28.32, 47.15, 61.03, 61.81, 81.11, 116.32, 119.78, 123.35, 124.23, 125.04, 127.73, 129.51, 150.02, 158.42, 171; Anal. Calc. for $C_{19}H_{22}N_2O_5$; C,63.68; H, 6.19; N, 7.82; found: C, 63.61; H, 6.31; N, 7.96%; ESI-MS: 359.10 $[M+H]^+$.

Tert-Butyl 2-((3-oxo-3H-benzo[f]chromen-2-yl)carbamoyl)pyrrolidine-1-carboxylate (25). Pale yellow solid, Yield: 76%; *M.P*: 192–196 °C; IR (KBr) 3382, 3340, 3069, 2972, 2897, 1715, 1687, 1589, 1575, 1516, 1462, 1437, 1408, 1344, 1253, 1220, 1193, 1111, 1088, 996, 974, 951, 806, 779 cm^{-1}; ^{1}H-NMR(400 MHz, $CDCl_3$): δ 1.55 (s, 9 H), 1.68 (s, 2 H), 1.97–2.32 (m, 1 H), 2.44 (s, 1 H), 3.46–3.60 (m, 2 H), 4.41–4.56 (m, 1 H), 7.46 (d, $J = 8.8$ Hz, 1 H), 7.58–7.61 (m, 1 H), 7.68–7.72 (m, 1 H), 7.91 (d, $J = 8.4$ Hz, 2 H), 8.33 (d, $J = 8.0$ Hz, 1 H), 9.53 (s, 1 H); ^{13}C-NMR(100 MHz, $CDCl_3$): δ ppm 24.69, 24.91, 28.38, 47.24, 61.08, 81.20, 114.14, 116.35, 116.43, 119.50, 119.61, 122.36, 124.06, 126.15, 126.25, 127.92, 128.81, 129.07, 130.66, 130.89, 148.93, 158.59, 169.59.; Anal. Calc. for $C_{23}H_{24}N_2O_5$; C, 67.63; H, 5.92; N, 6.86; found: C, 67.68; H, 5.99; N, 6.93%.

General procedure for Boc-deprotection

To a solution of compound **14/24/25** (1.0 mmol), DCM (10 mL) was added trifloroacetic acid (TFA) (0.1 mL). The resulting solution was stirred at room temperature for overnight. The completion of reaction was monitored by TLC. After completion of reaction, reaction mixture was concentrated to give residue. The residue was taken in water, neutralized with saturated $NaHCO_3$ solution, and extracted with DCM (3×15 mL). The organic layer was dried over anhydrous Na_2SO_4, filtered and concentrated to give compound **15/26/27** as solid. The product was used in next step without any further purification. (Yield = 96–98%).

Characterization data for Boc-deprotected compounds 15, 26, and 27

N-(4-Methyl-2-oxo-2H-chromen-7-yl)pyrrolidine-2-carboxamide (15). Light pink solid, Yield: 98%; *M.P*: 152–154 °C; IR (KBr) 3304, 3272, 3173, 3082, 2961, 2930, 2864, 1689, 1616, 1595, 1524, 1443, 1392, 1347, 1326, 1272, 1222, 1177, 1112, 1020, 963, 873, 845, 719 cm^{-1}; ^{1}H-NMR(400 MHz, $CDCl_3$): δ 1.77–1.85 (m, 2 H), 2.04–2.12 (m, 2 H), 2.21–2.28 (m, 1 H), 2.41 (d, $J = 1.2$ Hz, 3 H), 2.99–3.05 (m, 1 H), 3.10–3.14 (m, 1 H), 3.91 (dd, $J = 9.2$, 5.2 Hz, 1 H), 6.19 (s, 1 H), 7.53 (d, $J = 8.4$ Hz, 1 H), 7.59 (dd, $J = 8.4$, 2.0 Hz, 1 H), 7.64 (d, $J = 1.6$ Hz, 1 H), 10.05 (s,1H); ^{13}C-NMR (100 MHz, $CDCl_3$): δ ppm 18.67, 26.41, 30.76, 47.42, 61.02, 106.66, 113.26, 115.27, 115.94, 125.22, 141.09, 152.31,

154.32, 161.24, 174.08; Anal. Calc. for $C_{15}H_{16}N_2O_3$; C, 66.16; H, 5.92; N, 10.29; found: C, 66.29; H, 5.98; N, 10.38%

N-(2-Oxo-2H-chromen-3-yl)pyrrolidine-2-carboxamide (26). Pale yellow solid, Yield: 96%; *M.P*: 145–158 °C; IR (KBr) 3187, 3073, 2947, 2876, 1724, 1679, 1619, 1546, 1501, 1453, 1415, 1361, 1317, 1293, 1200, 1131, 1039, 1005, 947, 884, 863, 832, 799, 751 cm^{-1}; ^{1}H-NMR(400 MHz, $CDCl_3$): δ 1.79–1.86 (m, 2 H), 2.01–2.09 (m, 1 H), 2.25–2.33 (m, 1 H), 3.13–3.16 (m, 2 H), 4.06 (br s, 1 H), 7.25–7.33 (m, 2 H), 7.41–7.46 (m, 2 H), 8.68 (s, 1 H), 10.41 (s, 1 H); ^{13}C-NMR (100 MHz, CDCl3): δ ppm 26.16, 30.87, 47.33, 61.00, 116.32, 119.84, 123.19, 123.91, 125.02, 127.71, 129.54, 150.14, 158.59, 174.97; Anal. Calc. for $C_{14}H_{14}N_2O_3$; C, 65.11; H, 5.46; N, 10.85; found: C, 65.19; H, 5.58; N, 10.98%

N-(3-Oxo-3H-benzo[f]chromen-2-yl)pyrrolidine-2-carboxamide (27). Pale white solid, Yield: 92%; *M.P*: 250–255 °C; IR (KBr) 3390, 3111, 2881, 2710, 2649, 2559, 2505, 2442, 1722, 1689, 1587, 1548, 1513, 1461, 1438, 1420, 1402, 1387, 1338, 1315, 1248, 1227, 1197, 1128, 1101, 900, 813, 782, 754 cm^{-1}; ^{1}H-NMR(400 MHz, $CDCl_3$): δ 1.94–2.05 (m, 3 H), 2.49–2.50 (m, 1 H), 3.34 (m, 2 H), 4.64–4.68 (m, 1 H), 7.59–7.67 (m, 2 H), 7.76 (t, $J = 7.2$ Hz, 1 H), 8.08 (d, $J = 8$ Hz 1 H), 8.13 (d, $J = 8.8$ Hz 1 H), 8.23 (d, $J = 8.8$ Hz 1 H), 9.36 (s, 1 H), 10.69 (s, 1 H); ^{13}C-NMR (100 MHz, $CDCl_3$): δ ppm 24.04, 30.44, 46.27, 59.88, 113.45, 116.82, 122.03, 122.52, 124.34, 126.66, 128.76, 128.83, 129.49, 130.68, 131.88, 149.66, 157.57, 169.49; Anal. Calc. for $C_{18}H_{16}N_2O_3$; C, 70.12; H, 5.23; N, 9.09; found: C, 70.24; H, 5.34; N, 9.15%; ESI-MS: 309 $[M + H]^+$.

General procedure for synthesis of coumarin-benzenesulphonamide derivatives 16a–c, 28a–c, and 29a–c

To a solution of compound **15** (1.0 mmol) and sodium bicarbonate (3.0 mmol) in dichloro methane (DCM): water (1:1) (25 mL) un/substituted benzenesulphonyl chloride (1.1 mmol) was added. The resulting mixture was stirred at room temperature for 18 h. The completion of reaction was monitored by TLC. After completion of the reaction, the reaction mixture was concentrated to give residue. The residue was neutralized with dil HCl, filtered, washed with water (3 × 5 mL), pet.ether (5 mL) and dried to give compounds **16a–c**. 3-Aminocoumarin derivatives **28a–c** and **29a–c** were synthesized using same procedure as used for compound**16a–c**.

Characterization data for compounds 16a–c, 28a–c, and 29a–c

N-(4-Methyl-2-oxo-2H-chromen-7-yl)-1-(phenylsulfonyl)pyrrolidine-2-carboxamide (16a). Pale white solid, Yield: 89%; *M.P*: 225–228 °C; IR (KBr) 3313, 3194, 3068, 2953, 2872, 1718, 1695, 1616, 1579, 1570, 1523, 1444, 1417, 1390, 1348, 1309, 1217, 1166, 1093, 1070, 1008, 995, 893, 854, 752, 723 cm^{-1}; ^{1}H-NMR (400 MHz, $CDCl_3$): δ 1.29–1.81 (m, 3 H), 2.45 (s, 4 H), 3.29–3.33 (m, 1 H), 3.70 (s, 1 H), 4.24–4.27 (m, 1 H), 6.24 (s, 1 H), 7.31–7.47 (m, 1 H), 7.56–7.74 (m, 4 H), 7.85–7.95 (m, 3 H), 9.11 (s, 1 H); ^{13}C-NMR (100 MHz, $CDCl_3$): δ ppm 19.15, 25.10, 30.09, 50.80, 63.60, 77.00, 78.27, 108.10, 114.21, 116.35, 116.99, 125.69, 128.47, 130.16, 134.39, 135.96, 141.32, 152.70,

154.87,161.60, 169.96;; Anal. Calc. for $C_{21}H_{20}N_2O_5S$; C, 61.15; H, 4.89; N, 6.79; S, 7.77; found: C, 61.23, H, 4.92; N, 6.91; S, 7.86; ESI-MS: 413.05 $[M+H]^+$.

N-(4-Methyl-2-oxo-2H-chromen-7-yl)-1-tosylpyrrolidine-2-carboxamide (16b). Pale white solid, Yield: 86%; *M.P*: 216–220 °C; IR (KBr) 3562, 3369, 3290, 3140, 3059, 2987, 2953, 2891, 1724, 1697, 1689, 1618, 1597, 1568, 1523, 1506, 1440, 1411, 1396, 1346, 1332, 1313, 1294, 1157, 1182, 1093, 1003, 966, 941, 871, 827, 756, 725 cm^{-1}; ^{1}H-NMR(400 MHz, $CDCl_3$): δ 1.60–1.70 (m, 2 H), 1.82–1.84 (m, 1 H), 2.35–2.43 (m, 1 H), 2.44 (s, 3 H), 2.48 (s, 3 H), 3.25–3.30 (m, 1 H), 3.64–3.69 (m, 1 H), 4.20 (dd, $J = 8.8$, 2.8 Hz, 1 H), 6.24 (s,1H), 7.40–7.44 (m, 3 H), 7.56 (d, $J = 8.4$ Hz, 1 H), 7.78 (d, $J = 8.0$ Hz, 2 H), 7.84 (d, $J = 2.0$ Hz, 1 H), 9.11 (s, 1 H); ^{13}C-NMR (100 MHz, $CDCl_3$): δ ppm 18.65, 21.67, 24.52, 29.42, 50.27, 62.99, 107.52, 113.66, 115.75, 116.41, 125.11, 127.95, 130.22, 132.14, 140.71, 144.95, 152.12, 154.30, 161.09, 169.45; Anal. Calc. for $C_{22}H_{22}N_2O_5S$; C, 61.96; H, 5.20; N, 6.57; S, 7.52; found: C, 61.81; H, 4.98; N, 6.34; S, 7.48% ESI-MS: 427.10 $[M+H]^+$.

1-((4-Chlorophenyl)sulfonyl)-N-(4-methyl-2-oxo-2H-chromen-7-yl)pyrrolidine-2-carboxamide (16c). Pale white solid, Yield: 87%; *M.P*: −230–234 °C; IR (KBr) 3338, 3196, 3111, 3059, 2991, 2868, 1716, 1695, 1622, 1579, 1533, 1475, 1460, 1437, 1415, 1388, 1338, 1267, 1226, 1180, 1157, 1087, 1064, 1026, 1008, 974, 922, 850, 860, 761 cm^{-1}; ^{1}H-NMR(400 MHz, $CDCl_3$): δ 1.61–1.76 (m, 2 H), 1.87 (br s, 1 H) 2.43 (s, 4 H), 3.21–3.27 (m, 1 H), 3.67–3.71 (m, 1 H), 4.19 (d, $J = 6.8$ Hz, 1 H), 6.23 (s, 1 H), 7.44 (d, $J = 7.6$ Hz, 1 H), 7.55–7.60 (m, 3 H), 7.84–7.86 (m, 3 H), 9.01 (s, 1 H); ^{13}C-NMR (100 MHz, $CDCl_3$): δ ppm 18.65, 24.53, 29.59, 50.29, 63.03, 107.55, 113.72, 115.75, 116.49, 125.16, 129.30, 129.94, 133.73, 140.61, 152.12, 154.28, 161.04, 169.09; Anal. Calc. for $C_{21}H_{19}ClN_2O_5S$; C, 56.44; H, 4.29; N, 6.27; S, 7.17, found: C, 56.60; H, 4.32; N, 6.18; S, 7.30; ESI-MS: 447.00 $[M+H]^+$.

N-(2-Oxo-2H-chromen-3-yl)-1-(phenylsulfonyl)pyrrolidine-2-carboxamide (28a). Pale white solid, Yield: 92%; *M.P*: 186–188 °C; IR (KBr) 3350, 3084, 3064, 3037, 2985, 2937, 2872, 1724, 1693, 1626, 1602, 1572, 1518, 1460, 1444, 1363, 1350, 1309, 1294, 1257, 1222, 1180, 1165, 1132, 1111, 1091, 1074, 1049, 1004, 995, 968, 947, 923, 904, 860, 850, 773, 759, 721 cm^{-1}; ^{1}H-NMR(400 MHz, $CDCl_3$): δ 1.73 (m, 1 H), 1.86–1.88 (m, 2 H), 2.3–2.4 (m,1H), 3.29–3.36 (m, 1 H) 3.60–3.65 (m, 1 H), 4.34 (dd, $J = 8.4$, 3.0 Hz, 1 H), 7.29–7.31 (dt, $J = 7.6$, 1.2 Hz, 1 H), 7.35 (br, d, $J = 8.00$ Hz, 1 H), 7.45–7.49 (m, 1 H), 7.51 (dd, $J = 8$, 1.4 Hz, 1 H), 7.59–7.63 (m, 2 H), 7.67–7.70 (m, 1 H), 7.95–7.97 (m, 2 H), 8.69 (s, 1 H), 9.38 (s, 1 H); ^{13}C-NMR (100 MHz, $CDCl_3$): δ ppm 24.66, 30.47, 49.91, 62.77, 116.44, 119.64, 123.70, 123.74, 125.11, 127.84, 128.10, 129.48, 129.87, 133.68, 135.94, 150.23, 158.37, 170.87; Anal. Calc. for $C_{20}H_{18}N_2O_5S$; C, 60.29; H, 4.55; N, 7.03; S, 8.05; found: C, 60.33; H, 4.48; N, 6.98; S, 8.08; ESI-MS: 399.05 $[M+H]^+$.

N-(2-Oxo-2H-chromen-3-yl)-1-tosylpyrrolidine-2-carboxamide (28b). Pale white solid, Yield: 90%; *M.P*: 170–172 °C; IR (KBr) 3367, 3088, 3066, 2955, 2879, 1728, 1718, 1697, 1629, 1597, 1514, 1485, 1458, 1354, 1294, 1163, 1111, 1091, 1058, 1004, 950, 923, 904,

850, 754, 665 cm^{-1}; ^{1}H-NMR(400 MHz, $CDCl_3$): δ 1.66 (br s, 1 H), 1.75–1.85 (m, 2 H), 2.24 (br s, 1 H), 2.46 (s, 3 H) 3.29–3.31 (m, 1 H), 3.60 (br s, 1 H),4.31 (br d, 1 H), 7.28–7.40 (m, 4 H), 7.45–7.52 (m, 2 H), 7.83 (d, $J = 7.6$ Hz, 2 H), 8.69 (s, 1 H), 9.40 (s, 1 H); ^{13}C-NMR (100 MHz, $CDCl_3$): δ ppm 21.64, 24.67, 30.45, 49.90, 62.74, 116.44, 119.66, 123.69, 123.74, 125.09, 127.83, 128.17, 129.84, 130.08, 132.93, 144.68, 150.23, 158.37, 171.01; Anal. Calc. for $C_{21}H_{20}N_2O_5S$; C, 61.15; H, 4.89; N, 6.79; S, 7.77, found: C, 61.31; H, 4.91; N, 6.79; S, 7.77; ESI-MS: 413.05 $[M + H]^+$.

1-((4-Chlorophenyl)sulfonyl)-N-(2-oxo-2H-chromen-3-yl)pyrrolidine-2-carboxamide (28c). Pale white solid, Yield: 95%; *M.P*: 202–206 °C; IR (KBr) 3311, 3248, 3093, 3084, 2955, 2875, 1722, 1693, 1626, 1604, 1537, 1487, 1460, 1448, 1356, 1329, 1296, 1276, 1222, 1205, 1157, 1101, 1085, 1070, 1022, 1006, 949, 904, 881, 856, 767, 756 cm^{-1}; ^{1}H-NMR(400 MHz, $CDCl_3$): δ 1.71 (s, 1 H), 1.81–1.91 (m, 2 H), 2.27 (br s, 1 H), 3.26–3.32 (m, 1 H) 3.61 (br s, 1 H), 4.32–4.33 (br d, 1 H), 7.29–7.36 (m, 2 H), 7.45–7.57 (m, 2 H) 7.58 (d, $J = 8.4$ Hz, 2 H), 7.90 (d, $J = 8.4$ Hz, 2 H), 8.68 (s, 1 H), 9.30 (s, 1 H); ^{13}C-NMR (100 MHz, $CDCl_3$): δ ppm 24.69, 30.54, 49.89, 62.75, 116.45, 119.60, 123.62, 123.83, 125.16, 127.87, 129.51, 129.81, 129.94, 134.57, 140.38, 150.21, 158.41, 170.60; Anal. Calc. for $C_{20}H_{17}ClN_2O_5S$; C, 55.49; H, 3.96; N, 6.47; S, 7.41; found: C, 55.58; H, 3.89; N, 6.39; S, 7.30; ESI-MS: 433.00 $[M + H]^+$.

N-(3-Oxo-3H-benzo[f]chromen-2-yl)-1-(phenylsulfonyl)pyrrolidine-2-carboxamide (29a). Pale white solid, Yield: 90%; *M.P*: 206–208 °C; IR (KBr) 3068, 2956, 2889, 1713, 1691, 1536, 1516, 1503, 1463, 1445, 1328, 1237, 1222, 1203, 1192, 1164, 1185, 1090, 994, 814 cm^{-1}; ^{1}H-NMR(400 MHz, $CDCl_3$): δ 1.80–1.84 (m, 1 H), 1.86–1.95 (m, 2 H), 2.29–2.33 (m, 1 H), 3.32–3.39 (br m, 1 H), 3.64–3.69 (m, 1 H), 4.39 (dd, $J = 8.4$, 3.2 Hz, 1 H), 7.48 (d, $J = 8.8$ Hz, 1 H), 7.57–7.64 (m, 3 H), 7.67–7.71 (m, 2 H), 7.92 (d, $J = 8.8$ Hz, 2 H), 7.98–8.00 (m, 2 H), 8.31 (d, $J = 8.4$ Hz, 1 H), 9.46 (s, 1 H), 9.52 (s, 1 H); ^{13}C-NMR (100 MHz, $CDCl_3$): δ ppm 24.72, 30.47, 49.94, 62.83, 113.97, 116.48, 119.92, 122.30, 123.66, 126.20, 127.89, 128.13, 128.86, 129.07, 129.51, 130.66, 131.09, 133.70, 135.96, 149.18, 158.30, 170.98; Anal. Calc. for $C_{24}H_{20}N_2O_5S$; C, 64.27; H, 4.50; N, 6.25; S, 7.15; found: C, 64.34; H, 4.47; N, 6.18; S, 7.30; ESI-MS: 449.01 $[M + H]^+$.

N-(3-Oxo-3H-benzo[f]chromen-2-yl)-1-tosylpyrrolidine-2-carboxamide (29b). Pale white solid, Yield: 87%; *M.P*: 202–206 °C; IR (KBr) 2918, 2887, 1706, 1702, 1696, 1516, 1504, 1464, 1347, 1319, 1237, 1137, 1192, 1158, 1089, 898, 814 cm^{-1}; ^{1}H-NMR(400 MHz, $CDCl_3$): δ 1.76–1.84 (m, 1 H), 1.86–1.94 (m, 2 H), 2.29–2.31 (m, 1 H), 2.47 (s, 3 H), 3.30–3.37 (br m, 1 H), 3.62–3.66 (m, 1 H), 4.37 (dd, $J = 8.4$, 3.2 Hz, 1 H), 7.41 (d, $J = 8.0$ Hz, 2 H), 7.49 (d, $J = 8.8$ Hz, 1 H), 7.58–7.62 (m, 1 H), 7.68–7.72 (m, 1 H), 7.87 (d, $J = 8.0$ Hz, 2 H), 7.92 (d, $J = 2.0$ Hz, 1 H), 7.94 (d, $J = 2.8$ Hz, 1 H), 8.33–8.36 (m, 1 H), 9.50 (s, 1 H), 9.55 (s, 1 H); ^{13}C-NMR (100 MHz, $CDCl_3$): δ ppm 21.67, 24.72, 30.44, 49.93, 62.79, 114.01, 116.37, 116.51, 119.92, 122.33, 122.42, 123.72, 126.19, 127.89, 128.20, 128.86, 129.10, 130.11, 130.67, 130.92, 131.07, 132.94, 144.70, 149.20, 158.32, 171.13; Anal. Calc. for $C_{25}H_{22}N_2O_5S$; C, 64.92; H, 4.79; N, 6.06; S, 6.93; found: C, 64.99; H, 4.72; N, 6.12; S, 7.09; ESI-MS: 463.13 $[M + H]^+$.

1-((4-Chlorophenyl)sulfonyl)-N-(3-oxo-3H-benzo[f]chromen-2-yl)pyrrolidine-2-carboxamide (29c). Pale white solid, Yield: 91%; *M.P*: 230–234 °C; IR (KBr) 2870, 2848, 1715, 1706, 1694, 1533, 1516, 1464, 1343, 1238, 1224, 1203, 1187, 1166, 1102, 1089, 1010, 812 cm^{-1}; ^{1}H-NMR(400 MHz, $CDCl_3$): δ 1.81–1.90 (m, 1 H), 1.92–2.01 (m, 2 H), 2.31–2.35 (m, 1 H), 3.30–3.36 (m, 1 H), 3.63–3.67 (m, 1 H), 4.38 (dd, $J = 8.0$, 2.8 Hz, 1 H), 7.50 (d, $J = 8.8$ Hz, 1 H), 7.58–7.62 (m, 3 H), 7.70 (t, $J = 7.2$ Hz, 1 H), 7.92–7.95 (m, 4 H), 8.33 (d, $J = 8.4$ Hz, 1 H), 9.39 (s, 1 H), 9.54 (s, 1 H); ^{13}C-NMR (100 MHz, $CDCl_3$): δ ppm 24.74, 30.54, 49.93, 62.80, 113.96, 116.48, 120.05, 122.30, 123.59, 126.24, 127.94, 128.88, 129.08, 129.54, 129.84, 130.68, 131.18, 134.58, 140.41, 149.21, 158.36, 170.72; Anal. Calc. for $C_{24}H_{19}ClN_2O_5S$; C, 59.69; H, 3.97; N, 5.80; S, 6.64, found: C, 59.38; H, 3.95; N, 5.75; S, 6.44%; ESI-MS: 483.06 $[M + H]^+$.

Full experimental detail, IR, ^{1}H and ^{13}C NMR spectra. This material can be found via the "Supplementary Content" section of this article's webpage

Acknowledgements

Authors are thankful to The Head, Department of Chemistry, Faculty of Science, The M. S. University of Baroda for providing laboratory facilities, Department of Zoology for screening compounds for anticancer activity and Zydus Research Center, Ahmedabad, for the ESI-MS analyses and antidiabetic activity. DST purse, M.S University of Baroda for single crystal analyses.

References

[1] World Health Organization. *Cancer Fact Sheet September 2018*; World Health Organization: Geneva, **2018**.

[2] Supuran, C. T.; Casini, A.; Mastrolorenzo, A.; Scozzafava, A. COX-2 Selective Inhibitors, Carbonic Anhydrase Inhibition and Anticancer Properties of Sulfonamides Belonging to This Class of Pharmacological Agents. *Mrmc.* **2004**, *4*, 625–632. DOI: 10.2174/1389557043403792.

[3] Abbate, F.; Casini, A.; Owa, T.; Scozzafava, A.; Supuran, C. T. Carbonic Anhydrase Inhibitors: E7070, a Sulfonamide Anticancer Agent, Potently Inhibits Cytosolic Isozymes I and II, and Transmembrane, Tumor-Associated Isozyme IX. *Bioorg. Med. Chem. Lett.* **2004**, *14*, 217–223. DOI: 10.1016/j.bmcl.2003.09.062.

[4] Abd El-Karim, S. S.; Anwar, M. M.; Syam, Y. M.; Nael, M. A.; Ali, H. F.; Motaleb, M. A. Rational Design and Synthesis of New Tetralin-Sulfonamide Derivatives as Potent anti-Diabetics and DPP-4 Inhibitors: 2D &3D QSAR, in Vivo Radiolabeling and Bio Distribution Studies. *Bioorg. Chem.* **2018**, *81*, 481–493. DOI: 10.1016/j.bioorg.2018.09.021.

[5] Bouchain, G.; Leit, S.; Frechette, S.; Khalil, A. E.; Lavoie, R.; Moradei, O.; Woo, S. H.; Fournel, M.; Yan, P. T.; Kalita, A.; et al. Development of Potential Antitumor Agents. Synthesis and Biological Evaluation of a New Set of Sulfonamide Derivatives as Histone Deacetylase Inhibitors. *J. Med. Chem.* **2003**, *46*, 820–830. DOI: 10.1021jm020377a.

[6] Mirian, M.; Zarghi, A.; Sadeghi, S.; Tabaraki, P.; Tavallaee, M.; Dadrass, O.; Sadeghi-Aliabadi, H. Synthesis and Cytotoxic Evaluation of Some Novel Sulfonamide Derivatives against a Few Human Cancer Cells, Iran. *J. Pharm. Res.* **2011**, *10*, 741–748.

[7] Smyth, J. F.; Aamdal, S.; Awada, A.; Dittrich, C.; Caponigro, F.; Schöffski, P.; Gore, M.; Lesimple, T.; Djurasinovic, N.; Baron, B.; et al. Phase II Study of E7070 in Patients with Metastatic Melanoma. *Ann. Oncol.* **2005**, *16*, 158–161. DOI: 10.1093/annonc/mdi016.

[8] Talbot, D. C.; Pawel, V. J.; Cattell, E.; Yule, S. M.; Johnston, C.; Zandvliet, A. S.; Huitema, A. D.; Norbury, C. J.; Ellis, P.; Bosquee, L.; Reck, M. A Randomized Phase II Pharmacokinetic and Pharmacodynamics Study of Indisulam as Second-Line Therapy in

Patients with Advanced Non-Small Cell Lung Cancer. *Clin. Cancer Res.* **2007**, *13*, 1816–1822. DOI: 10.1158/1078-0432.CCR-06-0249.

[9] Zhao, G.; Taunk, P. C.; Magnin, D. R.; Simpkins, L. M.; Robl, J. A.; Wang, A.; Robertson, J. G.; Marcinkeviciene, J.; Sitkoff, D. F.; Parker, R. A.; et al. Diprolyl Nitriles as Potent Dipeptidyl Peptidase IV Inhibitors. *Bioorg. Med. Chem. Lett.* **2005**, *15*, 3992–3995. DOI: 10.1016/j.bmcl.2005.06.043.

[10] Hiroshi, S.; Hiroshi, K.; Mitsuharu, N.; Fumihiko, A.; Yoshiharu, H. 1-((S)-c-Substituted Prolyl)-(S)-2-Cyanopyrrolidine as a Novel Series of Highly Potent DPP-IV Inhibitors. *Bioorg. Med. Chem. Lett.* **2005**, *15*, 2441–2445. DOI: 10.1016/j.bmcl.2005.03.077.

[11] Sharma, R.; Soman, S. S. Design and Synthesis of Novel Diamide Derivatives of Glycine as Antihyperglycemic Agents. *Synth. Commun.* **2016**, *46*, 1307–1317. DOI: 10.1080/00397911.2016.1203435.

[12] Larsson, S. C.; Christos, S. M.; Wolk, A. Diabetes Mellitus and Risk of Breast Cancer: A Meta-Analysis. *Int. J. Cancer* **2007**, *121*, 856–862. DOI: 10.1002/ijc.22717.

[13] Larsson, S. C.; Orsini, N.; Brismar, K.; Wolk, A. Diabetes Mellitus and Risk of Bladder Cancer: A Meta-Analysis. *Diabetologia* **2006**, *49*, 2819–2823. DOI: 10.1007/s00125-006-0468-0.

[14] Vigneri, P.; Frasca, F.; Sciacca, L.; Pandini, G.; Vigneri, R. Diabetes and Cancer. *Endocr. Relat. Cancer* **2009**, *16*, 1103–1123. DOI: 10.1677/ERC-09-0087.

[15] Leone, A.; Di, Gennaro, E.; Bruzzese, F.; Avallone, A.; Budillon, A. New Perspective for an Old Antidiabetic Drug: Metformin as Anticancer Agent. *Cancer Treat. Res.* **2014**, *159*, 355–376. DOI: 10.1007/978-3-642-38007-5_21.

[16] Evans, J. M.; Donnelly, L. A.; Emslie-Smith, A. M.; Alessi, D. R.; Morris, A. D. Metformin and Reduced Risk of Cancer in Diabetic Patients. *BMJ* **2005**, *330*, 1304–1305. DOI: 10.1136/bmj.38415.708634.F7.

[17] Nair, R. V.; Fisher, E. P.; Safe, S. H.; Cortez, C.; Harvey, R. G.; DiGiovanni, J. Novel Coumarins as Potential Anticarcinogenic Agents. *Carcinogenesis* **1991**, *12*, 65–69. DOI: 10.1093/carcin/12.1.65.

[18] Curini, M.; Epifano, F.; Maltese, F.; Marcotullio, M. C.; Gonzales, S. P.; Rodriguez, J. C. Synthesis of Collinin, an Antiviral Coumarin. *Aust. J. Chem.* **2003**, *56*, 59–60. DOI: 10.1071/CH02177.

[19] Gormley, N. A.; Orphanides, G.; Meyer, A.; Cullis, P. M.; Maxwell, A. The Interaction of Coumarin Antibiotics with Fragments of DNA Gyrase B Protein. *Biochemistry* **1996**, *35*, 5083–5092. DOI: 10.1021/bi952888n.

[20] Sashidhara, K. V.; Kumar, A.; Chatterjee, M.; Rao, K. B.; Singh, S.; Verma, A. K.; Palit, G. Discovery and Synthesis of Novel 3-Phenylcoumarin Derivatives as Antidepressant Agents. *Bioorg. Med. Chem. Lett.* **2011**, *21*, 1937–1941. DOI: 10.1016/j.bmcl.2011.02.040.

[21] Fylaktakidou, K. C.; Hadjipavlou-Litina, D. J.; Litinas, K. E.; Nicolaides, D. N. Natural and Synthetic Coumarin Derivatives with Anti-Inflammatory/Antioxidant Activities. *Cpd.* **2004**, *10*, 3813–3833.DOI: 10.2174/1381612043382710.

[22] Kostova, I.; Bhatia, S.; Grigorov, P.; Balkansky, S.; Parmar, V. S.; Prasad, A. K.; Saso, L. Coumarins as Antioxidants. *Cmc.* **2011**, *18*, 3929–3951. DOI: 10.2174/092986711803414395.

[23] Soni, R.; Soman, S. S. Design and Synthesis of Aminocoumarin Derivatives as DPP-IV Inhibitors and Anticancer Agents. *Bioorg. Chem.* **2018**, *79*, 277–284. DOI: 10.1016/j.bioorg.2018.05.008.

[24] Wu, L.; Wang, X.; Xu, W.; Farzaneh, F.; Xu, R. The Structure and Pharmacological Functions of Coumarins and Their Derivatives. *Cmc.* **2009**, *16*, 4236–4260. DOI: 10.2174/092986709789578187.

[25] Heide, L. The Aminocoumarins: Biosynthesis and Biology. *Nat. Prod. Rep.* **2009**, *26*, 1241–1250. DOI: 10.1039/b808333a.

[26] Keri, R. S.; Sasidhar, B. S.; Nagaraja, B. M.; Amelia, S. M. Recent Progress in the Drug Development of Coumarin Derivatives as Potent Antituberculosis Agents. *Eur. J. Med. Chem.* **2015**, *100*, 257–269. DOI: 10.1016/j.ejmech.2015.06.017.

[27] Sharma, R.; Soman, S. S. Design and Synthesis of Sulphonamide Derivatives of Pyrrolidine and Piperidine as anti-Diabetic Agents. *Eur. J. Med. Chem.* **2015**, *90*, 342–350. DOI: 10.1016/j.ejmech.2014.11.041.

[28] Durgapal, S. D.; Soni, R.; Umar, S.; Suresh, B.; Soman, S. S. Anticancer Activity and DNA Binding Studies of Novel 3,7-Disubstituted Benzopyrones. *Chem. Select* **2017**, *2*, 147–153. DOI: 10.1002/slct.201601361.

Journal of Molecular Liquids 297 (2020) 111920

Contents lists available at ScienceDirect

Journal of Molecular Liquids

journal homepage: www.elsevier.com/locate/molliq

Synthesis and mesomorphic properties of coumarin derivatives with chalcone and imine linkages

Sunil Dutt Durgapal, Rina Soni, Shubhangi S. Soman *, A.K. Prajapati

Department of Chemistry, Faculty of Science, The M. S. University of Baroda, Vadodara, 390 002, India

ARTICLE INFO

Article history:
Received 10 August 2019
Received in revised form 1 October 2019
Accepted 12 October 2019
Available online 16 October 2019

Keywords:
Coumarin
Chalcone
Imine
Thermotropic liquid crystals
Single crystal study

ABSTRACT

We report here design and synthesis of two new mesogenic homologous series of coumarin derivatives consisting of chalcone and imine central linkages along with terminal *n*-alkoxy chain. All the compounds were synthesized and characterized by combination of elemental analysis and standard spectroscopic methods. All compounds were screened under polarising optical microscope (POM) for liquid crystalline properties, thermogram of all compounds were studied using differential scanning calorimetry (DSC) to get phase transition temperatures, enthalpy and entropy. X-ray single crystal study of *n*-octyloxy coumarin derivative 16 g was resolved with imine central linkage, which showed linear rod like geometry.

1. Introduction

Liquid crystalline material contains properties of both liquid and crystal [1]. Due to their dual properties, earlier application of these materials was as liquid crystal displays [2]. Recently, applications of liquid crystalline material are extended to liquid crystal thermometers, optical storage, chemical and biological sensors [3–5]. As a result of wide range of applications of liquid crystalline materials, there is increase in need to develop new liquid crystalline materials specially of thermotropic class [6]. Design of rod like thermotropic liquid crystal material mainly consists of phenyl rings in rigid core while alkyl chains in flexible terminal core. To develop thermotropic liquid crystalline compounds containing heterocyclic ring is one of the interesting area of research [7–9]. As heteroatoms present in ring not only affect type of mesophase exhibited by molecules and its transition temperature, but also affect the other properties of molecules including dipole moment, polarizablility, dielectric constant, photoluminescence [10]. Heterocyclic liquid crystalline materials have shown applications in both photonic and electronic displays devices. Recently there are reports on such materials comprising of organic compounds as well as organic-inorganic hybrids [11,12]. Chalcone linkage has been used in liquid crystalline compounds due to its geometrical shape, thermal stability, charge transfer property by π-bond conjugation and high photosensitivity [13–20]. Imine group is also well explored in liquid crystalline compounds due to its stepped structure, molecular linearity, ability to self-organize and property of incorporating mesophases in molecules [21–23]. Major disadvantage of imine is their inherent chemical, thermal and photo-physical instability, which reduces its potential applications in electro-optic displays [24].

Coumarins are one of the largest classes of naturally occurring compounds. Coumarins derivatives with liquid crystalline and gel properties can be seen as new type of photo cross-linkable materials for their practical applications [25,26]. Coumarin derivatives have been used in material chemistry as optical materials, fluorescent whiteners, fluorescent tags, laser dyes, non-linear optical chromophores [27–32]. Position of substituents and type of substituents on coumarin ring play very important role to overall optical properties of coumarin derivatives. Polymeric and non-polymeric coumarin derivatives have been reported for their liquid crystalline properties [33–35]. Coumarin derivatives with alkyne-, ester- and azo-linkages have been reported and explored for their mesogenic properties (Fig. 1).

Trivedi et al. and Dave et al. have reported coumarin ester derivatives as liquid crystalline compounds [36,37]. Merlo et al. have reported alkyne linked coumarin derivative 2 with their applications in solar cell [38]. Srinivasa et al. have synthesized ethyl 7-hydroxycoumarin-3-carboxylate derivatives 3–4 with ester linkage, which showed excellent liquid crystal behaviour majorly smectic A (SmA) and nematic phase [39,40]. Hagar et al. have reported 7-hydroxy-4-methyl-coumarin derivatives 5–6 with ester and azoester for mesophase study (Fig. 1) [41].

Hereby we report synthesis of coumarin derivatives and the effect of chalcone and imine linkages on the mesomorphic properties for thermotropic liquid crystals. The mesomorphic properties were studied by Differential Scanning Calorimetry (DSC) and Polarising Optical

* Corresponding author.
E-mail address: shubhangiss@rediffmail.com (S.S. Soman).

https://doi.org/10.1016/j.molliq.2019.111920
0167-7322/

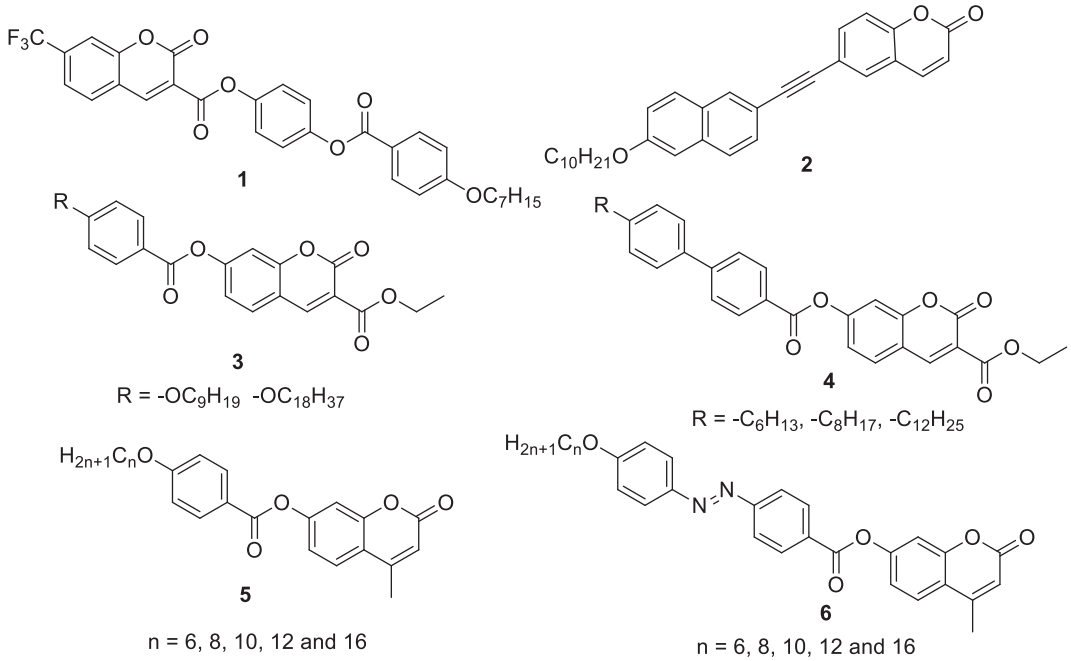

Fig. 1. Coumarin derivatives with liquid crystalline properties.

Microscope (POM). The mesomorphic behaviour of the homologous compounds with two different linkages is rationalized based on the varying lengths of the alkyl chain.

2. Experimental

2.1. Material and methods

Reagent grade chemicals and solvents were purchased from commercial supplier and used after purification. Thin-layer chromatography (TLC) was performed on silica gel F254 plates (Merck). Acme's silica gel (60–120 mesh) was used for column chromatographic purification. All reactions were carried out in nitrogen atmosphere. Melting points are uncorrected and were measured in open capillary tubes, using a Rolex melting point apparatus. IR spectra were recorded as potassium bromide (KBr) pellets on PerkinElmer RX 1 spectrometer. ^{1}H NMR and ^{13}C NMR spectral data were recorded on Advance Bruker 400 spectrometer (400 MHz) with Deuterated chloroform ($CDCl_3$) or Deuterated dimethyl sulfoxide (DMSO-d_6) as solvent and tetramethyl silane (TMS) as internal standard. *J* values are in Hz. Mass spectra were determined by ESI-MS, using a Shimadzu LCMS 2020 apparatus. Elemental analyses were recorded on Thermosinnigan Flash 11–12 series EA. Thermograms were recorded on DSC (DSC-822, Mettler Toledo having Stare software). Photographs were obtained by Polarising optical microscope Leica DM200P attached with camera Leica DFC295 and separate heating unit with controller Linkpad by Linkam. UV-Vis spectra were recorded on PerkinElmer UV/Vis Spectrometer Lambda 35 with WinLab software.

2.2. Synthesis

2.2.1. Synthesis of 3-acetyl-7-hydroxy coumarin (8)

To a solution of 2,4-dihydroxy benzaldehyde (15.0 g, 0.108 mol, 1.0 eq) in ethanol (50 mL) was added ethyl acetoacetate (13.62 mL, 0.108 mol, 1.0 eq) followed by catalytic amount of piperidine (0.1 mL). The resulting mixture was refluxed for 18 h. The completion of reaction was checked by thin-layer chromatography (TLC). After completion of reaction, reaction mixture was allowed to cool down to room temperature and concentrated on a rotavapor. The viscous liquid obtained was poured into ice cold water to give solid. The solid obtained was filtered, washed with water, dried and recrystallized from ethanol to give compound 8 as green crystals. Yield: 95%; M.P. 236–238 °C (Lit [42] M.P. 238 °C).

2.2.2. (E)-7-Hydroxy-3-(3-(4-hydroxyphenyl)acryloyl)-2H-chromen-2-one (10)

To a solution of compound 8 (1.02 g, 5.0 mmol) in ethanol (50 mL) was added 4-hydroxy benzaldehyde (0.61 g, 5.0 mmol) and stirred for 10–15 min. To this mixture, catalytic amount of pyrrolidine and acetic acid were added and resulting mixture was refluxed at 78–80 °C for 36 h. The completion of reaction was checked by TLC. After completion of reaction, the reaction mixture was allowed to cool to room temperature (rt), concentrated on rotavapor and poured into ice cold water to give brown solid. The crude product was filtered, washed with water, and dried. The crude compound was purified by column chromatography using petroleum ether:ethyl acetate (7:3) to give pure compound 10 as bright orange solid. Yield: 48%; M.P: >260 °C; ^{1}H NMR (400 MHz, DMSO-d_6): δ 6.7 (d, 1H), 6.82–6.86 (m, 3H), 7.58 (d, J = 8.4 Hz, 2H), 7.62 (d, J = 15.6 Hz, 1H), 7.62 (d, J = 15.6 Hz, 1H), 7.77 (d, J = 8.4 Hz, 1H), 8.61 (s, 1H), 10.16 (s, 1H); ^{13}C NMR (100 MHz, DMSO-d_6): δ ppm 102.28, 111.55, 114.60, 116.44, 120.81, 121.68, 126.13, 131.21, 132.79, 144.18, 148.37, 157.47, 159.56, 160.69, 164.35, 186.58.

2.2.3. Synthesis of alkoxy coumarin chalcone derivatives 11a-j

To compound 10 (1.00 mmol) in *N*,*N*-dimethyl formamide (DMF) (20 mL) was added anhy. K_2CO_3 (4.0 mmol) and stirred for 10–15 min at rt. To this alkyl halide (2.0 mmol) was added and resulting solution was heated at 70–72 °C for 18–20 h. The completion of reaction was monitored with TLC. After completion of reaction, mixture was cooled to room temperature and poured into ice cold water to give solid. The solid was filtered, washed with water and air dried. The crude compound was purified by column

chromatography using pet.ether:ethyl acetate (9:1 to 8:2) to give compounds 11a-k.

2.3. Characterization data of all even members alkyl chain derivatives

2.3.1. (E)-7-Ethoxy-3-{3-[4-(ethoxy)phenyl]acryloyl}-2H-chromen-2-one (11a)

Yellow solid, Yield: 95%; M.P: 166–168 °C; IR (KBr): 3092, 3047, 2982, 2933, 2872, 1729, 1656, 1599, 1507, 1425, 1354, 1292, 1254, 1167, 1113, 1040, 918, 826, 794 cm^{-1}; ^1H NMR (400 MHz, $CDCl_3$): δ 1.45 (t, J = 7.0 Hz, 3H), 1.50 (t, J = 7.2 Hz, 3H), 4.07–4.10 (q, J = 7.0 Hz 2H), 4.15 (q, J = 7.2 Hz, 2H), 6.85 (d, J = 2.4 Hz, 1H), 6.90–6.95 (m, 3H), 7.57 (d, J = 8.8 Hz 1H), 7.65 (d, J = 8.8 Hz, 2H), 7.86 (d, J = 16.0 Hz, 1H), 7.93 (d, J = 15.6 Hz, 1H), 8.60 (s, 1H); ^{13}C NMR (100 MHz, $CDCl_3$): δ ppm 14.52, 14.75, 63.65, 64.56, 100.68, 112.31, 114.16, 114.81, 121.42, 121.73, 127.61, 130.77, 131.25, 144.62, 148.40, 157.63, 159.96, 161.24, 164.48, 186.33; Anal. Calc. for $C_{22}H_{20}O_5$; C, 70.51; H, 5.53; found: C, 70.68; H, 5.42%; ESI-MS: 365.10 $[M+H]^+$.

2.3.2. (E)-7-Butoxy-3-{3-[4-(butoxy)phenyl]acryloyl}-2H-chromen-2-one (11b)

Yellow solid, Yield: 92%; M.P: 132–134 °C; IR (KBr): 3082, 3045, 2953, 2870, 1723, 1653, 1595, 1567, 1505, 1467, 1426, 1376, 1251, 1165, 1059, 991, 957, 823 cm^{-1}; ^1H NMR (400 MHz, $CDCl_3$): δ 1.02–1.03 (m, 6H), 1.47–1.58 (m, 4H), 1.76–1.87 (m, 4H), 4.02 (t, J = 6.6 Hz, 2H), 4.08 (t, J = 6.6 Hz, 2H), 6.85 (s, 1H), 6.89–6.94 (m, 3H), 7.56 (d, J = 8.4 Hz, 1H), 7.64 (d, J = 8.4 Hz, 2H), 7.85 (d, J = 15.6 Hz, 1H), 7.93 (d, J = 15.6 Hz, 1H), 8.60 (s, 1H); ^{13}C NMR (100 MHz, $CDCl_3$): δ ppm 13.81, 13.87, 19.16, 19.22, 30.90, 31.20, 67.85, 68.69, 100.68, 112.27, 114.19, 114.83, 121.36, 121.69, 127.54, 130.75, 131.23, 144.64, 148.41, 157.64, 159.98, 161.46, 164.69, 186.34; Anal. Calc. for $C_{26}H_{28}O_5$; C, 74.26; H, 6.71; found: C, 74.28; H, 6.55%; ESI-MS: 421.15 $[M+H]^+$.

2.3.3. (E)-7-(Hexyloxy)-3-{3-[4-(hexyloxy)phenyl]acryloyl}-2H-chromen-2-one (11d)

Yellow solid, Yield: 96%; M.P: 138–140 °C; IR (KBr): 3096, 2923, 2854, 1717, 1655, 1596, 1543, 1507, 1466, 1426, 1372, 1296, 1254, 1163, 1066, 1016, 985, 826, 720 cm^{-1}; ^1H NMR (400 MHz, $CDCl_3$): δ 0.91–0.95 (m, 6H), 1.34–1.39 (m, 8H), 1.45–1.52 (m, 4H), 1.78–1.88 (m, 4H), 4.02 (t, J = 6.6 Hz, 2H), 4.07 (t, J = 6.6 Hz, 2H), 6.85 (d, J = 2.4 Hz, 1H), 6.90–6.94 (m, 3H), 7.57 (d, J = 8.8 Hz, 1H), 7.64 (d, J = 8.8 Hz, 2H), 7.85 (d, J = 15.6 Hz, 1H), 7.93 (d, J = 16.0 Hz, 1H), 8.60 (s, 1H); ^{13}C NMR (100 MHz, $CDCl_3$): δ ppm 14.06, 14.07, 22.59, 22.62, 25.62, 25.70, 28.86, 29.13, 31.51, 31.58, 68.17, 69.01, 100.68, 112.27, 114.20, 114.83, 121.35, 121.68, 127.54, 130.76, 131.23, 144.64, 148.41, 157.63, 159.98, 161.46, 164.69, 186.34; Anal. Calc. for $C_{30}H_{36}O_5$; C, 75.60; H, 7.61; found: C, 75.68; H, 7.60; %; ESI-MS: 477.35 $[M+H]^+$.

2.3.4. (E)-7-(Octyloxy)-3-{3-[4-(octyloxy)phenyl]acryloyl}-2H-chromen-2-one (11f)

Yellow solid, Yield: 95%; M.P: 116–118 °C; IR (KBr): 3097, 2930, 2863, 1718, 1654, 1596, 1543, 1507, 1466, 1424, 1373, 1292, 1251, 1163, 1123, 1062, 985, 827 cm^{-1}; ^1H NMR (400 MHz, $CDCl_3$): δ 0.90–0.92 (m, 6H), 1.31–1.36 (br s, 16H), 1.44–1.52 (m, 4H), 1.78–1.88 (m, 4H), 4.01 (t, J = 6.6 Hz, 2H), 4.07 (t, J = 6.6 Hz, 2H), 6.85 (d, J = 2.0 Hz, 1H), 6.90–6.94 (m, 3H), 7.56 (d, J = 8.8 Hz, 1H), 7.64 (d, J = 8.8 Hz, 2H), 7.85 (d, J = 15.6 Hz, 1H), 7.93 (d, J = 15.6 Hz, 1H), 8.60 (s, 1H); ^{13}C NMR (100 MHz, $CDCl_3$): δ ppm 14.13, 22.67, 25.94, 26.02, 28.89, 29.16, 29.21, 29.25, 29.29, 29.35, 31.79, 31.82, 68.18, 69.01, 100.69, 112.27, 114.18, 114.84, 121.37, 121.70, 127.55, 130.74, 131.21, 144.62, 148.38, 157.64, 159.96, 161.46, 164.69, 186.32; Anal. Calc. for $C_{34}H_{44}O_5$; C, 76.66; H, 8.33; found: C, 76.52; H, 8.48%; ESI-MS: 533.07 $[M+H]^+$.

2.3.5. (E)-7-(Decyloxy)-3-{3-[4-(decyloxy)phenyl]acryloyl}-2H-chromen-2-one (11 g)

Yellow solid, Yield: 89%; M.P: 118–120 °C; IR (KBr): 3082, 2921, 2850, 1733, 1653, 1597, 1507, 1468, 1420, 1338, 1299, 1258, 1165, 1068, 1051, 852, 825, 719 cm^{-1}; ^1H NMR (400 MHz, $CDCl_3$): δ 0.90 (t, J = 6.8 Hz, 6H), 1.29–1.34 (br s, 24H), 1.44–1.51 (m, 4H), 1.78–1.88 (m, 4H), 4.01 (t, J = 6.6 Hz, 2H), 4.07 (t, J = 6.6 Hz, 2H), 6.85 (d, J = 2.4 Hz, 1H), 6.90–6.94 (m, 3H), 7.56 (d, J = 8.8 Hz, 1H), 7.64 (d, J = 8.4 Hz, 2H), 7.86 (d, J = 15.6 Hz, 1H), 7.93 (d, J = 15.6 Hz, 1H), 8.60 (s, 1H); ^{13}C NMR (100 MHz, $CDCl_3$): δ ppm 14.15, 22.70, 25.93, 26.01, 28.89, 29.16, 29.32, 29.39, 29.55, 29.57, 31.90, 68.18, 69.01, 100.69, 112.27, 114.19, 114.84, 121.38, 121.70, 127.55, 130.75, 131.21, 144.63, 148.38, 157.64, 159.97, 161.46, 164.69, 186.33; Anal. Calc. for $C_{38}H_{52}O_5$; C, 77.51; H, 8.90; found: C, 77.65; H, 9.02%; ESI-MS: 589.36 $[M+H]^+$.

2.3.6. (E)-7-(Dodecyloxy)-3-{3-[4-(dodecyloxy)phenyl]acryloyl}-2H-chromen-2-one (11h)

Yellow solid, Yield: 92%; M.P: 124–126 °C; IR (KBr): 2953, 2921, 2850, 1733, 1654, 1596, 1508, 1468, 1421, 1339, 1299, 1260, 1166, 1144, 1068, 1023, 987, 953, 852, 851, 825, 804, 744, 721 cm^{-1}; ^1H NMR (400 MHz, $CDCl_3$): δ 0.90 (t, J = 6.8 Hz, 6H), 1.28–1.36 (br s, 32H), 1.44–1.49 (m, 4H), 1.78–1.88 (m, 4H), 4.01 (t, J = 6.6 Hz, 2H), 4.06 (t, J = 6.4 Hz, 2H), 6.84 (d, J = 2.0 Hz, 1H), 6.89–6.94 (m, 3H), 7.56 (d, J = 8.8 Hz, 1H), 7.64 (d, J = 8.8 Hz, 2H), 7.85 (d, J = 15.6 Hz, 1H), 7.93 (d, J = 15.6 Hz, 1H), 8.60 (s, 1H); ^{13}C NMR (100 MHz, $CDCl_3$): δ ppm 14.16, 22.72, 25.93, 26.02, 28.90, 29.17, 29.33, 29.37, 29.40, 29.55, 29.59, 29.61, 29.65, 29.67, 31.94, 68.18, 69.01, 100.69, 112.27, 114.18, 114.83, 121.36, 121.69, 127.54, 130.75, 131.21, 144.62, 148.38, 157.64, 159.96, 161.46, 164.69, 186.31; Anal. Calc. for $C_{42}H_{60}O_5$; C, 78.22; H, 9.38; found: C, 78.40; H, 9.42%

2.3.7. (E)-7-(Tetradecyloxy)-3-{3-[4-(tetradecyloxy)phenyl]acryloyl}-2H-chromen-2-one (11i)

Yellow solid, Yield: 85%; M.P: 122–124 °C; IR (KBr): 3070, 3046, 2918, 2850, 1720, 1658, 1613, 1568, 1510, 1469, 1425, 1373, 1294, 1254, 1197, 1170, 1071, 979, 828, 774, 723 cm^{-1}; ^1H NMR (400 MHz, $CDCl_3$): δ 0.89 (t, J = 6.4 Hz, 6H), 1.28–1.33 (br s, 40H), 1.43–1.48 (m, 4H), 1.77–1.88 (m, 4H), 4.0 (t, J = 6.6 Hz, 2H), 4.06 (t, J = 6.4 Hz, 2H), 6.84 (d, J = 2.0 Hz, 1H), 6.89–6.94 (m, 3H), 7.56 (d, J = 8.8 Hz, 1H), 7.64 (d, J = 8.8 Hz, 2H), 7.85 (d, J = 15.6 Hz, 1H), 7.93 (d, J = 15.6 Hz, 1H), 8.60 (s, 1H); ^{13}C NMR (100 MHz, $CDCl_3$): δ ppm 14.16, 22.72, 25.94, 26.02, 28.90, 29.17, 29.34, 29.39, 29.55, 29.60, 29.62, 29.68, 29.71, 31.94, 68.18, 69.01, 100.68, 112.26, 114.18, 114.83, 121.34, 121.68, 127.54, 130.74, 131.21, 144.63, 148.38, 157.63, 159.96, 161.46, 164.69, 186.29; Anal. Calc. for $C_{46}H_{68}O_5$; C, 78.81; H, 9.78; found: C, 78.74; H, 9.92%

2.3.8. (E)-7-(Hexadecyloxy)-3-{3-[4-(hexadecyloxy)phenyl]acryloyl}-2H-chromen-2-one (11j)

Yellow solid, Yield: 90%; M.P: 120–122 °C; IR (KBr): 3070, 3047, 2917, 2850, 1720, 1658, 1614, 1568, 1510, 1469, 1425, 1374, 1253, 1198, 1167, 1022, 980, 831, 774, 722 cm^{-1}; ^1H NMR (400 MHz, $CDCl_3$): δ 0.89 (t, J = 6.8 Hz, 6H), 1.27 (br s, 48H), 1.47–1.49 (m, 4H), 1.78–1.88 (m, 4H), 4.01 (t, J = 6.6 Hz, 2H), 4.06 (t, J = 6.4 Hz, 2H), 6.85 (d, J = 2.0 Hz, 1H), 6.90–6.94 (m, 3H), 7.56 (d, J = 8.4 Hz, 1H), 7.64 (d, J = 8.4 Hz, 2H), 7.85 (d, J = 15.6 Hz, 1H), 7.93 (d, J = 15.6 Hz, 1H), 8.60 (s, 1H); ^{13}C NMR (100 MHz, $CDCl_3$): δ ppm 14.17, 22.72, 25.94, 26.02, 28.90, 29.17, 29.34, 29.39, 29.56, 29.60, 29.62, 29.69, 29.72, 31.95, 68.18, 69.01, 100.68, 112.27, 114.19, 114.83, 121.36, 121.68, 127.54, 130.75, 131.22, 144.64, 148.40, 157.64, 159.97, 161.46, 164.69, 186.33; Anal. Calc. for $C_{50}H_{76}O_5$; C, 79.32; H, 10.12; found: C, 79.51; H, 10.05%

2.3.9. (E)-7-(Octadecyloxy)-3-{3-[4-(octadecyloxy)phenyl]acryloyl}-2H-chromen-2-one (11k)

Yellow solid, Yield: 94%; M.P: 118–120 °C; IR (KBr): 2918, 2849, 1716, 1655, 1601, 1568, 1508, 1467, 1425, 1253, 1172, 1069, 1026, 977, 828, 801, 776, 720 cm^{-1}; ^1H NMR (400 MHz, $CDCl_3$): δ 0.89 (t, $J = 6.6$ Hz, 6H), 1.27 (br s, 56H), 1.47–1.48 (m, 4H), 1.77–1.86 (m, 4H), 4.01 (t, $J = 6.6$ Hz, 2H), 4.06 (t, $J = 6.4$ Hz, 2H), 6.84 (s, 1H), 6.89–6.94 (m, 3H), 7.56 (d, $J = 8.8$ Hz, 1H), 7.64 (d, $J = 8.4$ Hz, 2H), 7.85 (d, $J = 15.6$ Hz, 1H), 7.93 (d, $J = 15.6$ Hz, 1H), 8.60 (s, 1H); ^{13}C NMR (100 MHz, $CDCl_3$): δ ppm 14.16, 22.72, 25.94, 26.02, 28.90, 29.17, 29.34, 29.39, 29.56, 29.60, 29.62, 29.69, 29.72, 31.95, 68.18, 69.01, 100.68, 112.27, 114.19, 114.83, 121.36, 121.69, 127.54, 130.75, 131.21, 144.63, 148.39, 157.64, 159.96, 161.46, 164.69, 186.31; Anal. Calc. for $C_{54}H_{84}O_5$; C, 79.75; H, 10.41; found: C, 79.81; H, 10.43%

2.3.10. Synthesis of 3-acetamido-7-hydroxy coumarin (12)

To a stirring solution of 2,4-dihydroxybenzaldehyde 7 (20.0 g, 144.92 mmol, 1.0 eq) in acetic anhydride (68.36 mL, 724.6 mmol, 5.0 eq) *N*-acetylglycine (16.9 g, 144.92 mmol, 1.0 eq) and sodium acetate (47.55 g, 579.68 mmol, 4.0 eq) were added and the resulting mixture was heated at 100–110 °C for 7 h or till the completion of reaction as monitored by TLC. On completion of reaction it was cooled to room temperature, water (20 mL) was added and the resulting solid was filtered, dried and then recrystallized from absolute ethanol to give 3-acetamido-7-hydroxy coumarin 12 as crystalline solid. % Yield: 48%; M.P.: 242–244 °C (Lit [43]. M. P. 244–246 °C).

2.3.11. Synthesis of 3-amino-7-hydroxycoumarin (13)

To a solution of above obtained 3-acetamido-7-hydroxy-coumarin 12 (20.0 g) in ethanol (150 mL), conc HCl (30 mL) was added and the resulting solution was refluxed for an hour. On completion of reaction it was cooled to room temperature, concentrated to a small volume and then neutralized with sodium bicarbonate solution to yield crude compound. The resulting solid was filtered, dried and then recrystallized from absolute ethanol to give pure crystalline 3-amino-7-hydroxy-coumarin 13. % Yield: 66%; M.P. 248–250 °C (Lit [43] M.P. 250 °C).

2.3.12. Synthesis of 3-amino 7-alkoxy coumarin derivatives (14)

To a solution of 3-amino 7-hydroxycoumarin (1.0 eq) in dimethyl formamide (DMF) (20 mL) was added anhy. K_2CO_3 (2.5 eq) and stirred at room temperature for 10–15 min. To this mixture, alkyl bromide (1.0 mmol) was added and resulting solution was stirred at room temperature (rt) for 22–24 h. The completion of reaction was checked by TLC. After completion of reaction, the reaction mixture was poured into ice-cold water to give solid. The solid was filtered, washed with water, dried and recrystallized from ethanol to give compound 13 as off white solid. These compounds 14a-l were directly used for next step.

2.3.13. Synthesis of 4-alkyloxybenzaldehyde derivatives (15)

Compounds 15a-l were prepared using same method as described for compounds 14a-l. The crude compounds were obtained as colourless oil. All the compounds were purified by column chromatography and used for next step.

General procedure for Synthesis of (*E*)-7-alkoxy-3-((4-alkoxybenzylidene)amino)-2*H*-chromen-2-one (16a-l).

To a solution of 3-amino 7-alkoxy coumarin 14a-l (1.0 eq) and 4-alkoxy benzaldehyde 15a-l (1.0 eq) in ethanol (10 mL) was refluxed for 18–20 h in presence of catalytic amount of acetic acid (0.1–0.2 mL). The reaction mixture was allowed to cool down to room temperature and concentrated to half volume. The solid separated out on standing was filtered, washed with cold ethanol, cold petrolium ether and dried to give compound 16a-l.

2.4. Characterization data of all even members alkyl chain derivatives

2.4.1. (E)-7-Butoxy-3-{[4-(butoxy)benzylidene]amino}-2H-chromen-2-one (16c)

Yellow solid, Yield: 61%, M.P:142–144 °C; IR (KBr): 3080, 2956, 2872, 1421, 1614, 1569, 1504, 1473, 1285, 1240, 1166, 1654, 961, 769 cm^{-1}; ^1H NMR (400 MHz, $CDCl_3$) δ ppm: 1.00–1.03 (m, 6H), 1.48–1.58 (m, 4H), 1.78–1.86 (m, 4H), 4.02–4.06 (m, 4H), 6.84–6.89 (m, 2H), 6.98 (d, $J = 8.8$ Hz, 2H), 7.41 (d, $J = 8.4$ Hz, 1H), 7.55 (s, 1H), 7.87 (d, $J = 8.8$ Hz, 2H), 9.10 (s, 1H), ^{13}C NMR (100 MHz, $CDCl_3$) δ ppm: 13.8, 13.9, 19.2, 19.2, 31.0, 31.2, 67.9, 68.3, 100.9, 113.3, 114.6, 128.5, 129.0, 130.8, 132.4, 132.8, 153.7, 159.0, 161.6, 162.3, 162.4; Anal. Calc. for $C_{24}H_{27}NO_4$; C, 73.26; H, 6.92; N, 3.56; found: C, 73.41; H, 6.80; N, 3.62%

2.4.2. (E)-7-(Hexyloxy)-3-{[4-(hexyloxy)benzylidene]amino}-2H-chromen-2-one (16e)

Yellow solid, Yield: 66%, M.P: 140–142 °C; IR (KBr): 2923, 2854, 1720, 1622, 1251, 1171, 1153, 1133, 843, 769 cm^{-1}; ^1H NMR (400 MHz, $CDCl_3$) δ ppm: 0.91–0.95 (m, 6H), 1.38–1.39 (m, 8H), 1.45–1.52 (m, 4H), 1.79–1.86 (m, 4H), 4.00–4.05 (m, 4H), 6.84–6.88 (m, 2H), 6.97 (d, $J = 8.8$ Hz, 2H), 7.41 (d, $J = 8.8$ Hz, 1H), 7.55 (s, 1H), 7.87 (d, $J = 8.8$ Hz, 2H), 9.09 (s, 1H), ^{13}C NMR ($CDCl_3$, 100 MHz) δ ppm 14.1, 22.6, 25.6, 25.7, 29.0, 29.1, 31.5, 31.6, 68.2, 68.6, 100.8, 113.3, 114.6, 128.5, 129.0, 130.8, 132.4, 132.8, 153.7, 159.0, 161.6, 162.2, 162.4; Anal. Calc. for $C_{28}H_{35}NO_4$; C, 74.80; H, 7.85; N, 3.12; found: C, 74.66; H, 7.80; N, 3.01%

2.4.3. (E)-7-(Octyloxy)-3-{[4-(octyloxy)benzylidene]amino}-2H-chromen-2-one (16 g)

Yellow solid, Yield: 63%, M.P: 140–142 °C; IR (KBr): 2922, 2854, 1720, 1623, 1250, 1152, 1132, 842, 766 cm^{-1}; ^1H -NMR (400 MHz, $CDCl_3$) δ ppm: 0.89–0.93 (m, 6H), 1.26–1.40 (m, 16H), 1.45–1.52 (m, 4H), 1.79–1.86 (m, 4H), 4.01–4.06 (m, 4H), 6.85–6.88 (m, 2H), 6.97 (d, $J = 8.8$ Hz, 2H), 7.41 (d, $J = 8.4$ Hz, 1H), 7.55 (s, 1H), 7.87 (d, $J = 8.8$ Hz, 2H), 9.10 (s, 1H). ^{13}C NMR (100 MHz,$CDCl_3$) δ ppm: 14.1, 22.6, 25.9, 26.0, 29.0, 29.1, 29.2, 29.2, 29.3, 29.3, 31.7, 31.8, 68.2, 68.6, 100.9, 113.3, 113.4, 114.7, 128.5, 129.1, 130.8, 132.5, 132.8, 153.7, 158.6, 158.9, 161.6, 162.3, 162.4; Anal. Calc. for $C_{32}H_{43}NO_4$; C, 76.00; H, 8.57; N, 2.77; found: C, 75.84; H, 8.80; N, 2.52%

2.4.4. (E)-7-(Decyloxy)-3-{[4-(decyloxy)benzylidene]amino}-2H-chromen-2-one (16h)

Yellow solid, Yield: 55%, M.P: 134–136 °C; IR (KBr): 2921, 2852, 1720, 1624, 1606, 1567, 1507, 1332, 1135, 843, 769 cm^{-1}; ^1H NMR (400 MHz, $CDCl_3$) δ ppm: 0.89 (t, 6H), 1.34–1.36 (m, 24H), 1.44–1.50 (m, 4H), 1.79–1.86 (m, 4H), 4.00–4.05 (m, 4H), 6.84–6.88 (m, 2H), 6.97 (d, $J = 8.8$ Hz, 2H), 7.41 (d, $J = 8.4$ Hz, 1H), 7.55 (s, 1H), 7.87 (d, $J = 8.8$ Hz, 2H), 9.10 (s, 1H); ^{13}C NMR (100 MHz, $CDCl_3$) δ ppm: 14.2, 22.7, 26.0, 26.0, 29.0, 29.2, 29.3, 29.4, 29.4, 29.6, 31.9, 68.2, 68.6, 100.9, 113.4, 114.6, 114.7, 128.5, 129.0, 130.9, 132.5, 132.8, 153.7, 159.0, 161.6, 162.4, 162.4; Anal. Calc. for $C_{36}H_{51}NO_4$; C, 76.97; H, 9.15; N, 2.49; found: C, 76.96; H, 9.11; N, 2.50%, ESI-MS: 563.2 $[M+H]^+$.

2.4.5. (E)-7-(Dodecyloxy)-3-{[4-(dodecyloxy)benzylidene]amino}-2H-chromen-2-one (16i)

Yellow solid, Yield: 62%, M.P: 138–140 °C; IR (KBr): 2920, 2851, 1721, 1623, 1607, 1570, 1507, 1470, 1425, 1399, 1381, 1293, 1253, 1171, 1153, 1053, 1023, 977, 843, 769 cm^{-1}; ^1H NMR (400 MHz, $CDCl_3$) δ ppm: 0.90 (t, $J = 6.4$ Hz, 6H), 1.28–1.50 (br s, 32H), 1.64 (s, 4H), 1.81–1.85 (m, 4H), 4.01–4.05 (m, 4H), 6.84–6.89 (m, 2H), 6.97 (d, $J = 8.8$ Hz, 2H), 7.41 (d, $J = 8.4$ Hz, 1H), 7.56 (s, 1H), 7.87 (d, $J = 8.8$ Hz, 2H), 9.10 (s, 1H); Anal. Calc. for $C_{40}H_{59}NO_4$; C, 77.75; H, 9.62; N, 2.27; found: C, 77.52; H, 9.62; N, 2.23%

2.4.6. (E)-7-(Tetradecyloxy)-3-{[4-(tetradecyloxy)benzylidene]amino}-2H-chromen-2-one (16j)

Yellow solid, Yield: 59%, M.P: 132–134 °C; IR (KBr): 2919, 2850, 1720, 1622, 1570, 1470, 1426, 1380, 1292, 1252, 1152, 1135, 1058, 1010, 910, 843, 802, 768 cm^{-1}; ^1H NMR ($CDCl_3$, 400 MHz) δ ppm: 0.90 (t, $J = 6.4$ Hz, 6H), 1.28 (br s, 40H), 1.45–1.48 (m, 4H), 1.79–1.85 (m, 4H), 4.01–4.05 (m, 4H), 6.81–6.89 (m, 2H), 6.97 (d, $J = 8.8$ Hz, 2H), 7.41 (d, $J = 8.4$ Hz, 1H), 7.56 (s, 1H), 7.87 (d, $J = 8.8$ Hz, 2H), 9.10 (s, 1H); Anal. Calc. for $C_{44}H_{67}NO_4$; C, 78.41; H, 10.02; N, 2.08; found: C, 78.25; H, 10.14; N, 2.12%

2.4.7. (E)-7-(Hexadecyloxy)-3-{[4-(hexadecyloxy)benzylidene]amino}-2H-chromen-2-one (16k)

Yellow solid, Yield: 67%, M.P: 130–132 °C; IR (KBr): 2919, 2851, 1721, 1623, 1570, 1509, 1470, 1293, 1254, 1171, 1153, 1058, 1021, 910, 843, 802, 769 cm^{-1}; ^1H NMR (400 MHz, $CDCl_3$) δ ppm: 0.90 (t, $J = 6.4$ Hz, 6H), 1.28 (br s, 48H), 1.45–1.49 (m, 4H), 1.79–1.85 (m, 4H), 4.01–4.05 (m, 4H), 6.85–6.88 (m, 2H), 6.97 (d, $J = 8.8$ Hz, 2H), 7.41 (d, $J = 8.4$ Hz, 1H), 7.55 (s, 1H), 7.87 (d, $J = 8.4$ Hz, 2H), 9.10 (s, 1H); Anal. Calc. for $C_{48}H_{75}NO_4$; C, 78.96; H, 10.35; N, 1.92; found: C, 78.98; H, 10.54; N, 1.87%

2.4.8. (E)-7-(Octadecyloxy)-3-{[4-(octadecyloxy)benzylidene]amino}-2H-chromen-2-one (16l)

Yellow solid, Yield: 55%, M.P: 126–128 °C; IR (KBr): 2919, 2850, 1721, 1624, 1570, 1508, 1470, 1293, 1254, 1171, 1152, 1136, 1058, 910, 843, 803, 769 cm^{-1}; ^1H NMR (400 MHz, $CDCl_3$) δ ppm: 0.90 (t, $J = 6.4$ Hz, 6H), 1.28 (br s, 56H), 1.49 (br s, 4H), 1.83 (br s, 4H), 4.03 (s, 4H), 6.85–6.88 (m, 2H), 6.98 (d, $J = 8.4$ Hz, 2H), 7.41 (d, $J = 8.4$ Hz, 1H), 7.56 (s, 1H), 7.87 (d, $J = 8.8$ Hz, 2H), 9.10 (s, 1H); Anal. Calc. for $C_{52}H_{83}NO_4$; C, 79.44; H, 10.64; N, 1.78; found: C, 79.28; H, 10.72, N; 1.69%.

3. Results and discussion

3.1. Chemistry

3-Acetyl-7-hydroxy-2H-chromen-2-one 8 was prepared by Knoevenangel condensation of 2,4-dihydroxy benzaldehyde 7 with ethyl acetoacetate using catalytic amount of piperidine in ethanol. Compound 8 on reaction with 4-hydroxy benzaldehyde 9 by refluxing for 36 h in presence of catalytic amount of pyrrolidine and acetic acid in ethanol gave (*E*)-7-hydroxy-3-[3-(4-hydroxyphenyl)acryloyl]-2*H*-chromen-2-one 10. Compound 10 was alkylated with different *n*-alkyl bromides using anhydrous K_2CO_3 in *N*,*N*-dimethyl formamide (DMF) at 70–72 °C to give *bis*-alkyloxy derivatives 11a-k of Series-I (Scheme 1).

The structures of compounds 11a-k were confirmed by different analytical techniques such as ^1H NMR, ^{13}C NMR, IR, ESI-MS and CHN analysis. In general, compounds 11a-k exhibited three peaks in the range 3095-2840 cm^{-1} for the alkyl chain in IR spectra, while carbonyl stretching frequency of lactone was observed at 1730-1718 cm^{-1}, carbonyl group of chalcone was observed at 1660-1650 cm^{-1}. In the ^1H NMR spectra of compounds 11a-k, terminal methyl groups of both alkyl chain were observed as triplet in the upfield region of δ 0.88–1.00 while methylene protons were observed as multiplet at δ 1.33–1.88. Methylene protons attached with oxygen were observed as triplets in the region of 3.99–4.08 ppm. All aromatic protons of coumarin and phenyl rings were observed between δ ~6.84–7.65. Chalcone protons were observed as a doublet at 7.83–7.95 ppm with trans coupling (*J*) value of 16.0 Hz and proton of 4th position of coumarin were observed as singlet around δ 8.60 ppm.

In the ^{13}C NMR spectra of 11a-k, peaks for methyl and other alkyl carbons were in range of δ 14–31 ppm, two methylene carbons adjacent to oxygen were observed at δ 68 and 69 ppm. All aromatic carbons were appeared in range of δ 100–161 ppm, coumarin lactone carbonyl carbon at 164 ppm and carbonyl carbon of chalcone at 184 ppm. The ESI-MS of all the compounds were recorded giving molecular ion peak corresponding to molecular weight of compounds.

In another series, chalcone linkage was replaced by imine linakge. Alkylation of 3-amino-7-hydroxy-2H-chromen-2-one and 4-hydroxybenzaldehyde were done separately using different *n*-alkyl bromides and anhydrous K_2CO_3 in dry DMF at room temperature. Resulting alkylated compounds were reacted in ethanol using catalytic amount of acetic acid to give Schiff bases 16a-l Series-II (Scheme 2).

The structures of all the compounds 16a-l were confirmed by using different analytical techniques such as ^1H NMR, ^{13}C NMR, IR, ESI-MS and CHN analysis. In IR spectra of compounds 16a-l exhibited band at 2922-2854 cm^{-1} for the C–H stretching of alkyl chain, band at 1720 cm^{-1} for carbonyl stretching of lactone ring, 1623 cm^{-1} for carbonyl stretching of chalcone moiety. In the ^1H NMR spectra of compounds 16a-l, two terminal methyl groups of alkyl chain were observed as triplet in the upfield region of δ ~0.88–0.93. Methylene protons at δ 1.20–1.88 were observed as multiplet, methylene groups adjacent to oxygen were overlapped and appeared as multiplet in region of 4.02–4.05 ppm, All aromatic protons were observed in region of δ 6.84–7.88 ppm, while imine proton was appeared as singlet around δ 9.10 ppm.

In the ^{13}C NMR spectra of 16a-l, two methyl carbons and methylene carbons were observed around δ 14–31 ppm, methylene carbon adjacent to oxygen were observed at 68–69 ppm. All aromatic carbons were observed in range of 100–161 ppm lactone carbonyl carbon observed at 162 ppm. All compounds 16a-l were analysed by ESI-MS to give $[M+H]^+$ peak corresponding to their molecular weight.

3.2. Mesomorphic properties

3.2.1. Differential scanning calorimetry study (DSC)

The phase transition temperatures, enthalpy-entropy changes and mesophase textures of the pure compounds 11a-k and 16a-l are summarised in Tables 1 and 2. Clear-cut transition temperatures and textures could be obtained from DSC curves and POM observations for all of the compounds, and they were in good agreement with each other for the multiple heating/cooling cycles. Thermograms were calculated by DSC (DSC-822,

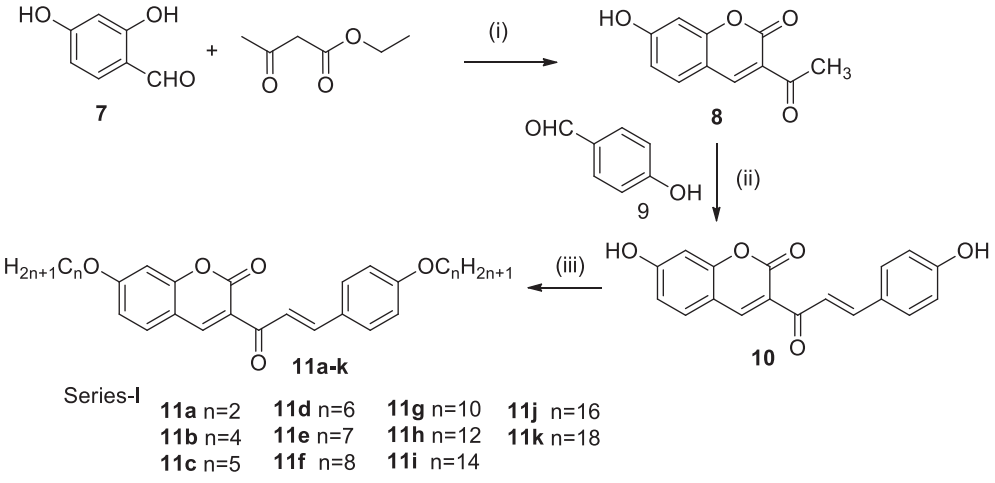

Reagents and conditions: (i) piperidine, ethanol, reflux,16 h; (ii) pyrrolidine, acetic acid, ethanol reflux, 36 h; (iii) dry K_2CO_3, *n*-alkyl bromide, DMF reflux.

Scheme 1. Synthesis of chalcone containing coumarin derivatives.

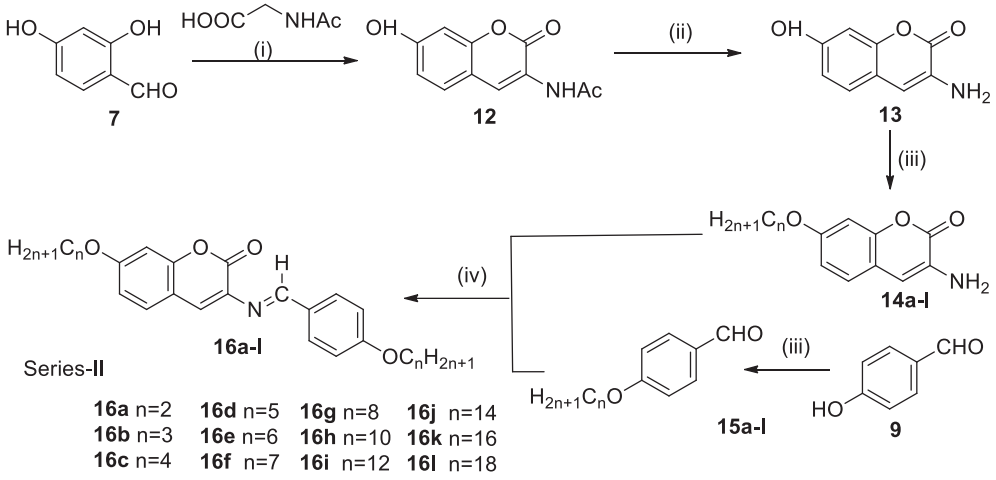

Reagents and condition: (i) acetic anhydride, sodium acetate, reflux, 5h (ii) HCl, ethanol, reflux, 1h (iii) K_2CO_3, n-alkyl Bromide, DMF, r.t, 18-20 h (iv) catalytic acetic acid, ethanol reflux, 16-18h.

Scheme 2. Synthesis of imine containing coumarin derivatives.

Table 1
DSC phase transition temperature, enthalpy and entropy of alkoxy coumarin chalcone linked compounds 11a-11k[a].

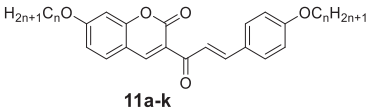

11a-k

Compd	n	Heating Temp ºC (ΔH KJmol^{-1}, ΔS Jmol^{-1}K^{-1})			Cooling Temp ºC (ΔH KJmol^{-1}, ΔS Jmol^{-1}K^{-1})		
		SmA	N	Iso	N	SmA	Cr
11a	2			169.56 (3.64, 8.22)			88.35 (2.39, 6.62)
11b	4			132.45 (6.19, 15.28)			90.43 (2.28, 6.29)
11c	5			126.66 (8.32, 20.81)			64.33 (14.16, 41.97)
11d	6		116.88 (5.28, 13.54)	138.01 (0.45, 1.10)	135.06 (1.17, 2.87)		46.03 (1.89, 5.92)
11e	7		96.33 (3.61, 9.57)	104.00 (0.84, 2.27)	102.00 (2.94, 7.84)		79.00 (1.37, 3.89)
11f	8	86.94 (1.54, 4.28)	108.91 (5.75, 15.09)	115.48 (0.40, 1.03)	111.56 (0.25, 0.66)	105.21 (0.07, 0.18)	83.09 (4.06, 11.41)
11 g	10	83.71 (5.02, 14.07)		118.66 (0.86, 2.20)		117.87 (1.18, 3.01)	73.62 (4.70, 13.58)
11h	12	74.29 (1.31, 3.77)		124.91 (1.92, 4.82)		121.14 (1.86, 4.71)	73.60 (3.02, 8.71)
11i	14	83.78 (3.91, 10.96)		121.83 (1.51, 3.83)		118.89 (1.39, 3.55)	73.55 (3.05, 8.80)
11j	16	93.22 (7.95, 21.73)		119.99 (1.42, 3.61)		117.39 (1.68, 4.30)	80.11 (6.24, 17.67)
11k	18	96.38 (4.24, 11.48)		118.66 (0.49, 1.24)		116.73 (0.79, 2.03)	83.20 (4.66, 13.08)

[a] SmA = Smectic A phase, N = Nematic phase, Iso = Isotropic phase, Cr = Crystalline solid.

Table 2
DSC phase transition temperature, enthalpy and entropy of all alkoxy coumarin imine linkage compounds 16a-l[a].

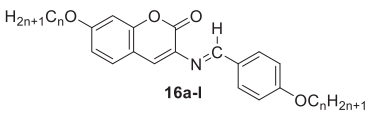

16a-l

Compd	n	Heating Temp ºC (ΔH KJmol-1, ΔS Jmol-1K-1)			Cooling Temp ºC (ΔH KJmol-1, ΔS Jmol-1K-1)		
		SmA	N	Iso	N	SmA	Cr
				129.83 (4.57, 11.34)			91.91 (2.96, 8.13)
16b	3		105.00 (9.55, 25.26)	133.00 (0.31, 0.76)	128.00 (0.14, 0.35)		82.5 (5.55, 15.61)
16c	4		113.10 (4.93, 12.76)	143.35 (0.14, 0.33)	140.07 (0.17, 0.41)		56.77 (8.92, 27.05), 40.03 (2.20, 7.03)
16d	5		77.00 (5.85, 16.71)	129.00 (1.65, 4.10)	128.00 (0.23, 0.701)		55.00 (7.14, 17.80)
16e	6		82.95 (10.33, 29.09)	139.99 (0.57, 1.38)	136.75 (0.59, 1.44)		80.04 (0.26, 0.74) 60.18 (1.65, 4.95)
16f	7		84.00 (4.72, 13.22)	112.00 (1.89, 4.90)	107.00 (0.40, 1.05)		68.50 (8.13, 23.84)
16 g	8	99.86 (3.55, 9.54)	126.66 (0.23, 0.58)	139.96 (0.76, 1.84)	136.76 (0.39, 0.95)	123.40 (0.20, 0.50)	70.42 (9.15, 26.64)
16h	10	93.12 (10.03, 27.40)		136.67 (0.85, 2.07)		124.05 (0.47, 1.18)	70.24 (10.60, 30.90)
16i	12	99.71 (13.63, 36.64)		136.63 (2.52, 6.18)		134.11 (1.99, 4.89)	80.22 (9.94, 28.15)
16j	14	96.48 (1.08, 2.94)		132.38 (0.88, 2.17)		126.06 (1.29, 3.23)	64.54 (1.87, 5.54)
16k	16	105.85 (11.30, 29.89)		131.35 (2.21, 5.47)		128.72 (1.52, 3.79)	92.19 (10.93, 29.94)
16l	18	109.89 (9.67, 25.31)		126.69 (1.20, 3.01)		123.39 (0.76, 2.06)	96.99 (15.12, 40.97)

[a] SmA = Smectic A phase, N = Nematic phase, Iso = Isotropic phase, Cr = Crystalline solid.

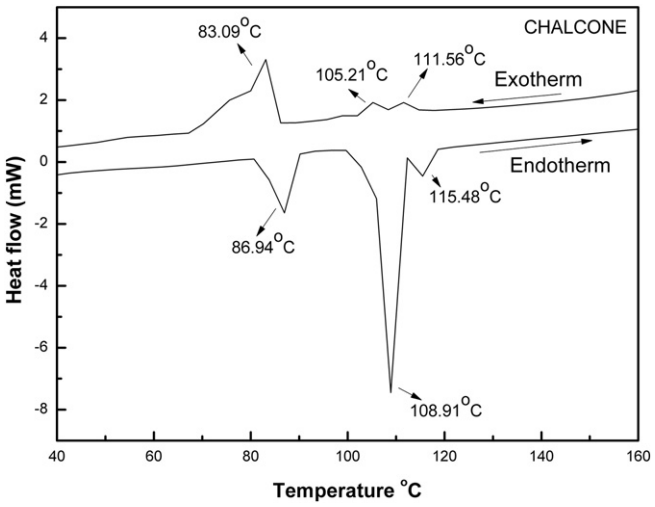

Fig. 2. DSC plot of octyloxy coumarin chalcone derivative 11f in both heating and cooling cycle along with transition temperatures.

Mettler Toledo having Stare software). Phase transitions of all the compounds were measured in both heating and cooling cycle at rate of 10 °C/min. Chalcone derivatives of coumarin compounds 11a, 11b and 11c showed one endotherm for crystalline to isotropic liquid phase (Cr-Iso) on heating and one exotherm from isotropic liquid phase to crystallization (Iso-Cr) on cooling without any mesogenic property.

Compounds 11d and 11e exhibited two endotherms from crystalline solid to nematic phase (Cr–N) and nemtic phase to isotropic liquid phase (N-Iso) on heating. Similarly on cooling two exotherms are observed corresponding to isotropic liquid phase to nematic phase (Iso-N) and nematic phase to crystalline solid state (N–Cr). Compound 11f showed three endotherms for heating cycle and three exotherms on cooling cycle, while heating first transition was observed from crystalline solid to smectic A phase (Cr-SmA), second transition was observed for smectic A phase to nematic phase (SmA-N) and third transition was observed for nematic mesophase to isotropic liquid phase (N-Iso). In cooling cycle, compound 11f showed three exotherms for Isotropic liquid phase to nematic phase (Iso-N), nematic to smectic A phase (N-SmA) and smectic A phase to crystalline solid (SmA-Cr) (Fig. 2, Table 1). Compounds 11 g-11k showed only two transitions in both heating and cooling cycles corresponding to smectic A mesophase in between crystal and isotropic phases.

DSC thermograms for alkoxy coumarin derivatives 16a-l with imine linkage were evaluated, which was used for calculations of enthalpy and entropy values for all the synthesized compounds. Compound 16a exhibited one endotherm from Cr-Iso in heating cycle with no mesogenic property. Compounds 16b-16f showed two endotherms in heating cycle from Cr–N and N-Iso. In cooling cycle, compounds 16b, 16d and 16f exhibited two exotherms for Iso-N and N–Cr transitions, whereas compound 16c and 16e exhibited three exotherms from Iso-N, nematic phase to crystal-1 and crystal-1 to crystalline solid (Fig. 3a, Table 2).

Compound 16 g showed three endotherms on heating first for Cr-SmA, second for SmA –N and third corresponding to N-Iso, while three exotherms during cooling are observed corresponding to Iso-N, N-SmA and SmA-Cr transitions (Fig. 3b, Table 2). Compounds 16h-l showed two endotherms for Cr-SmA and SmA-Iso transitions on heating and two exotherms for Iso-SmA and SmA-Cr transitions on cooling. Only SmA phase was observed in both heating and cooling cycle for compounds 16h-l (Table 2).

3.2.2. Polarising optical microscopy (POM) study

The mesogenic properties of all the compounds 11a-k and 16a-l were observed by using Leica DM2500P attached with camera Leica DFC295 along with the separate heating plate on microscope. Thin film of the samples was prepared by sandwiching a small amount of each compound between slide and coverslip.

Lower members of *n*-alkoxy coumarin chalcone derivatives with ethyl (11a), butyl (11b) and pentyl (11c) chain did not show any mesomorphic properties. Compounds 11d and 11e having *n*-hexyl and *n*-heptyl chain showed nematic phase, 11f with *n*-octyl chain length showed two phases viz Nematic phase (Fig. 4a) and smectic A (Fig. 4b) respectively on cooling. All the higher members 11 g-11k showed only smectic A phase similar to compound 11f as shown in Fig. 4b.

Coumarin imine linkage derivatives 16a-l showed different textures under polarising optical microscope. Compound 16a did not show any mesogenic phase, while compounds 16b to 16f showed marble texture, characteristic of nematic phase during heating and colloing cycles. Compound 16 g showed both smectic A and nematic phases on heating cycle. During cooling cycle for compound 16 g, isotropic phase was first transformed into tiny spherical droplets (Fig. 4c) later coalesced into the Schlieren texture characteristic of nematic phase (Fig. 4d and e), which on further cooling exhibited focal conic texture characteristic of smectic A phase (Fig. 4f) before crystallization. Compounds 16h-16l exhibited only focal conic texture characteristic of smectic A phase on both heating and cooling cycle.

3.3. Structure-mesomorphic property relationship

The graph of phase-transition temperatures against the number of carbons in chalcone and imine derivatives of the *n*-alkoxy chain enabled to identify the effects of the terminal chain on the mesomorphic properties. The relationship was established from two different plots (Fig. 5). Based on Fig. 5a and b, the transition curves Cr-SmA/N/Iso, SmA/N-Iso, SmA-Iso, are obtained.

The Cr-SmA/N/Iso transition curve exhibited sharp falling tendency up to *n*-dodecyloxy derivative 11 h and covers large area which may be responsible for the enantiotropy nature of the series. From compounds 11h to 11k ascending trend was observed this may be due to the excessive van der Waals attractive forces between the long alkyl chains, the melting temperatures increased from the carbon chain length 12 to 18 members [44]. The lower members with short chain 11a, 11b and 11c did not show any mesogenic properties.

The isotropic liquid of lower members does not supercool sufficiently for monotropic nematic mesophase to be obtained. Lower members are in fact not mesomorphic, the high melting points of these lower members of series may be partially responsible for the lack of mesophase formation. Mesophases are most commonly observed when a suitable compound is heated to a temperature above that at which the crystal lattice is stable. All the compounds of the present series comprised of a molecules which are long, narrow, and linear containing dipolar groups, which should give strong intermolecular attractions. It seems that these intermolecular attractions are too strong, selective weakening of the cohesive forces may not occur until high temperatures are reached, and when the melting process does begin, the thermal vibrations may be too great to allow an ordered arrangement of the molecules to persist. Middle members 11d, 11e and 11f showed falling tendency and pronounce odd-even effect for the N-Iso transition temperatures. Smectic A phase commences from compound 11f and persist up to the last homologue synthesized in the series. SmA-Iso transition temperature curve showed descending trend from compound 11h to 11k (Fig. 5a).

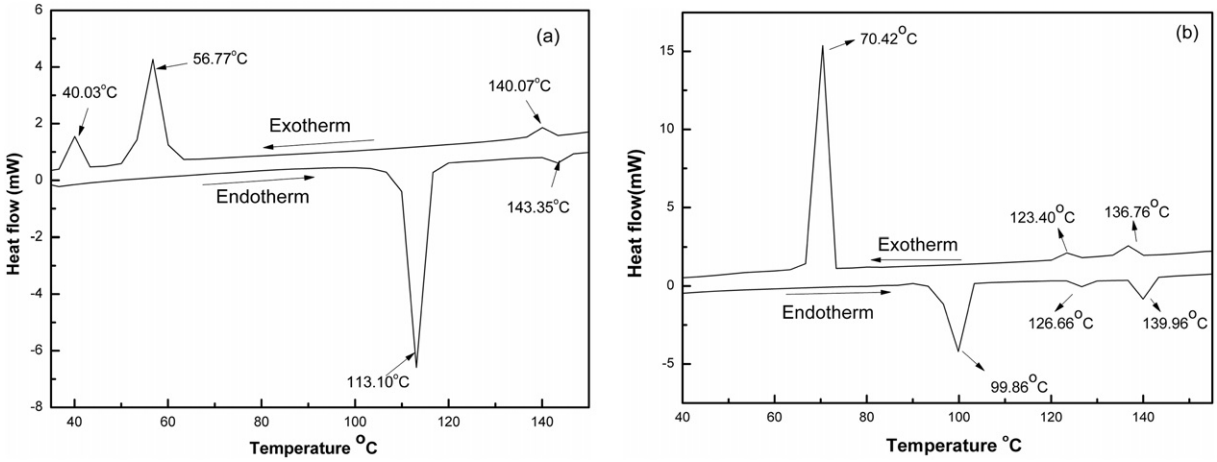

Fig. 3. DSC plots of imine derivatives (a) compound 16c with butyloxy showing cryst-1 to cryst modification in cooling cycle and (b) compound 16 g octyloxy at different temperature.

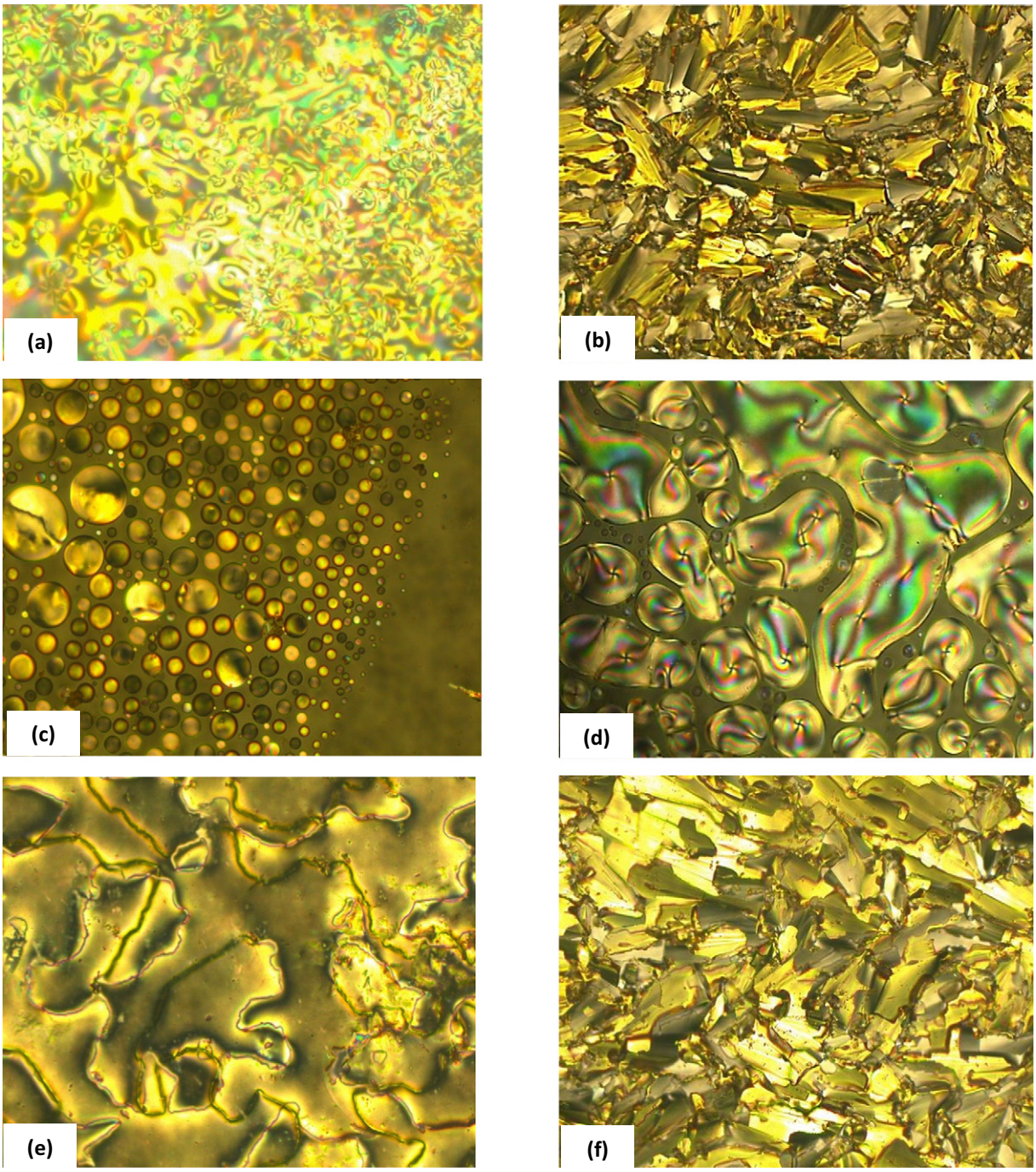

Fig. 4. POM images of compound 11f and 16 g. Optical photomicrographs were taken during the cooling cycle of compound 11f showed transition from isotropic liquid to Nematic Schlieren texture (a) at 111.56 °C, further on cooling nematic to focal conic Smectic-A phase (b) was observed at 105.21 °C. On cooling compound 16 g from isotropic liquid, nematic droplets (c) appeared at 136.76 °C and coalesced to form the typical schlieren texture (d) at 136.00 °C, On further cooling gives marble texture (e) of nematic phase at 134.28 °C and finally transition from nematic to focal conic smectic A (f) at 123.40 °C was observed.

Similarly, the phase diagram for coumarin derivatives with imine central linkage was also plotted against the transition temperatures versus the number of carbon atoms present in the *n*-alkoxy terminal chain (Fig. 5b). Compound 16a with ethoxy chain did not exhibit any mesogenic property. Mesophase was observed from compound 16b till the last member long chain synthized in this series. Only Nematic mesophase was observed for compound 16b with *n*-propyloxy to compound 16 g with *n*-octyloxy. The N-Iso, transition temperatures exhibited falling tendency with marked odd-even effect (Fig. 5b). The SmA mesophase commences from *n*-octyloxy derivative 16 g as an enantiotropy and persist up to the last member synthesized in this series. SmA-Iso transition temperatures exhibited smooth falling tendency from compound 16 g to compound 16l.

All the compounds of series-I exhibited lower mesophase range and thermal stability as compared to compounds of series-II. Both the series have common coumarin ring as a core moiety substituted at 3rd and 7th positions and differ at the central linkage only. Series-I has chalcone central linkage whereas series II has imine central linkage. It seems that chalcone central linkage increases the breadth of the molecule of series I little as compared to molecules of series II, which may be responsible for the lower mesophase range and thermal stability (Mesophase-Isotropic transition) of compounds of series-I [45].

3.4. X-ray diffraction study

Compound 16 g with imine linkage and octyloxy substituent was further studied by X-ray single crystal diffraction (CCDC No. 1943900). The structure is shown in Fig. 6 and data is given in Table 3.

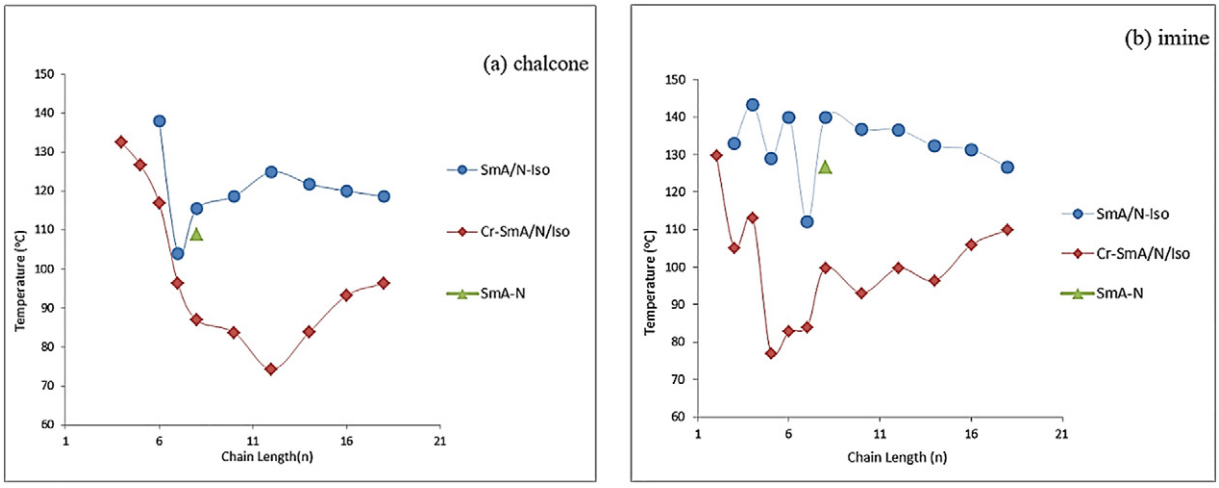

Fig. 5. Mesomorphic behaviour as a function of the number of carbon atoms (n) in the terminal alkoxy chain (a) Series-I with chalcone central linkage in heating cycle (b) Series-II with imine central linkage in heating cycle.

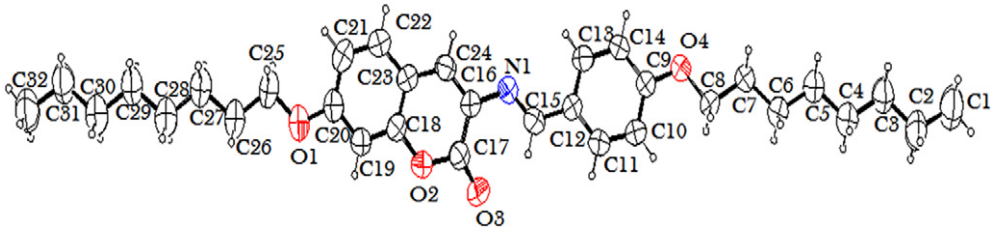

Fig. 6. Single crystal of compound 16 g with coumarin imine *n*-octyl derivative.

The crystal packing of molecules in the unit cell were arranged in a linear fashion one on other. Three π···π stackings were observed by one molecule as shown in Fig. 7a, first was between phenyl rings of two different molecules at a distance of 3.381 Å, second was observed at distance of 3.328 Å between carbonyl carbon of lactone of two different molecules and third was observed between phenyl rings of coumarin moiety of two different molecules.

Short contacts were observed with value of 2.64 Å between oxygen of alkoxy and C–H of benzene ring (O···C–H) on head to head manner as shown in Fig. 7b. The results of X-ray single crystal undoubtedly indicated that the molecule is linear and each molecule is stacked on other by intermolecular interactions. Single crystal data for compound 11 h was also obtained and provided in supporting information.

Ball and stick model of *n*-dodecyloxy coumarin chalcone derivative 11 h and *n*-octyloxy coumarin imine derivative 16 g were shown in Fig. 8. From ball and stick model obtained from X-ray single crystal was used for calculation of length/breadth ratio, which showed that L/B ratio for compound with chalcone linkage was lower than L/B ratio for compound with imine linkage.

3.5. UV-Vis study

Compounds 11f and 16 g were analysed for UV-Vis absorption spectra in chloroform (1×10^{-5} M) at room temperature (Fig. 9). Compound 11f with chalcone linkage showed broad absorption bands at 269 and 391 nm. Shoulder peak at 383 nm was observed in π-π* transition peak due to shifting of electron density from donor alkoxy moiety to the aromatic core. Compound 16 g with imine linkage showed two intense absorption bands at 286 and 341 nm. Effect of octyloxy group on absorption spectra can be seen due to push-pull effect between alkoxy group and aromatic ring (Fig. 9). The absorbance maximum attributed to the π-π* transition were chosen as excitation wavelength for fluorescence measurements. Compounds 11f and 16 g were excited at 391 and 341 nm respectively and emission spectra were recorded in chloroform. Both compounds showed very low emission in chloroform this is probably due to non radiative decay of the compounds.

4. Conclusion

We have designed and synthesized two new homologous series of *n*-alkoxy coumarin derivatives with chalcone and imine linkages. The effect of chalcone and imine linkages on mesophase appearance and stability were studied using DSC and POM. All the compounds from both the series up to *n*-heptyl chain length showed only nematic phase. POM study of compound 11f with chalcone linkage and 16 g with imine linkage with *n*-octyl chain, showed two phases. Focal conic phase is indicative of smectic A phase and nematic phase with different textures, which was further confirmed by DSC study. All the higher members from both the series with alkyl chain length *n*-decyl and

Table 3
Crystal data and structure refinement for compound 16 g

Empirical formula	$C_{32}H_{43}NO_4$	$\rho_{calc}g/cm^3$	1.139
Formula weight	505.67	μ/mm^{-1}	0.074
Temperature/K	293	F(000)	548.0
Crystal system	triclinic	Crystal size/mm^3	0.4 × 0.13 × 0.1
Space group	P-1	Radiation	MoKα (λ = 0.71073)
a/Å	10.6388(19)	2Θ range for data collection/°	6.26 to 58
b/Å	11.6468(17)	Index ranges	−13 ≤ h ≤ 14, −15 ≤ k ≤ 15, −17 ≤ l ≤ 17
c/Å	12.6960(18)	Reflections collected	32012
α/°	74.709(13)	Independent reflections	7150 [R_{int} = 0.1022, R_{sigma} = 0.1175]
β/°	76.399(14)	Data/restraints/parameters	7150/0/336
γ/°	88.388(14)	Goodness-of-fit on F [2]	0.986
Volume/$Å^3$	1473.9(4)	Final R indexes [I ≥ 2σ (I)]	R_1 = 0.0793, wR_2 = 0.1567
Z	2	Final R indexes [all data]	R_1 = 0.2599, wR_2 = 0.2329

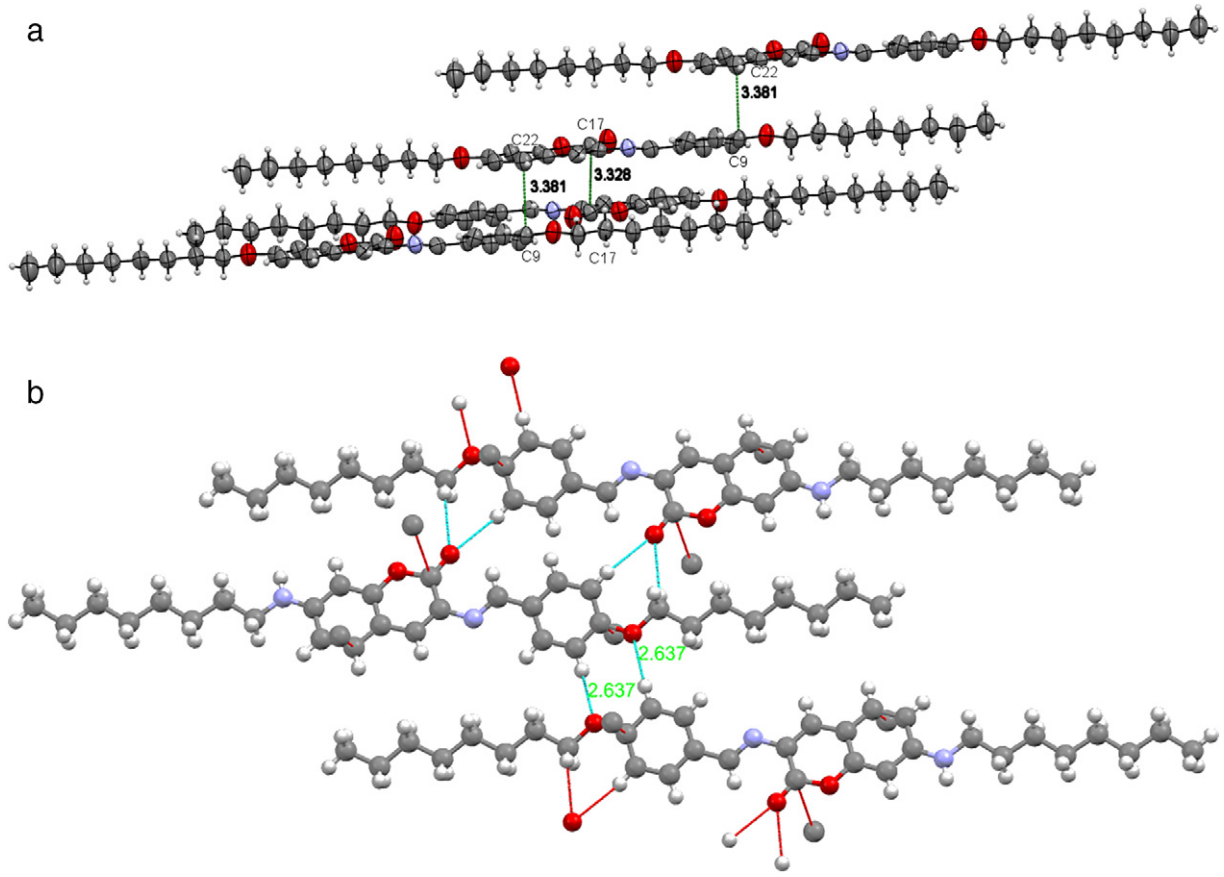

Fig. 7. a: X-ray single crystal analysis showing strong π-π stacking between two layers in compound 16 g. b: Short contacts between oxygen of alkoxy and hydrogen of benzene ring in compound 16 g.

above showed only focal conic smectic A phase. The mesophase range and thermal stability of coumarin derivatives with chalcone linkage was lower as compared to the coumarin derivatives with imine linkage.

Acknowledgements

One of the authors (RS) is thankful to Department of Science & Technology, Government of India for financial support vide reference no. SR/WOS-A/CS-1028/2014 under Women Scientist Scheme. Authors are also thankful to The Head, Department of Chemistry, Faculty of Science, The M. S. University of Baroda for providing laboratory facilities, DST-FIST for providing NMR, POM and DSC facilities, DST-PURSE for providing X-ray single crystal facility, Zydus Research Centre, Ahmedabad, for the ESI-MS analyses.

Appendix A. Supplementary data

Supplementary data to this article can be found online at https://doi.org/10.1016/j.molliq.2019.111920.

Conflicts of interest

The authors declare that there is no conflict of interest regarding the publication of this paper.

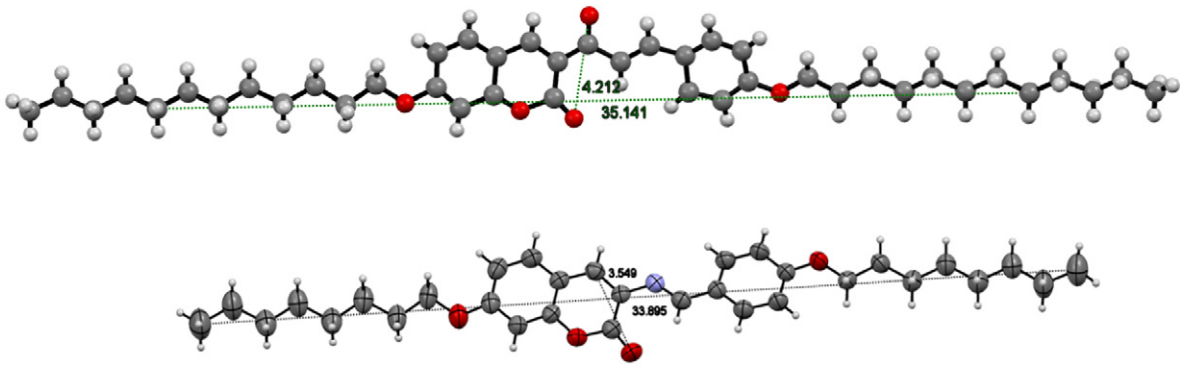

Fig. 8. Ball and stick model of chalcone and imine derivative along with the molecular length and breadth. X-ray single crystal spectroscopic technique, Mercury 3.10 software was used to obtain Dimensions of *n*-octyloxy derivatives for chalcone (a) L/B ratio 8.343 and imine (b) with L/B ratio 9.550.

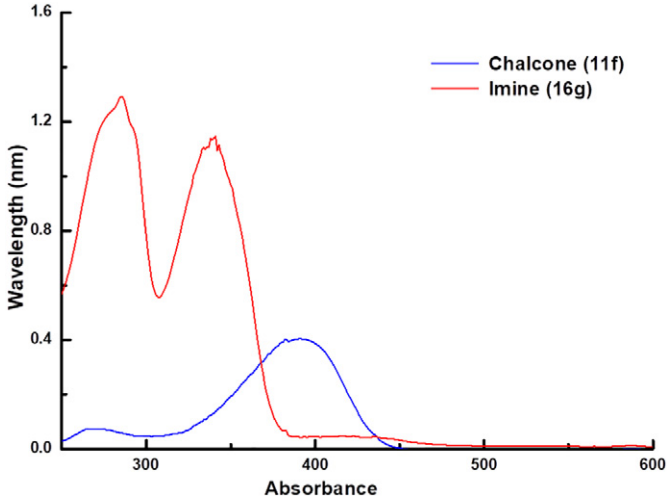

Fig. 9. UV-Vis absorbance spectra for compounds 11f and 16 g in chloroform.

References

[1] G.W. Gray, Advances in Liquid Crystals, vol. 2, Academic Press Inc, New York and London, 1972.
[2] D.K. Yang, S.T. Wu, Fundamentals of Liquid Crystal Devices, second ed. Wiley, Chichester, United Kingdom, 2014.
[3] D. Andrienko, Introduction to liquid crystals, J. Mol. Liq. 267 (2018) 520–541.
[4] A.S. Matharu, S. Jeeva, P. Ramanujam, Liquid crystals for holographic optical data storage, Chem. Soc. Rev. 36 (2007) 1868–1880.
[5] J.P.F. Lagerwall, G.A. Scalia, New era of liquid crystal research: applications of liquid crystals in soft matter nano-, bio- and microtechnology, Curr. Appl. Phys. 12 (2012) 1387–1412.
[6] S. Singh, D.A. Dunmur, Liquid Crystals: Fundamentals, World Scientific Publishing Co. Pte. Ltd., London, 2002.
[7] V.V. Titov, A.I. Pavlyuchenko, Thermotropic liquid crystals in the heterocyclic series, Chem. Heterocycl. Comp. 16 (1980) 1–13.
[8] A. Seed, Synthesis of self-organizing mesogenic materials containing a sulfur-based five-membered heterocyclic core, Chem. Soc. Rev. 36 (2007) 2046–2069.
[9] J. Han, 1,3,4-Oxadiazole based liquid crystals, J. Mater. Chem. C. 1 (2013) 7779–7797.
[10] M.P. Aldred, P. Vlachos, D. Dong, S.P. Kitney, W.S. Tsoi, M. O'Neill, S.M. Kelly, Heterocyclic reactive mesogens: synthesis, characterisation and mesomorphic behaviour, Liq. Cryst. 32 (2005) 951–965.
[11] T.D. Nguyen, E. Ehrenfreund, Z.V. Vardeny, The spin-polarized organic light emitting diode, Synth. Met. 173 (2013) 16–21.
[12] A.J.M. Al-Karawi, From mesogens to metallomesogens. Synthesis, characterization, liquid crystals and luminescent properties, Liq. Cryst. 44 (2017) 2285–2300.
[13] N.K. Chudgar, S.N. Shah, New fluorescentmesogens with a chalcone central linkage, Liq. Cryst. 4 (1989) 661–6681989.
[14] G.-Y. Yeap, I. Susanti, B.-S. Teoh, W.A.K. Mahmood, W.T.A. Harrison, Synthesis and phase transition in new chalcone derivatives: crystal structure of 1-phenyl-3-(4'-undecylcarbonyloxyphenyl)-2-propen-1-one, Mol. Cryst. Liq. Cryst. 442 (2005) 133–146.
[15] C.V. Yelamaggad, A.S. Achalkumar, N.L. Bonde, A.K. Prajapati, Liquid crystal abrikosov flux lattice: the exclusive wide thermal range enantiotropic occurrence, Chem. Mater. 18 (2006) 1076–1078.
[16] C.V. Yelamaggad, N.L. Bonde, A.S. Achalkumar, D.S. Shankar Rao, S.K. Prasad, A.K. Prajapati, Frustrated liquid crystals: synthesis and mesomorphic behavior of unsymmetrical dimers possessing chiral and fluorescent entities, Chem. Mater. 19 (2007) 2463–2472.
[17] B.T. Thaker, P.H. Patel, A.D. Vansadiya, J.B. Kanojiya, Substitution effects on the liquid crystalline properties of thermotropic liquid crystals containing schiff base chalcone linkages, Mol. Cryst. Liq. Cryst. 515 (2009) 135–147.
[18] B.T. Thaker, J.B. Knojiya, Synthesis, characterization and mesophase behavior of new liquid crystalline compounds having chalcone as a central linkage, Mol. Cryst. Liq. Cryst. 542 (2011) 606–620.
[19] V.S. Sharma, R.H. Vekariya, A.S. Sharma, R.B. Patel, Mesomorphic properties of liquid crystalline compounds with chalconyl central linkage in two phenyl rings, Liq. Cryst. Today 26 (2017) 46–54.
[20] A.J.M. Al-Karawia, A.J. Hammooda, A.A. Awada, A.A.B. OmarAlia, S.R. Khudhaierb, D.T.A. Al-Heetimic, S.G. Majeed, Synthesis and mesomorphism behaviour of chalcones and pyrazoles type compounds as photo-luminescent materials, Liq. Cryst. 45 (2018) 1603–1619.
[21] S.T. Ha, T.L. Lee, S.L. Lee, S. Sreehari Sastry, Y.F. Win, Schiff base liquid crystals with terminal iodo group: synthesis and thermotropic properties, Sci. Res. Essays 6 (2011) 5025–5035.
[22] A. Gowda, A. Roy, S. Kumar, Synthesis and mesomorphic properties of novel schiff base liquid crystalline EDOT derivatives, J. Mol. Liq. 225 (2017) 840–847.
[23] L. Fritsch, A.A. Merlo, An old dog with new tricks: schiff bases for liquid crystals materials based on isoxazolines and isoxazoles, Chemistry Select 1 (2016) 23–29.
[24] A.A. Merlo, H. Gallardo, T.R. Taylor, T. Kroin, Mol. Cryst. Liq. Cryst. 250 (1994) 31–39.
[25] Y.Q. Tian, E. Akiyama, Y. Nagase, J. Mater. Chem. 13 (2003) 1253–1258.
[26] Y.Q. Tian, E. Akiyama, Y. Nagase, et al., Macromol. Chem. Phys. 201 (2000) 1640–1652.
[27] S. Zhou, J. Jia, J. Gao, L. Han, Y. Li, W. Sheng, The one-pot synthesis and fluorimetric study of 3-(20-benzothiazolyl) coumarins, Dyes Pigments 86 (2010) 123–128.
[28] I. Esnal, G. Duran-Sampedro, A.R. Agarrabeitia, J. Bañuelos, I. Gracia-Moreno, M.A. Macias, E. Peña-Cabrera, I. López-Arbeloa, S. De la Moya, M.J. Ortiz, Coumarin-BODIPY hybrids by heteroatom linkage: versatile, tunable and photostable dye lasers for UV irradiation, Phys. Chem. Chem. Phys. 17 (2015) 8239–8247.
[29] A. Concellón, R. Termine, A. Golemme, P. Romero, M. Marcos, J.L. Serrano, High hole mobility and light-harvesting in discotic nematic dendrimers prepared via 'click' chemistry, J. Mater. Chem. C. 7 (2019) 2911–2918.
[30] S.Y. Ahn, Y.B. Cha, M. Kim, K.H. Ahn, Y.C. Kim, Synthesis, characterization, and electroluminescence properties of a donor-acceptor type molecule for highly efficient non-doped green organic light-emitting diodes, Synth. Met. 199 (2015) 8–13.
[31] V. Leandri, J.M. Gardner, M. Johnson, Coumarin as a quantitative probe for hydroxyl radical formation in heterogeneous photocatalysis, J. Phys. Chem. C 123 (2019) 6667–6674.
[32] G. Deng, H. Xu, L. Kuang, C. He, B. Li, M. Yang, X. Zhang, Z. Li, J. Liu, Novel nonlinear optical chromophores based on coumarin: synthesis and properties studies, Opt. Mater. 88 (2019) 218–222.
[33] H. Kang, D. Kang, Photoalignment behavior on polystyrene fllms containing coumarin moieties, Mol. Cryst. Liq. Cryst. 623 (2015) 45–55.
[34] J. Buchs, M. Gäbler, D. Janietz, H. Sawade, Coumarin-based emissive liquid crystals, Liq. Cryst. 41 (2014) 1605–1618.
[35] Y. Tian, E. Akiyama, Y. Nagase, A. Kanazawa, O. Tsutsumi, T. Ikeda, Synthesis and investigation of photophysical and photochemical properties of new side-group liquid crystalline polymers containing coumarin moieties, J. Mater. Chem. 14 (2004) 3524–3531.
[36] K.N. Trivedi, N.N. Thaker, Mesomorphic heterocyclic homologous series: I.7-(4'-*n*-Alkoxybenzoyloxy)-3-acetylcoumarins II. 4'-Formylphenyl 7-*n*-alkoxycoumarin-3-carboxylates, Mol. Cryst. Liq. Cryst. 78 (1981) 263.
[37] J.S. Dave, M.R. Menon, P.R. Patel, Synthesis and mesomorphic characterization of azoesters with a coumarin ring, Liq. Cryst. 29 (2002) 543–549.
[38] A.A. Merlo, A. Tavares, S. Khan, M.J. Leite Santos, S.R. Teixeira, Liquid-crystalline coumarin derivatives: contribution to the tailoring of metal-free sensitizers for solar cells, Liq. Cryst. 45 (2018) 310–322.
[39] H.T. Srinivasa, H.N. Harishkumar, B.S. Palakshamurthy, New coumarin carboxylates having trifluoromethyl, diethylamino and morpholino terminal groups: synthesis and mesomorphic characterisations, J. Mol. Struct. 1131 (2017) 97–102.
[40] H.T. Srinivasa, B.S. Palakshamurthy, A.T. Mohammad, Ethyl 7-hydroxycoumarin-3-carboxylate derivatives: synthesis, characterization and effect of liquid crystal properties, J. Mol. Struct. 1155 (2018) 513–519.
[41] M. Hagar, H.A. Ahmed, O.A. Alhaddadd, DFT calculations and mesophase study of coumarin esters and its azoesters, Crystals 8 (2018) 359–370.
[42] S.D. Durgapal, R. Soni, S. Umar, B. Suresh, S.S. Soman, Anticancer activity and DNA binding studies of novel 3,7-disubstituted benzopyrones, Chemistry 2 (2017) 147–153.
[43] A.A. Kudale, J. Kendall, C.C. Warford, N.D. Wilkins, G.J. Bodwell, Hydrolysis-free synthesis of 3-amino coumarins, Tetrahedron Lett. 48 (2007) 5077–5080.
[44] P.J. Collings, M. Hird, Introduction to Liquid Crystals: Chemistry and Physics, Taylor & Francis Ltd, London, 1998.
[45] A. Lesac, U. Baumeister, I. Dokli, Z. Hameršak, T. Ivšić, D. Kontrec, M. Viskić, A. Knežević, R.J. Mandle, Geometric aspects influencing N-NTB transition implication of intramolecular torsion, Liq. Cryst. 45 (2018) 1101–1110.

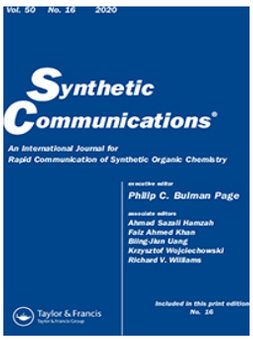

Taylor & Francis
Taylor & Francis Group

Synthetic Communications

An International Journal for Rapid Communication of Synthetic Organic Chemistry

ISSN: 0039-7911 (Print) 1532-2432 (Online) Journal homepage: https://www.tandfonline.com/loi/lsyc20

Synthesis and studies of flavone and bis-flavone derivatives

Sunil Dutt Durgapal, Shubhangi S. Soman, Shweta Umar & Suresh Balakrishnan

To cite this article: Sunil Dutt Durgapal, Shubhangi S. Soman, Shweta Umar & Suresh Balakrishnan (2020) Synthesis and studies of flavone and bis-flavone derivatives, Synthetic Communications, 50:16, 2502-2510, DOI: 10.1080/00397911.2020.1781186

To link to this article: https://doi.org/10.1080/00397911.2020.1781186

SYNTHETIC COMMUNICATIONS®
2020, VOL. 50, NO. 16, 2502–2510
https://doi.org/10.1080/00397911.2020.1781186

Taylor & Francis
Taylor & Francis Group

Synthesis and studies of flavone and bis-flavone derivatives

Sunil Dutt Durgapal[a], Shubhangi S. Soman[a], Shweta Umar[b], and Suresh Balakrishnan[b]

[a]Department of Chemistry, Faculty of Science, The M. S. University of Baroda, Vadodara, India; [b]Department of Zoology, Faculty of Science, The M. S. University of Baroda, Vadodara, India

ABSTRACT

Flavonoids are widely occurring polyphenols of plant origin and well explored in the field of pharmacological activities. Recent studies showed this scaffold to be more dynamic as fluorescent probe. Very rare reports are there in literature on flavones as liquid crystals, for the first time we have synthesized and characterized flavone and bis-flavone derivatives for mesomorphic properties. Compounds **9a–d** and **13a–d** were studied for liquid crystalline properties by Differential scanning calorimetry (DSC) and Polarizing optical microscopy (POM) studies. The compounds **8, 9a–d, 12,** and **13a–d** were also studied for antioxidant property by DPPH assay.

GRAPHICAL ABSTRACT

We have synthesized new n-alkoxy flavone and Bis-flavone derivatives for liquid crystalline properties. The compounds were characterized by using different spectral techniques, all synthesized compounds did not show mesophase which was confirmed by differential scanning calorimetry (DSC) and polarizing optical microscopy (POM) study.

POM image of compound **9c** in heating (a) shows direct melting (92.2°C) of compound and cooling (b) goes to crystallization (65.8°C) with no phase.

Flavone derivatives are well reported to show broad pharmacological applications, we have also tested compounds for antioxidant properties by DPPH assay.

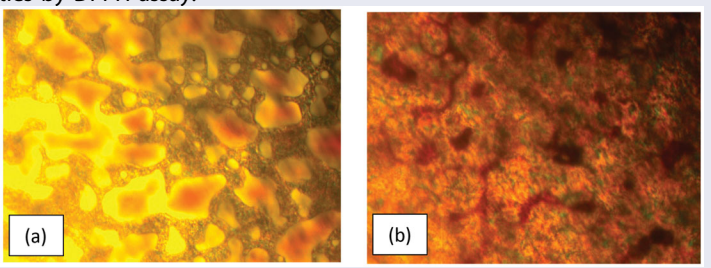

ARTICLE HISTORY

Received 14 April 2020

KEYWORDS

Antioxidant activity; bis-flavones; flavones; liquid crystals; synthesis

CONTACT Shubhangi S. Soman shubhangiss@rediffmail.com Department of Chemistry, Faculty of Science, The M. S. University of Baroda, Vadodara, India.

Supplemental data for this article can be accessed on the publisher's website.

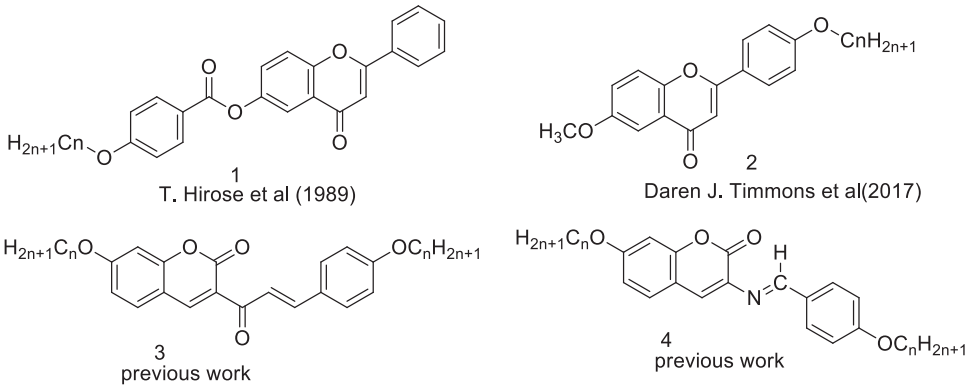

Figure 1. Chromene derivatives with liquid crystalline property.

Introduction

Flavonoids consist of group of naturally occurring compounds. They are major constituent of many fruits, vegetables, beverages and secondary metabolite. Flavonoids family members (e.g. flavones, isoflavones, and neoflavones) possess many medicinal properties.[1–3] Various naturally and synthetic occurring flavonoid derivatives are studied for variety of pharmacological activities to treat different diseases.[4] Special interest in these molecules attracted due to its potential health benefits such as antioxidant activities of these polyphenolic compounds.[5] Functional hydroxyl groups in flavonoids mediate their antioxidant effects by scavenging free radicals or chelating metal ions.[6] The design of heterocyclic compounds having liquid crystalline properties led to variety of mesogenic compounds with interesting properties. Flavonoid derivatives emerged as important framework which can detect cysteine intracellular which showed potential utility of flavones as fluorescent probe.[7,8] It is observed that simple heterocyclic core, terminal alkyl chains and various connecting moieties are not sufficient to introduce liquid crystalline (LC) properties.[9] There are very few reports in literature on flavone derivatives with mesogenic properties. Hirose et al. first time in 1989 synthesized 6-(4-n-alkoxybenzoyloxy)-flavone compound **1** (Figure 1) exhibiting nematic phase.[10]

Timmons et al. synthesized series of flavones compound **2** (Figure 1) with substitution on 4′, and 6 positions which gave nematic and smectic phase.[11] Mohammad et al. reported dimers of Isoflavone with ethylene/phenylenediamine bridge showed smectic and nematic mesophases.[12] In our previous work we have reported chromen-2-one containing chalcone, imine linkages **3** and **4** (Figure 1) with alkoxy group showed excellent mesomorphic properties.[13]

We report herein synthesis of chromen-4-one and bischromen-4-one derivatives for their mesomorphic phase study and antioxidant property.

Results and discussion

Chemistry

2,4-dihydroxy acetophenone **6** was prepared from resorcinol **5** by using standard method.[14] 2,4-dihydroxy acetophenone **6** was reacted with 4-hydroxy benzaldehyde in

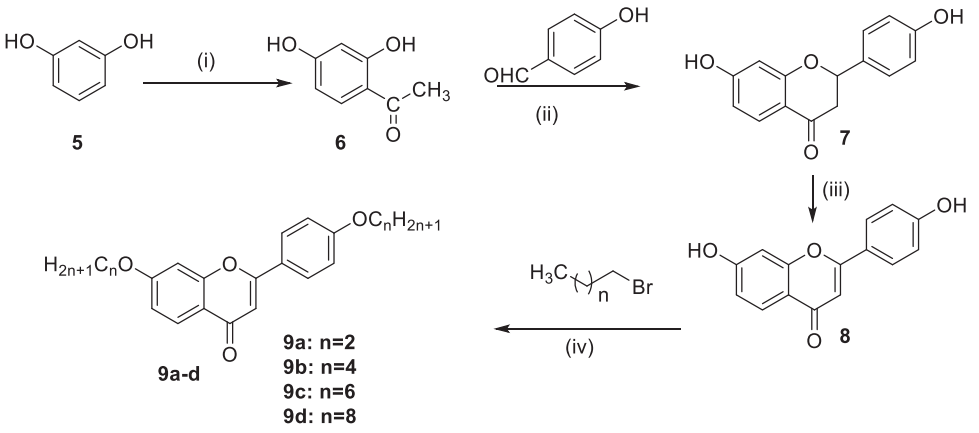

Reagent and conditions:- (i) Glacial AcOH/ $ZnCl_2$, 25-30 min, heat (ii) Ethanol, pyrrolidone, 2-3 drops acetic acid, 78-80°C, 48hrs (iii) I_2/DMSO, 120°C, 3hrs (iv) K_2CO_3, DMF, 80°C, Reflux

Scheme 1. Synthesis of 7-hydroxy-2-(4-hydroxyphenyl)-4H-chromen-4-one derivatives

ethanol using catalytic amount of piperidine and acetic acid to give flavanone **7** (Scheme 1). Compound **7** was purified by column chromatography and its structure was confirmed by ^{1}H-NMR. Compound **7** was oxidized using I_2/DMSO to give flavone **8**. Compound **8** was alkylated with different *n*-alkyl bromides using K_2CO_3 in N,N-dimethyl formamide (DMF) to give compounds **9a–d** (Scheme 1).

The IR spectrum of compounds **8** exhibited one broad band in the range of 3214 cm^{-1} for O–H stretching vibrations and another strong band at 2929 cm^{-1} for C–H Stretching vibrations. Carbonyl stretching frequency was observed at 1630 cm^{-1}. In ^{1}H-NMR of compound **8** showed singlet for proton at 3rd position of flavone ring at δ 6.28 ppm and seven protons were observed in aromatic region of δ 6.40–8.14 ppm, –OH proton was observed at 13.5 ppm. In ^{13}C-NMR for compound **8** peaks from δ 102–162 were observed for all aromatic carbons. Carbonyl carbon peak was observed at 176 ppm.

IR spectrum of compound **9a–d** showed bands from 3058 to 2956 cm^{-1} for C–H stretching, band at 1637 cm^{-1} observed for carbonyl stretching and bands at 1250–1110 cm^{-1} observed for C–O stretching vibrations. Formation of compounds **9a–d** was confirmed by ^{1}H, ^{13}C-NMR, IR and Mass analysis. In general ^{1}H NMR of compound **9a–d** showed triplets from δ 0.99 to 1.04 for six protons of two terminal methyl groups, peaks from δ 1.51 to 1.87 indicated methylene protons of different alkoxy group, triplet in range from δ 4.04–4.11 ppm is for $-OCH_2$ protons attached at 7th and 4th position. Singlet Peak around δ 6.7 ppm is for proton at 3rd position of flavone ring. Multiplet from δ 6.95–7.03 ppm is for protons of aromatic ring at 2nd position of chromen-4-one. Doublet at δ 7.86 and 8.12 ppm is observed for 5th and 6th position proton of flavone ring.

Resorcinol on acylation with acetic anhydride and $ZnCl_2$ gave 1,1′-(4,6-dihydroxy-1,3-phenylene) diethanone **10** (Scheme 2). Compound **10** on reaction with two equivalents of 4-hydroxy benzaldehyde in ethanol using catalytic amount of pyrrolidine and acetic acid gave mixture of two products **11a** and **11b** on TLC which were separated by column chromatography.

The formation of Compounds **11a** and **11b** was confirmed by IR, ^{1}H NMR, ^{13}C NMR, Mass spectra. ESI-Mass of **11a** showed M + H peak at 403.1. While ESI-MS of compound **11b** showed M + H peak at 299.09 thus proved formation of monoreacted compound **11b**

The IR spectrum of compounds **11a** exhibited one broad band in the range of 3381–3158 cm^{-1} for O–H stretching vibrations. Carbonyl stretching frequencies for ketone of chalcone and for chromen-4-one were observed at 1635 and 1675 cm^{-1}, respectively. ^{1}H NMR of compound **11a** exhibited three doublet of doublets at δ 2.78, 3.28, and 5.61 ppm for one proton each indicated protons at 3rd and 2nd positions, respectively. Aromatic protons of 4-hydroxy phenyl ring and olefinic protons were observed as doublets in region of δ 6.81, 6.85, 7.35, and 7.80 ppm. Protons of 5th and 8th position of aromatic ring of flavanone were observed at δ 6.52 and 8.62 ppm. Phenolic protons were observed at δ 9.62, 10.21, and 13.56 ppm. In ^{13}C NMR of compound **11a** exhibited sharp peaks for aliphatic carbons of flavanone ring at δ 43.47 and 79.79, peaks for aromatic carbons were observed from 104 to 168 ppm. Carbonyl carbon of chromen-4-one ring and chalcone were observed at δ 190 and 193 ppm, respectively.

Compound **11a** was subjected to oxidation/oxidative cyclization using catalytic amount of I_2 (0.2 equivalent) in DMSO to give compound **12** (Scheme 2) with high yield of 92%. Further compound **12** was alkylated using alkyl bromides with K_2CO_3 in DMF to give compounds **13a–d**.

^{1}H-NMR of compound **12** showed singlet at δ 6.86 for two protons, indicated flavone ring protons at 3rd position. While two singlets at δ 8.05 and 8.57 ppm, indicated protons at 5th and 8th position. Protons of 4-hydroxyphenyl rings were observed as doublet at δ 6.95 and 7.98 ppm with coupling constant (J = 8.8 Hz) indicated ortho coupled protons. In general, the IR spectrum of compound **13a–d** showed bands from 3077 to 2856 cm^{-1} for C–H stretching vibrations. Here, disappearance of broad band indicated alkylation of free –OH has occurred. Band at 1640 cm^{-1} indicated carbonyl stretching

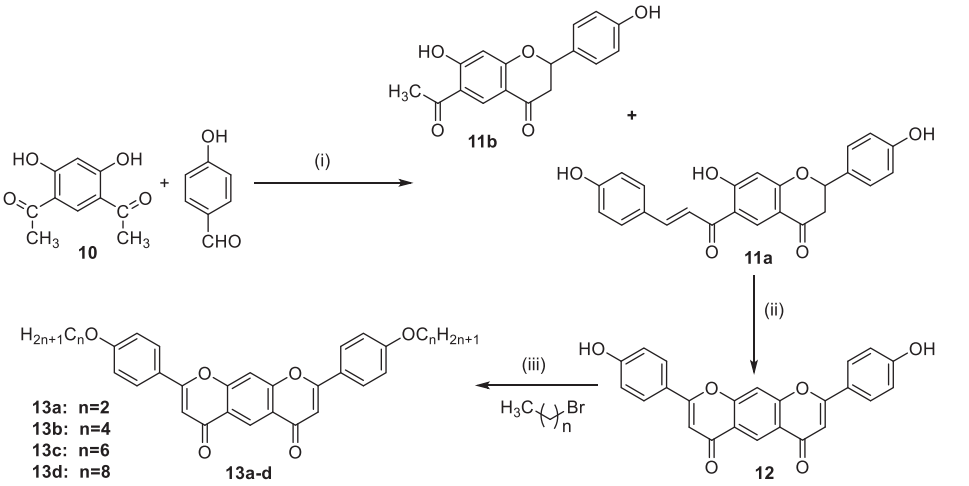

Reagent and conditions: (i) Ethanol, Pyrrolidine, AcOH, 78-80 °C, Reflux, 20 hrs (ii) I_2/DMSO, 3hr reflux (iii) K_2CO_3, DMF, 16hr reflux

Scheme 2. Synthesis of 2,8-bis(4-hydroxyphenyl)-4H,6H-pyrano[3,2-g]chromene-4,6-dione derivatives.

frequency and band at 1250–1050 cm^{-1} indicated C–O stretching vibrations. ^{1}H-NMR of compound **13a–d** showed peaks in range from δ 1.00 to 2.19 for aliphatic protons of alkyl chain, triplet at 4.06–4.09 ppm is observed for methylene protons of alkoxy group. Aromatic protons of flavones were observed in region from δ 6.72 to 9.07 ppm. ^{13}C-NMR of compound **13b–d** showed peaks from 14 to 68 ppm for aliphatic carbons. Peak from δ 105 to 163 ppm corresponds to aromatic carbons. Peak at 177 ppm is for carbonyl carbon of chromone.

Mesomorphic phase study

Long alkyl chain compounds of chromen-2-one as rigid structure showed liquid crystalline properties.[11] Flavone compounds containing long alkyl chain **9a–d** and **13a–d** were chosen for liquid crystal phase study. All compounds were screened for phase transition temperature by differential scanning calorimetry which showed one sharp peak on heating and cooling for crystalline to isotropic liquid phase with no phase transition (Figure 2).

To confirm that compounds are showing no liquid crystal phase polarizing optical microscope was used to observe photographs of compounds. Initially these compounds were subjected to heating rate of 20°C/min and 10°C/min to find phase transition between solid and liquid phase. Further, these compounds were studied at slower rate of heating and cooling rate of 5°/min and 2°C/min to find the phase transition under POM observation (Figure 3).

Crystal changed to dark region i.e. isotropic liquid while heating process, this observation indicated direct melting of the crystal phase to isotropic liquid phase. No liquid crystal texture was observed during cooling process. On cooling compounds directly

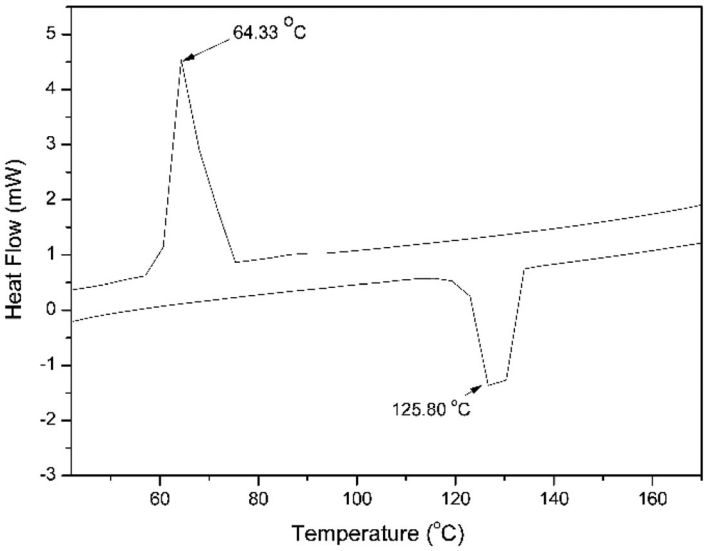

Figure 2. DSC of compound **9b** showing sharp melting point at 125.80 °C and crystallization at 64.33 °C.

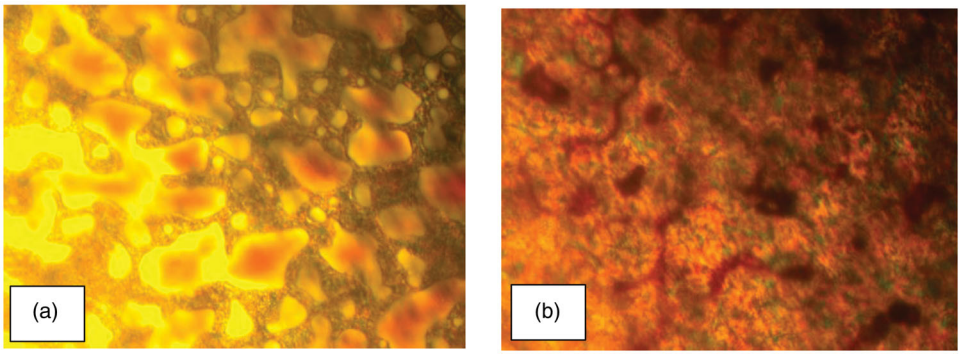

Figure 3. POM image of compound **9c** in heating (a) shows direct melting (92.2 °C) of compound and cooling (b) goes to crystallization (65.8 °C) with no phase.

Table 1. Anti-oxidant activity of compounds **8**, **9a–d, 12,** and **13a–d**.

Compoud No.	EC_{50} μg/mL[a]
8	17.27
9a	116.2
9b	2334
9c	7611
9d	8008
12	9.87
13a	321.9
13b	2695
13c	4851
13d	8641
Ascorbic acid	11

[a]EC_{50} values were determined using Graph Pad. Prism software by DPPH assay using DMF.

crystallized into a stable state of crystal without any transitions within the crystal region.

Antioxidant activity

Antioxidant activity of all synthesized compounds was tested by DPPH assay. Compound **8** showed moderate activity as compared to ascorbic acid. On alkylation of hydroxyl group of compound **8** by various n-alkyl chains in compounds **9a–d** showed decrease in antioxidant activity (Table 1). Bis-flavone derivatives **12** showed very good antioxidant activity with EC_{50} value of 9.87 μg/mL as compared to ascorbic acid. However, alkylated compounds **13a–d** showed very poor antioxidant activity with EC_{50} significantly higher than ascorbic acid in DPPH assay. In general compounds **8**, **12** with hydroxyl group showed good antioxidant activity but as the alkyl side chain increases loss in antioxidant properties was observed. The scavenging properties of antioxidant compounds are often associated with their ability to form stable radicals. It is well known that aromatic compounds containing free hydroxyl groups can give rise to stable radical.[15] All the compounds with alkyl chain failed to show good activity because of poor solubility of compounds in polar aprotic solvents like dimethyl sulphoxide (DMSO) and dimethyl formamide (DMF).

Conclusion

Synthesis of *n*-alkoxy derivatives of flavone and bisflavones is carried out for liquid crystalline properties, as well as antioxidant properties. All compounds were screened for liquid crystalline properties but fail to show activity. It is observed that since melting points of compounds **13a–d** were very high and solubility of compounds was very poor so higher n-alkoxy derivatives were not synthesized. Flavone derivatives also studied for antioxidant activity. Hydroxy flavone **8** and hydroxy bis-flavone **12** showed moderate to good activity as compared to ascorbic acid in DPPH assay. Since the solubility of *n*-alkylated compounds **9a–d**, **13a–d** was very poor in polar aprotic solvents, antioxidant activity was not observed.

Experimental

General method for alkylation of 7-hydroxy-2-(4-hydroxyphenyl)-4H-chromen-4-one (9a–d)

A mixture of compound **8** (1.968 mmol, 1.0 eq) and anhydrous potassium carbonate (4.92 mmol, 2.5 eq) in N,N-dimethyl formamide (DMF) (10.0 mL) was stirred for 10 min at rt. To this mixture, alkyl bromide (4.33 mmol, 2.2 eq) was added and resulting mixture was refluxed at 80°C for 12 h. The completion of reaction was checked by TLC. After completion of reaction, reaction mixture was poured into crushed ice. The solid separated out was filtered, washed with cold water and recrystallized from ethanol to give compounds **9a–d**.

Characterization data for compound (9b)

7-Butyloxy-2-(4-butyloxyphenyl)-4H-chromen-4-one

Color: light brown; Yield: 71.5%; M.P: 124–126 °C; IR(KBr): 3426, 3211, 2955, 2934, 2869, 1637, 1601, 1572, 1440, 1356, 1317, 1252, 1183, 1126, 1087, 1037, 1007, 971, 905, 839, 764, 669, 634 cm^{-1}; ^{1}H NMR ($CDCl_3$, 400 MHz) ppm: 1.0–1.04 (t, 6H), 1.51–1.59 (m, 4H), 1.79–1.89 (m, 4H), 4.04–4.11 (t, 4H), 6.70 (s, 1H), 6.96 (d, $J = 2.0$ Hz, 1H), 6.98 (dd, $J = 8.8$, 2.4 Hz, 1H), 7.03 (d, $J = 8.8$ Hz, 2H), 7.86 (d, $J = 8.8$ Hz, 2H), 8.13 (d, $J = 8.4$ Hz, 1H); ^{13}C NMR ($CDCl_3$, 100 MHz): 13.91, 13.94, 19.31, 31.15, 31.27, 68.08, 68.50, 100.92, 106.07, 114.65, 114.98, 117.71, 123.99, 127.00, 127.89, 158.01, 161.96, 163.19, 163.72, 178.01; Anal. Calc. for $C_{23}H_{26}O_4$; C, 75.38; H, 7.15; found: C, 75.14; H, 7.40%, $[M + H]^+$: 367.18

General method for synthesis of (13a-d): alkylation of 2,8-bis(4-hydroxyphenyl)pyrano[3,2-g]chromene-4,6-dione (12)

To a solution of compound **12** (0.2 g, 0.5 mmol, 1 eq) in anhydrous DMF (10 mL), anhydrous K_2CO_3 (0.185 g, 1.25 mmol, 2.5 eq) was added and then the reaction mixture was stirred for 15 min to obtain a clear orange solution. To this, alkyl bromides (1.1 mmol, 2.2 eq) were added to the stirred solution dropwise. The reaction mixture was heated at 68–70 °C for 16 h. The completion of reaction was checked by TLC. The reaction mixture was cooled to room temperature and poured into ice cold water to

give solid. The solid was filtered with vacuum and dried. The solid was dissolved in DCM (10 mL), dried over anhydrous Na_2SO_4, filtered and concentrated to give compounds **13a–d** as yellow solid.

Characterization data for compound (13d)

2,8-Bis(4-(octyloxy)phenyl)-4H,6H-pyrano[3,2-g]chromene-4,6-dione

Color: white; Yield: 68%, M. P: Above 256–258 °C; IR (KBr): 3079,3041, 2923, 2853, 1641, 1612, 1511, 1469, 1425, 1375, 1302, 1260, 1244, 1182, 1118, 1033, 902, 829, 640,617 cm^{-1}; ^1H ($CDCl_3$, 400 MHz) δ ppm: 0.89–0.92 (t, $J = 6.8$ Hz, 6H), 1.26–1.36 (m, 16H), 1.48–1.50 (m, 4H), 1.82–1.86 (m, 4H), 4.05 (t, $J = 6.4$ Hz, 4H), 6.72 (s, 2H), 7.02 (d, $J = 8.8$ Hz, 4H), 7.63 (s, 1H), 7.85 (d, $J = 8.8$ Hz, 4H), 9.07 (s, 1H); ^{13}C NMR ($CDCl_3$, 100 MHz): 14.10, 22.66, 26.01, 29.12, 29.23, 29.34, 29.70, 31.81, 68.42, 105.81, 106.10, 115.06, 121.56, 123.02, 125.76, 128.04, 158.38, 162.40, 163.79, 177.14; Anal. Calc. for $C_{40}H_{46}O_6$; C, 77.14; H, 7.45; found: C, 77.26; H, 7.63%, $[M + H]^+$: 623.33

Full experimental detail, IR, ^1H, ^{13}C NMR and ESI-MS spectra. This material can be found via the "Supplementary Content" section of this article's webpage

Acknowledgment

Authors are thankful to Head department of chemistry and department of Zoology, faculty of science, The Maharaja Sayajirao University of Baroda for laboratory facilities. DST-FIST for NMR facility in the department.

ORCID

Suresh Balakrishnan http://orcid.org/0000-0002-6559-022X

References

[1] Panche, A. N.; Diwan, A. D.; Chandra, S. R. Flavonoids: An Overview. *J. Nutr. Sci.* **2016**, *5*, 1–15. DOI: 10.1017/jns.2016.41.

[2] Middleton, E.; Kandaswami, C.; Theoharides, T. C. The Effects of Plant Flavonoids on Mammalian Cells: Implications for Inflammation, Heart Disease, and Cancer. *Pharmacol. Rev.* **2000**, *52*, 673–751.

[3] Suresh Babu, K.; Hari Babu, T.; Srinivas, P. V.; Hara Kishore, K.; Murthy, U. S.; Rao, J. M. Synthesis and Biological Evaluation of Novel C (7) Modified Chrysin Analogues as Antibacterial Agents. *Bioorg. Med. Chem. Lett.* **2006**, *16*, 221–224. DOI: 10.1016/j.bmcl.2005.09.009.

[4] Wang, Q.; Ge, X.; Tian, X.; Zhang, Y.; Zhang, J.; Zhang, P. Soy Isoflavone: The Multipurpose Phytochemical (Review). *Biomed. Rep.* **2013**, *1*, 697–701. DOI: 10.3892/br.2013.129.

[5] Firuzi, O.; Lacanna, A.; Petrucci, R.; Marrosu, G.; Saso, L. Evaluation of the Antioxidant Activity of Flavonoids by "Ferric Reducing Antioxidant Power" Assay and Cyclic Voltammetry. *Biochim. Biophys. Acta.* **2005**, *1721*, 174–184. DOI: 10.1016/j.bbagen.2004.11.001.

[6] Kumar, S.; Mishra, A.; Pandey, A. K. Antioxidant Mediated Protective Effect of Parthenium Hysterophorus against Oxidative Damage Using *In Vitro* Models. *BMC Complement Altern. Med.* **2013**, *13*, 120. DOI: 10.1186/1472-6882-13-120.

[7] Zhang, J.; Lv, Y.; Zhang, W.; Ding, H.; Liu, R.; Zhao, Y.; Zhang, G.; Tian, Z. A Flavone-Based Turn-On Fluorescent Probe for Intracellular Cysteine/Homocysteine Sensing with High Selectivity. *Talanta*. **2016**, *146*, 41–48. DOI: 10.1016/j.talanta.2015.08.025.

[8] Liu, B.; Wang, J.; Zhang, G.; Bai, R.; Pang, Y. Flavone-Based ESIPT Ratiometric Chemodosimeter for Detection of Cysteine in Living Cells. *ACS Appl Mater Interf.* **2014**, *6*, 4402–4407. DOI: 10.1021/am500102s.

[9] Srinivasa, H. T.; Harishkumar, H. N.; Palakshamurthy, B. S. New Coumarin Carboxylates Having Trifluoromethyl, Diethylamino and Morpholino Terminal Groups: Synthesis and Mesomorphic Characterisations. *J. Mol. Struct.* **2017**, *1131*, 97–102. DOI: 10.1016/j.molstruc.2016.11.047.

[10] Hirose, T.; Tsuya, K.; Nishigaki, T.; Idaka, E.; Yano, S. Phase Transitions of 6-(4-*n*-Alkoxybenzoyloxy)-Flavones and 3-Cyano-7-(4-*n*-Alkoxybenzoyloxy)-Coumarins. *Liq. Cryst.* **1989**, *4*, 653–659. DOI: 10.1080/02678298908033200.

[11] Timmons, D. J.; Jordan, A. J.; Kirchon, A. A.; Murthy, N. S.; Siemers, T. J.; Harrison, D. P.; Slebodnick, C. Asymmetric Flavone-Based Liquid Crystals: Synthesis and Properties. *Liq. Cryst.* **2017**, *44*, 1436–1449. DOI: 10.1080/02678292.2017.1281450.

[12] Mohammad, A. T.; Srinivasa, H. T.; Alrawi, R. Y. Isoflavone-Based Trimer Liquid Crystals: Synthesis, Characterization, Thermal and Mesomorphic Properties Evaluations. *Liq. Cryst.* **2020**, *47*, 28–35. DOI: 10.1080/02678292.2019.1622045.

[13] Durgapal, S. D.; Soni, R.; Soman, S. S.; Prajapati, A. K. Synthesis and Mesomorphic Properties of Coumarin Derivatives with Chalcone and Imine Linkages. *J. Mol. Liq*. **2020**, *297*, 111920. DOI: 10.1016/j.molliq.2019.111920.

[14] Killelea, J. R.; Lindwall, H. G. Preparation of Resacetophenone. *J. Am. Chem. Soc.* **1948**, *70*, 428–428. DOI: 10.1021/ja01181a522.

[15] Cotelle, N.; Bernier, J. L.; Catteau, J. P.; Pommery, J.; Wallet, J. C.; Gaydou, E. M. Antioxidant Properties of Hydroxy-Flavones. *Free Radic. Biol. Med.* **1996**, *20*, 35–43. DOI: 10.1016/0891-5849(95)02014-4.